



Hawken General Aviation's Hybrid Electric Air Transport (HEAT) Family

In response to AIAA's 2017-2018 Undergraduate
Hybrid Electric General Aviation Aircraft Competition
May 10, 2018



HAWKEN

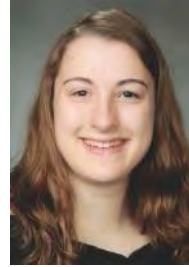
GENERAL AVIATION



Sean Berger
Team Lead



Bradley Polidoro
Propulsion



Carli Rau
Weights



Amelia Wentzel
Aerodynamics



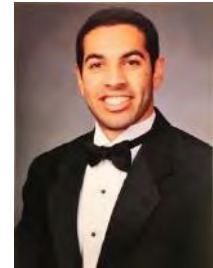
Nicholas Ferentinos
Structures & Materials
Cost



Zachary Stossel
Stability & Control
Acoustics



Josh Fang
Configuration



Kapil Gadre
Systems
Performance

Name	AIAA Number	Signature
Sean Berger	512397	<i>Sean Berger</i>
Bradley Polidoro	921454	<i>Bradley Polidoro</i>
Carli Rau	820377	<i>Carli Rau</i>
Amelia Wentzel	921519	<i>Amelia Wentzel</i>
Nicholas Ferentinos	921661	<i>Nicholas Ferentinos</i>
Zachary Stossel	921535	<i>Zachary Stossel</i>
Josh Fang	921534	<i>Josh Fang</i>
Kapil Gadre	823049	<i>Kapil Gadre</i>

Faculty Advisors

Dr. Pradeep Raj

Dr. Pat Artis

Contents

1	Executive Summary	1
2	3-View	2
3	Compliance Matrix	3
4	RFP Interpretation	4
4.1	Genesis of the Problem	4
4.2	RFP Requirements	4
4.3	Market Research	5
4.4	Concept of Operations	7
4.5	Measure of Merit and Design Driver	7
4.6	Technology	8
5	The HEAT Family	13
5.1	Conceptual Designs	13
5.1.1	Initial Concepts	13
5.1.2	Pros/Cons Matrix	14
5.2	Mission Profile	16
5.3	Initial Sizing	17
5.3.1	Design Space	17
5.3.2	Max Takeoff Weight Sizing	19
5.4	Configuration and Passenger Layout	22
5.5	Aerodynamic Design and Analysis	25
5.5.1	Wing Design	25
5.5.2	Airfoil Selection	26
5.5.3	Drag Build-Up	27
5.5.4	VLM Analysis	28
5.5.5	CFD Analysis	29
5.6	Propulsion	31
5.6.1	Hybrid Systems Considered	31
5.6.2	DEP Sizing	32
5.6.3	Hybrid Propulsion System Configuration	34
5.7	Structural Design and Material Selection	40
5.7.1	V-n Diagrams	40
5.7.2	Materials Selection	41
5.7.3	Wing	43
5.7.4	Fuselage	46
5.7.5	Empennage	46
5.8	Acoustics	48
5.8.1	Community Airport Noise	48
5.9	Systems	50
5.9.1	Landing Gear	50
5.9.2	Pneumatic/Fluid	51
5.9.3	De-Icing and Anti-Icing	51
5.9.4	Fuel System and Hydraulics	52
5.9.5	Fire and Heat Protection	53
5.9.6	Conventional Sensors	54
5.9.7	Avionics	54
5.9.8	Communication	56
5.9.9	Autonomous Systems Architecture	56
5.10	Weights and Center of Gravity	58
5.11	Stability and Control	62

5.11.1	Empennage	63
5.11.2	Static Stability	63
5.11.3	Dynamic Stability Analysis	65
5.11.4	Control Surface Sizing	66
5.12	Aircraft Performance	70
5.13	Maintenance and Reliability	74
5.14	Cost	74
5.14.1	Eastlake Model Assumptions	74
5.14.2	Market Analysis	75
5.14.3	Production Cost	76
5.14.4	Production Rate and Final Costs	78
6	Project Plans and Risks	79
6.1	Future Plans Through EIS	79
6.2	Risk Assessment	80
	References	83

List of Figures

1	A hybrid electric aircraft’s engine can be sized to cruise instead of takeoff or climb (not to scale) . . .	4
2	TRLs vary from 1 to 9 based upon a technology’s implementation into industry ²⁸	9
3	NASA is currently investigating DEP on a test aircraft called the X-57 Maxwell ²⁹	9
4	Battery energy density is anticipated to improve at an increasing rate over the next decade	11
5	Research suggests lithium-ion battery prices will fall between \$300 and \$150/kWh by 2024 ⁵	12
6	Initial aircraft concepts varied widely to flesh out a multitude of aircraft configurations	13
7	Hybrid propulsion allows for the HEAT family to meet RFP specified take-off and climb requirements, as well as extend an aircraft’s emergency range at 5000 ft. altitude	16
8	The design space for the HEAT family with the gray dot representing the design point	18
9	Hybrid MTOW sized by reducing engine size and adding DEP systems to TBM-930 MTOW estimation (meeting RFP requirements)	19
10	Empty weight trend line determined from 6 seat aircraft empty weights	20
11	The minimum MTOW was determined to occur with the smallest battery weight	21
12	Hawken is proud to present the HEAT Family Prometheus and Zeus	22
13	An average human can easily access both the aircraft’s cargo bay as well as the cabin	23
14	The seat pitch between the second and third row is 45 inches, giving commercial first-class level legroom to the passengers	24
15	Location of passenger accommodations	24
16	The easily accessible cargo bay provides ample storage for all passengers. Not pictured is a cargo net, which will prevent cargo from moving mid flight and disrupting the balance of the aircraft.	25
17	Top view of the wing planform. Split flaps, shown by dotted lines, provide additional lift during take-off and approach	26
18	The GAW-215 was selected due to its superior drag polar	27
19	The NACA 0012 was selected due to its drag polar	27
20	Drag Polar showing Cruise, Takeoff, and Landing Conditions	28
21	Surface mesh cells varied from 2 in ³ to 0.08 in ³ , with a target size of 0.5 in ³	30
22	CFD and VLM predictions for lift varied by less than 1% at angles of attack less than 10°	31
23	The Hawken team analyzed 3 hybrid propulsion systems	31
24	DEP closes the velocity gap required for take-off	33
25	DEP more than double’s the aircraft’s lift capability upon take-off	33
26	The propulsion system features 12 distributed motors and 1 primary internal combustion engine	34
27	The battery attachment pod allows for easy access, maintenance, and upgrades to the batteries	36
28	One of the six battery boxes located in the attachment pod	37
29	Folding propellers will allow the aircraft to reduce drag when DEP is not in use	38
30	The American Wire Gauge is a standard sizing methods for electrical wires	39
31	The 4 seat Prometheus’ final loading for the full mission profile	40
32	The 6 seat Zeus’ final loading for the full mission profile	41
33	Wing spar is linearly tapering box beam which reduces weight and provides enough structural support for all phases of flight	43
34	A design progression of wing spar cross-section designs was completed to find the lightest design for Aluminum 2024-T3	45
35	Final cross section shown to illustrate all volume requirements are met	45
36	A common fuselage structure is used for the HEAT family	46
37	A common empennage structure is used for the HEAT family	47
38	Anechoic chamber Aeronaut 16x8 three blade acoustic data at varying angles	49
39	Diagram of the HEAT family’s TKS de-ice and anti-ice system ³⁶	52
40	Fuel system features two wing tanks with fuel lines to the main engine	53
41	HEAT Family SkyVision Flight Deck is fully capable of VFR, IFR, and operating in all airspace classes	54
42	Fly-by-wire Actuation and Control Closed-loop Control System (with feedback)	56
43	The boxed region depicts the safe positions for CG travel with both HEAT family aircraft plotted	59
44	The boxed region depicts the safe position for CG travel for the Zeus and Prometheus (shown in blue and green respectively)	59

45	The weight build-up from zero fuel weight (MZFW) to max landing weight (MLW) to max takeoff weight (MTOW). Reserve fuel includes 45 minutes of additional flight ²⁵	61
46	To scale CG travel limits shown to give a better, physical representation of these limits	62
47	The aft limit is defined by the neutral point represented in orange. The forward limit, the green diamond, is set by the elevator moment. In between these is the CG with a blue square	62
48	Graph depicting optimal moment arm for the horizontal tail in terms of the length of the tail and horizontal stabilizer area	64
49	The ailerons are sized to meet both Mil-Spec and FAR roll requirements for enhanced maneuverability	67
50	Influence of the empennage design on the spin recovery characteristics ⁵⁵	68
51	Dimensioned vertical tail for the HEAT family aircraft	68
52	7 Initial layout for the elevator on the horizontal stabilizer	69
53	Dimensioned horizontal stabilizer with elevator shaded red	69
54	Hawken’s aircraft meet the range requirements of the RFP at MTOW	72
55	The 4 seat Prometheus can travel all the way from Virginia Tech To Pagosa Springs, CO at MTOW . .	73
56	As battery densities improve in the future, Hawken’s payload capacity will continue to improve as well	73
57	Each HEAT family is to be produced at 10 aircraft per month, and will be sold at \$925k and \$927k for the Prometheus and Zeus, respectively	78
58	Adequate time has been designated to certify the HEAT family as a single engine aircraft	80

List of Tables

1	More RFP requirements met results in increasing fuel costs ^{3,6-8,11,13,14,33,45,50,51,68-70}	6
2	China was projected to increase GA use in 2012 by a minimum of 25% by 2015, ⁶⁴	7
3	By 2024, TRL's of all utilized technologies are anticipated to increase to feasible levels for GA application with the exception of autonomous flight	8
4	Brushless Motors provide high power to weight ratios, ideal for application in the aerospace industry .	10
5	A Pros/Cons matrix allowed Hawken to select the best initial concepts for the final aircraft design . .	14
6	Fuel fractions accurately account for fuel use of a carbon engine-only aircraft	20
7	Total parasite drag for the HEAT family is .0357	28
8	Results from Tornado VLM Analysis of wing and empennage	29
9	Hawken CFD analysis used physics models representative of 3D incompressible flow	29
10	The 3 hybrid systems analyzed by Hawken vary by cost, weight, efficiency, and performance	32
11	Hawken's hybrid electric system's components are expected to be in service by 2024, with TBO values equal to or greater than current aircraft in the industry	34
12	The RED A05 Engine performs well in all phases of flight	35
13	EMRAX 208mm brushless 3-phase motors have the best price per pound	37
14	The further the DEP motor on the wing, the larger and heavier the wiring becomes	39
15	Hawken's hybrid propulsion system provides comparative propulsion efficiency to that of a traditionally powered aircraft, but increases mission flexibility and safety by allowing for battery charge in cruise	40
16	Materials and Weights Table for Structurally Designed Components	42
17	Takeoff was the most restrictive case with additional thrust from DEP system operations	44
18	Bending stress is dominant during takeoff	44
19	Aluminum 2024-T3 for its crack resistance and weight reduction	45
20	Fuselage structure specifications determined using plate buckling analysis of the skin	46
21	The empennage is adequately sized for all phases of flight	47
22	ANOPP results for airframe noise for ICAO chapter 14 requirements	49
23	HEAT family noise for ICAO chapter 10 requirements	49
24	The HEAT family aircraft are equipped with communication systems required for all phases of flight .	57
25	The weight breakdown for the Prometheus and Zeus, showing both the common and differing weights	60
26	Stability derivatives for the HEAT family	65
27	The HEAT family meet all but spiral Mil-spec dynamic stability requirements	66
28	Aileron size and location in ft and % span of the wing	66
29	Mil-spec and FAR roll requirements for the HEAT family aircraft provide enhanced safety and roll performance	67
30	Elevator sizing based on DEP use cases	69
31	The HEAT family greatly exceed the take-off and landing distance requirements set by the RFP	70
32	The Heat family take-off and landing performance is also great at 5000 ft AGL	71
33	Hawken's DEP system allows for the option to use reverse thrust, further improving landing distances	71
34	Ground effect was considered in take-off and landing distance calculations	71
35	Hawken's aircraft offer excellent low speed performance	72
36	Cost components for the Prometheus' final production or fly-away cost	77
37	Cost components for the Zeus' final production or fly-away cost	77
38	The Prometheus significantly reduces operating costs to \$58.50 per flight hour	79
39	The Zeus also significantly reduces from the competition to operating costs to \$57 per flight hour . . .	79
40	Risks identified by Hawken vary from High, Serious, Medium, and Low based upon severity and probability	80
41	Likelihood of risk was developed based upon probability	81
42	Severity of risk was based upon potential harm and cost to the aircraft and its occupants	81
43	The 5 major risks that Hawken identified were mitigated to acceptable levels	82

Nomenclature

Symbols

\$	US dollars	
α	Angle of attack	<i>degrees</i>
β	Effective propeller slipstream velocity multiplier	
ρ	Air density	<i>slugs/ft³</i>
σ	Stress	<i>ksi</i>
ζ	Damping ratio	
AR	Aspect ratio	
C_L	Lift coefficient	
C_{D_0}	Parasitic drag coefficient	
C_{L_α}	Lift coefficient with respect to angle of attack	<i>degree⁻¹</i>
C_{l_β}	Coefficient of rolling moment due to sideslip angle	<i>degree⁻¹</i>
$C_{L_{cruise}}$	Lift coefficient, cruise	
$C_{L_{max}}$	Max lift coefficient	
C_{l_p}	Coefficient of rolling moment due to roll rate	<i>degree⁻¹</i>
C_{l_r}	Coefficient of rolling moment due to rudder deflection	<i>degree⁻¹</i>
C_{m_0}	Moment coefficient at zero angle of attack	
C_{m_α}	Moment coefficient with respect to angle of attack	<i>degree⁻¹</i>
$C_{m_{cruise}}$	Moment coefficient in cruise	
C_{m_q}	Coefficient of pitching moment due pitching moment	<i>degree⁻¹</i>
C_{n_β}	Coefficient of yawing moment due to sideslip angle	<i>degree⁻¹</i>
C_{n_p}	Coefficient of yawing moment due to aileron deflection	<i>degree⁻¹</i>
C_{n_r}	Coefficient of yawing moment due to rudder deflection	<i>degree⁻¹</i>
C_{y_β}	Coefficient of side force due to sideslip angle	<i>degree⁻¹</i>
C_{y_p}	Coefficient of side force due to aileron deflection	<i>degree⁻¹</i>
C_{y_r}	Coefficient of side force due to rudder deflection	<i>degree⁻¹</i>
C_{Z_α}	Coefficient of roll due to sideslip angle	<i>degree⁻¹</i>
C_{Z_q}	Coefficient of roll due to aileron deflection	<i>degree⁻¹</i>
C_{Z_u}	Coefficient of roll due to rudder deflection	<i>degree⁻¹</i>
$CL_{Landing}$	Lift coefficient for landing	
CL_{TO}	Lift coefficient for take-off	
e	Oswald efficiency factor	

ft	Feet	
g	Gravitational acceleration	$32.2ft/s^2$
hp	Horsepower	
K_g	Ground effect induced drag parameter	
kg	Kilogram	
$KIAS$	Knots indicated air speed	
kWh	KiloWatt hour, unit of energy	
L/D	Lift to drag ratio	
lb	Pound	
P	Power	hp
$P_{Battery}$	Battery power	kW
P_{climb}	Power required for climb, horsepower	hp
P_{cruise}	Power required for cruise, horsepower	hp
P_{max}	Max Power required, horsepower	hp
S	Reference Area	ft^2
S_H	Horizontal tail area	ft^2
T	Period, seconds	s
V_A	Maneuver/Corner speed	$KIAS$
V_C	Design cruise speed	$KIAS$
V_D	Design dive speed	$KIAS$
V_S	Stall speed	$KIAS$
V_{APP}	Approach speed	$KIAS$
V_{AQUA}	Aquaplaning speed	$KTAS$
V_{HT}	Horizontal tail volume ratio	
V_{NE}	Never exceed speed	$KIAS$
V_{SO}	Stall speed	$KIAS$
V_{TD}	Touchdown speed	$KIAS$
V_{TO}	Takeoff speed	$KIAS$
V_{VT}	Vertical tail volume ratio	
W	Weight	lb
W/P	Power loading	lb/hp
W/S	Wing loading	lb/ft^2
W_{empty}	Empty aircraft weight	lb

W_{fuel} Fuel weight *lb*

Wh Watt hour

Acronyms

100/100LL Low lead gasoline commonly utilized in legacy general aviation aircraft

AC Alternating Current

AIAA American Institute of Aeronautics and Astronautics

ANOPP Airframe Noise Prediction Program

ATP Authorization To Proceed

AvGas Aviation Gasoline, also referred to as 100/100LL

AVIC Aviation Industry Corporation of China

BSFC Brake Specific Fuel Consumption

CFD Computational Fluid Dynamics

CFR Code of Federal Regulations

CG Center of Gravity

COTS Commercial Off-The-Shelf

CPI Consumer Price Index

DARPA Defense Advanced Research Projects Agency

dB Decibel, level of noise

DC Direct Current

DEP Distributed Electric Propulsion

EASA European Aviation Safety Administration

EIS Entry Into Service

EPN Effective Perceived Noise

FAA Federal Aviation Administration

FADEC Full Authority Digital Engine Control

FAR Federal Aviation Regulations

FBW Fly-By-Wire

FIKI Flight Into Known Icing

fpm Feet per minute

GA General Aviation

HEAT Hybrid Electric Air Transport

ICAO International Civil Aviation Organization

IFR Instrument Flight Rules

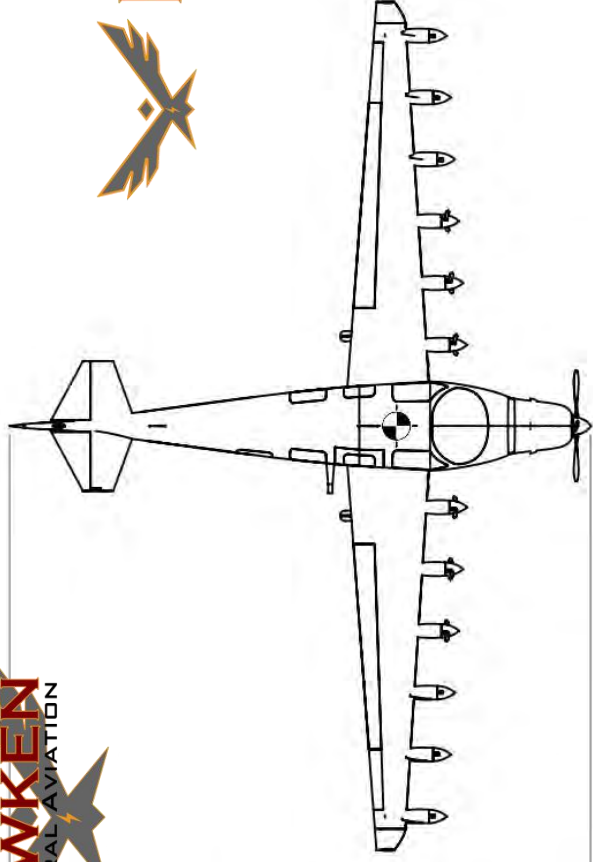
<i>Jet – A</i>	Most common fuel used in commercial aviation
<i>LCC</i>	Life Cycle Cost
<i>Li</i>	Lithium
<i>Li – S</i>	Lithium Sulfur
<i>LiDAR</i>	Light Detection and Ranging
<i>LOPA</i>	Layout of Passenger Arrangement
<i>MFD</i>	Multifunction Flight Display
<i>MLW</i>	Max Landing Weight
<i>MoM</i>	Measures of Merit
<i>MSL</i>	Mean Sea Level
<i>MTOW</i>	Max Take-Off Weight
<i>MZFW</i>	Zero Fuel Weight
<i>NACA</i>	National Aeronautics and Space Administration
<i>NASA</i>	National Aeronautics and Space Administration
<i>Ni</i>	Nickel
<i>NMC</i>	Nickel Metal Cadmium, a type of battery chemistry
<i>nmi</i>	Nautical miles
<i>O&M</i>	Operation and Maintenance
<i>PAX</i>	Passenger
<i>PFD</i>	Primary Flight Display
<i>RDT&E</i>	Research, Development, Test & Evaluation
<i>RED</i>	Raikhlin Aircraft Engine Developments
<i>RFP</i>	Request For Proposal
<i>STOL</i>	Short Take-Off and Landing
<i>TBO</i>	Time between overhaul, a measure of maintenance requirements for aircraft parts
<i>TKS</i>	Tecalemit Kilfrost Sheepbridge Stokes
<i>TRL</i>	Technology Readiness Level
<i>VFR</i>	Visual Flight Rules
<i>VLM</i>	Vortex Lattice Method
<i>VSP</i>	Vehicle Sketch Pad, open source software developed by NASA
<i>VTOL</i>	Vertical Take-Off and Landing

1 Executive Summary

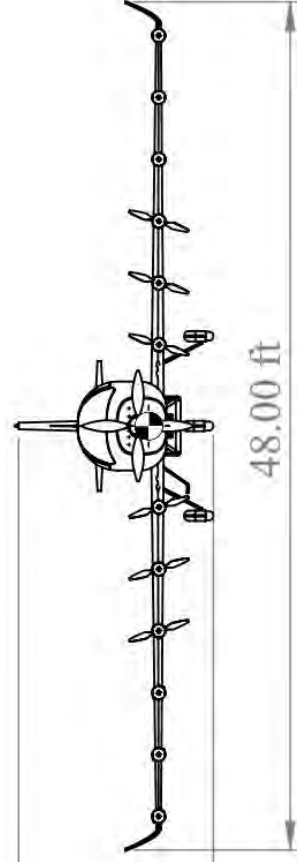
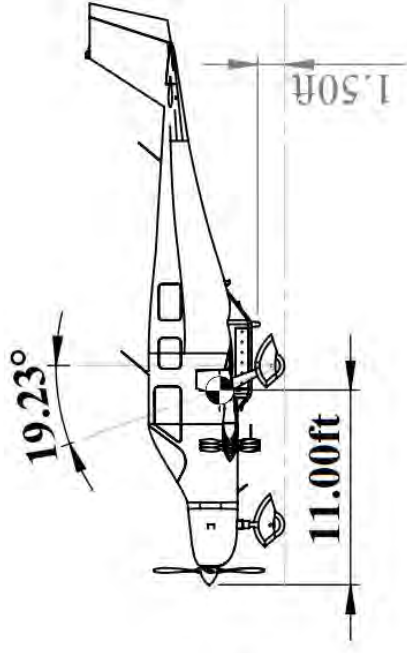
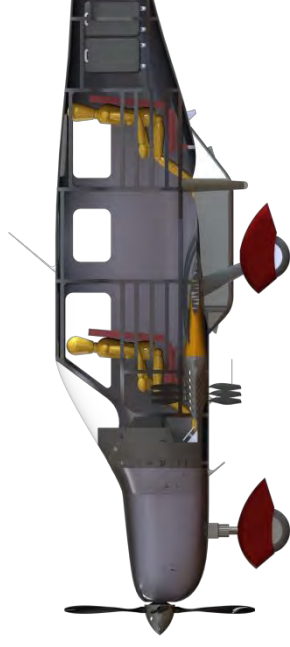
Hawken General Aviation is proud to present the HEAT (Hybrid Electric Air Transport) family aircraft in response to the 2018 AIAA HEGAA RFP. The main tasks set by the RFP were to design a family of hybrid-electric 4 and 6 seat general aviation aircraft, with an air frame and propulsion weight more than 75%. Additionally, there were the following performance requirements: 1500 and 1800 ft sea-level landing and takeoff distances and max payload ranges of 750 and 1000 nmi ranges, for the 4 and 6 seat variants respectively. Meeting these RFP requirements, the 4 seat, Prometheus, and the 6 seat, Zeus were designed with the goals of having competitive acquisition costs and reduced operating costs from the competition. With entry into service dates of 2028 and 2030, the Prometheus and Zeus, respectively, utilize Distributed Electric Propulsion (DEP) and 350 Wh/kg batteries as their hybrid-electric propulsion systems, giving adequate timing for technology certification in general aviation. However, the true benefit to DEP lies in supplementing power to the main engine during takeoff. In doing so, Federal Aviation Regulation stall speeds and RFP takeoff distances can be met with a reduced wing area, reducing drag during cruise. With a reduced wing area of 160 ft², the HEAT family also incorporate a 14.4 aspect ratio, further reducing drag and therefore operational costs. In the 4 seat category for general aviation aircraft, with a 180 knots cruise speed at 17,500 ft, the Prometheus reduces the average fuel cost per flight hour between the Cessna TTX, Cirrus SR22 and SR22T, and the Mooney Acclaim Ultra by 39%. Similarly, in the 6 seat category with a 177 knot cruise speed at 17,500 ft, the Zeus reduces the average fuel cost per flight hour between the Beechcraft Baron, the Piper Matrix, and the Daher TBM-930 by 68%.

As battery energy density improves to 450 Wh/kg in the next 20+ years, the HEAT family take advantage of this trend with an upgradable battery feature. By upgrading to 450 Wh/kg weight batteries, the Prometheus and Zeus payloads of 840 and 1260 lbs will increase by 13% and 11% for the same 1000 and 750 nmi ranges, respectively. In addition to this flexibility, manufacturing and maintenance costs are greatly reduced by exceeding the 75% weight commonality requirement to 94.8%. Such a high weight commonality was achieved using the same airframe and propulsion system with a weight difference from 2 seats, their respective furnishings, mounting supports to the airframe. Meeting all RFP requirements and implementing these design features, the Prometheus and Zeus are priced at \$925K and \$927k, respectively. Comparing this acquisition cost to the average cost of the noted 4 seat competitors, this is a 16% increase. However, the Zeus reduces its acquisition cost from the noted 6 seat competitors' average cost by 58%, giving the HEAT family competitive pricing.

PROMETHEUS



32.83ft

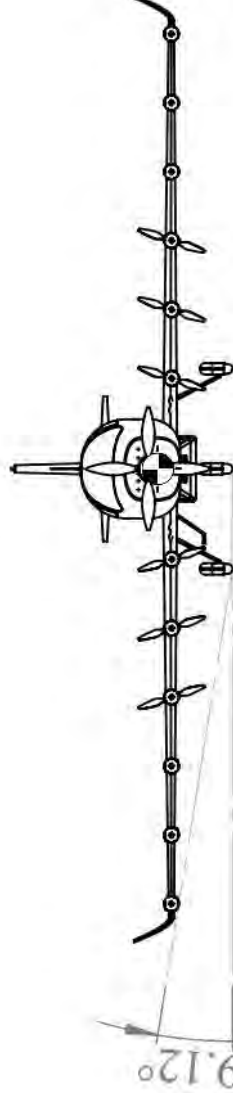
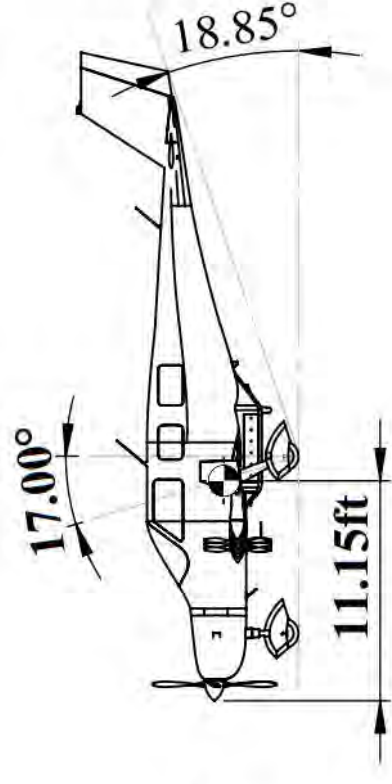
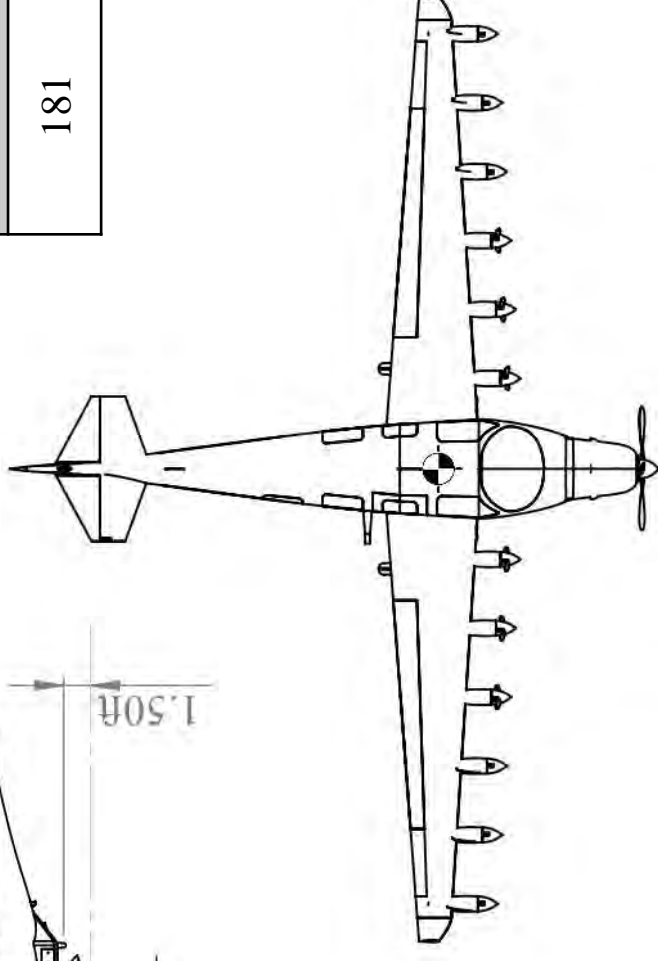
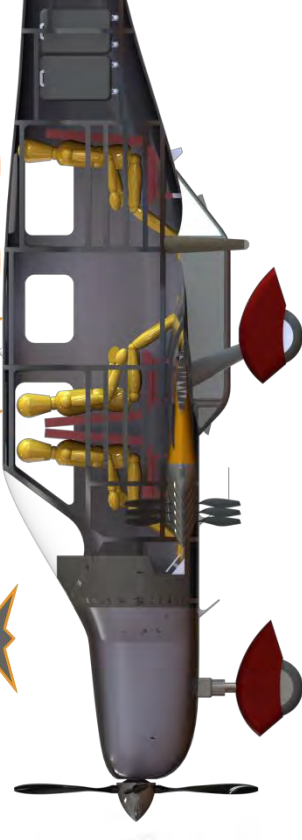


11.01ft

2. 3-Vu Drawings

HEAT FAMILY

Prometheus	Specifications	Zeus
32.5	W/S_{cruise} (psf)	35.6
17.7	W/P_{cruise} (lb/hp)	19.5
4776	MTOW (lb)	5280
319	Battery Weight (lb)	413
181	Cruise Speed (KIAS)	178



Common Specifications	Value
MAC location from nose (ft)	9.70
Tail Moment Arm (ft)	17.5
Cargo Bay Height (ft)	4.82

N.B. Non-bolded dimensions apply to both Prometheus and Zeus. Bolded dimensions are unique to each plane. This applies to CG location and LG to CG angle. Additionally, the outer three DEP propellers retract in at low power to meet tip-over angle requirements

3. Compliance Matrix

RFP Requirements						FAR Requirements				Design Data Requirements			
Description 4/6PAX	Compliance	Pg. #	Description 4/6PAX	Compliance	Pg. #	FAR	Description	Compliance	Pg. #	Description	Value	Pg. #	
Range of 1000/750 nmi	1338/1126 nmi	71	VFR and IFR with an autopilot	Yes	53	23.143	Airplane Must Remain Controllable During All Stages of Flight and Between All Stages of Flight	Yes	61	Payload range charts provided	Yes	54	
Max Takeoff Length 1500/1800 ft at Sea Level	870/964 ft	69	Flight in known icing conditions	Yes	50	23.149	Airplane Must Maintain Minimum Control Speed with Inoperative Engine	Yes	16	Mission profile described	Yes	16	
Max Landing Length at 5000 ft	1450/1620 ft	69	Takeoff and landing from dirt, grass, metal mat, gravel, asphalt, and concrete runways	Yes	49	23.2200	Flight Envelope Determined with Proper Load Limits	Yes	46	V-n diagrams including gust loads	Yes	46	
Climb Rate 1500/1300 fpm	1300/1500 fpm	16	Hybrid flight for takeoff, climb, go-around, and emergencies	Yes	16	23.2105	Pilot Must be of Average Skill to Operate the Airplane	Yes	53/64	Material selection for main structural groups	Yes	39	
Cruise Speed \geq 174 KIAS	180/177 KIAS	17	Production rate of 4-10 aircraft per month supported by brief market analysis	10	75	23.2230	Determine Structural Limit Loads and Ultimate Loads to a Factor of Safety of 1.5	Yes	42	Graphical flight envelope	Yes	46	
Commonality by Weight \geq 75%	94.8%	59	15% profit margin	Yes	75	23.2235	Structure Must be Able to Support Both Limit and Ultimate Loads	Yes	42	Geometric and dimensioned aircraft descriptions	Yes	2	
EIS for 4 and 6 PAX	2028/2030	76	Visually Appealing	Yes	14	23.2270	Airplane Must be Designed to Provide Occupant Protection in Case of an Emergency Landing	Yes	22	Aerodynamic performance and characteristic provide	Yes	25	
Autonomous Architecture	Yes	55	Aircraft reliability equal to or better than that of comparable aircraft	Yes	72	23.2315	Emergency Exits Must be Labeled Inside and Outside, Easily Opened, and Easily Accessible	Yes	22	Aircraft weight statement	Yes	59	
Emergency range at 5000 ft	32/34 nmi	17	Maintenance equal to or better than that of comparable aircraft	Yes	72	23.2320	Occupants Provided with Breathable Air Pressure	Yes	50	Center of Gravity envelope provided	Yes	58	
16/24 ft ³ cargo volume	16/24 ft ³	24	Climb, one engine inoperable (FAR 23.67)	Yes	16	23.2415	Power Plant Must be Protected from Ice	Yes	50	Description of propulsion system	Yes	31	
120/180 lb cargo weight	120/180 lb	59								Summary of basic stability characteristics	Yes	64/65	
										Summary of cost estimates	Yes	75/77	
										Business case analysis	Yes	5	
										Aircraft performance summary	Yes	69	

4 RFP Interpretation

4.1 Genesis of the Problem

In the field of aviation one statement is universally true, traditionally designed combustion engines are inherently inefficient for the majority of a normal flight profile. The greatest power required for flight occurs in the smallest portions of the overall mission: takeoff, climb, and go-around. For this reason, commercial and general aviation aircraft have engines that are oversized for the power required for the longest portion of flight, cruise. With recent advancements in hybrid power technologies, this fundamental design limitations can be avoided by designing an aircraft with a combustion engine sized solely for cruising flight, and supply the additional power for more demanding phases of flight with electric power, making the aircraft propulsion a hybrid system. A visual representation of this is represented in Figure 1.

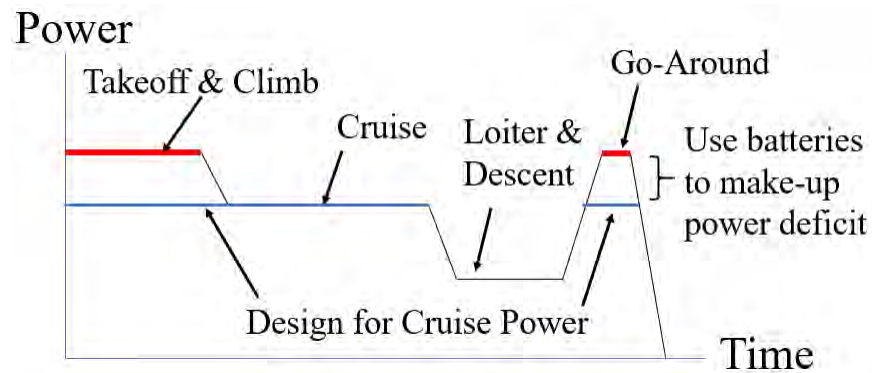


Figure 1: A hybrid electric aircraft's engine can be sized to cruise instead of takeoff or climb (not to scale)

The traditional engine is seen in red and an engine sized for a hybrid approach is seen in blue. Utilizing this revolutionary design approach, fuel is not only saved by capitalizing on the use of electric power from using a hybrid propulsion system, but also in the longest phase of flight, cruise, because a smaller engine will operate at the maximum efficiency point for the entire flight profile.

4.2 RFP Requirements

The AIAA RFP requires a design of a family of 4 seat and 6 seat hybrid-electric general aviation aircraft. The intent is to have sufficient energy storage for takeoff, climb, go-around, and emergencies via electric motors and batteries. An internal combustion engine provides additional power as needed for these specified hybrid portions of the mission.

The designs are required to have 75% commonality by weight to minimize development and manufacturing costs. The requirements are explicitly stated by the RFP and shown in Section 3 Compliance Matrix. Note, the page numbers of this report where the specific requirements are met have been included for the reader's convenience.

In order to make this family of aircraft certifiable by the FAA, the RFP requires compliance with applicable FAA 14 CFR, or Federal Aviation Regulations (FAR) Part 23. Other Parts, such as 67 and 91 were also considered. In December of 2016, many subparts of Part 23 applicable to this RFP were changed from strict requirements to demonstrated capability by the FAA, following the Small Airplane Revitalization Act of 2013. This act promoted innovation by removing several numerical restrictions and replaced them with more abstract goals to give aircraft manufacturers more leeway in aircraft design. Despite the recent change, the original FAR requirements were complied with in this aircraft family's design as they represent many years of aviation experience geared towards the safety of pilots and aircraft alike.

The primary design constraint was the inclusion of a hybrid electric propulsion system. The RFP requirements also dictate the requirement for high-performance specifications that are significantly higher than competitor general aviation aircraft on the market. These will be compared in Section 4.3 Market Research.

4.3 Market Research

Table 1 shows 4 and 6 seat general aviation comparator aircraft specifications. The Daher SOCATA TBM 930 was not listed as a competitor aircraft in the RFP, however, it met the most RFP requirements of any aircraft Hawken analyzed, and thus was added to the table.

Red boxes indicate performance specifications that do not meet RFP requirements. Yellow shows requirements are met, but under specific conditions only (e.g. for specific gross weight). Lastly, green shows RFP requirements that the competitor aircraft meet. Outside of hybrid requirements, the most frequently failed categories are the takeoff, landing, and range requirements. This exemplifies that the RFP performance requirements are unprecedented in the general aviation industry, particularly when measured at each aircraft's MTOW. The most significant metric from this table is the fuel cost per flight hour, shown in the bottom row. Here, a general correlation is evident: as the number of RFP requirements met increases, the fuel cost per flight hour increases. Thus, Hawken identified a market need for high-performance 4 and 6 seat aircraft with low fuel costs per flight hour at a competitive acquisition cost.

Table 1: More RFP requirements met results in increasing fuel costs^{3,6-8,11,13,14,33,45,50,51,68-70}

RFP Requirement	4 PAX General Aviation Aircraft				6 PAX General Aviation Aircraft		
	Cessna TTX	Cirrus SR22	Cirrus SR22T	Mooney Acclaim Ultra	Beechcraft Baron	Piper Matrix	Daher TBM 930
Electric Motor Propulsion	NO	NO	NO	NO	NO	NO	NO
Min Cruise Speed (KIAS): 174	197	170	171	175	190	188	252
Max Cruise Speed (KIAS): 200	235	183	213	242	202	213	330
Climb Rate (fpm)	1,400	1,300	1,203	1,375	1,700**	1,150	1,653
Takeoff Distance of 1500 ft. over 50 ft. Obstacle	1,280	1,594*	2,080	2,100	2,345	2,090	2,380*
Landing Distance of 1500 ft. over 50 ft. Obstacle	2,640	2,344	2,535	2,650	2,490	1,968	2,430*
Cruise Altitude (ft)	25,000	17,500	25,000	16,000	16,000	25,000	31,000
Range (nmi)	450**	900	900	1,275	1,480***	1,343	1,730*
Fuel Cost (per flight hr)	\$85.50	\$81.50	\$100.00	\$115.50	\$190.00	\$165.00	\$363.00

*at MTOW, **With 4 Occupants = 680 lbs, 55% Power, Max Endurance Range, *** based on a ferry mission with 1 pilot at LRC with 45-minute reserve

With a market need identified, and a profit margin set by the RFP, our customer base was identified as pilot owner/operators and businesses in the international market. For example: the Chinese general aviation industry. Between 2009 and 2012, the Aviation Industry Corporation of China (AVIC) bought Cirrus Aircraft, Continental™ Motors, and partnered with Cessna Aviation Co.² Additionally, research conducted in 2012 by the U.S.-China Aviation Cooperation Program forecasted China’s general aviation use for 2015. These results are highlighted in Table 2.⁶⁴ Based upon a 25% growth between 2002 and 2006, a minimum of 25% growth in the business jet category was expected for 2015, revealing China’s growing interest in the industry. By following Kodiak™’s proven business model, Hawken can effectively market to Chinese and American customers, while simultaneously meeting both U.S. and Chinese airworthiness standards. An FAA bilateral agreement allows certification in Chinese markets if the aircraft is certified by the FAA.²⁷ In order to ensure competitiveness in China, Hawken’s carbon-fuel engine will have to utilize Jet-A, since Jet-A fuel and parts are more readily available worldwide, in addition to being far less expensive than AvGas in a global market. With these considerations, Hawken will sell to both the international and U.S. markets, expecting greater profits from around the globe where bilateral agreements exist.

Table 2: China was projected to increase GA use in 2012 by a minimum of 25% by 2015,⁶⁴

GA Segment	Historical Trend	Growth Scenario (Low)	Growth Scenario (High)
Private Jet	China has latent demand of ~400 aircrafts	60 hours per aircraft annually	80 hours per aircraft annually
Training	n/a	5%	10%
Other (business jet, tourism)	25% growth from 2002-2006	25%	35%
Aerial seeding	China aims to increase forest coverage area from 12% to 16% of total land areas	14%	22%
Chemical Spraying	Historical CAGR 1994-2006, or 6%	6%	10%

4.4 Concept of Operations

To make our aircraft competitive with the current market, Hawken identified how the HEAT variants would be used. To bolster customer satisfaction, Hawken envisioned mission flexibility for the pilot, with mission types ranging from business leaders avoiding the hassle and delays of complicated transport to pilots taking their families on an exciting weekend excursion. Mission flexibility is ensured by meeting the following needs:

- Pilot workload to be less than or comparable to competitor aircraft on the ground and in the air, so that the HEAT aircraft will be attractive to pilots with varying levels of experience.
- Make aircraft systems more intuitive for both experienced and inexperienced pilots.
- Allow for easy swap of batteries to exploit future improvements of energy density.

4.5 Measure of Merit and Design Driver

In addition to the constraints set in the Concept of Operations, the RFP specifies a particular design constraint, or a dominant design driver, that affected all of Hawken’s design decisions. This driver was the inclusion of hybrid propulsion system. But, to make this design constraint desirable to the customer, Hawken wanted to make our hybrid aircraft a competitive alternative to carbon engine aircraft. Raymer defines life cycle cost (LCC) as the combination of Research, Development, Test and Evaluation (RDT&E) cost, the flyaway production cost, and Operational and Maintenance (O&M) cost.⁵⁵ Because the last two factors, the measure of merits selected to make Hawken’s aircraft

most desirable to the customer was a reduction in both production (flyaway) and operational costs. The flyaway cost of the aircraft is the price the end user pays, which values the aircraft at its marginal cost. According to the RFP requirements, Hawken must generate 15% profit for cost of the project, which is the total revenue generated minus the production cost of the aircraft. The primary factors that affect the flyaway cost of the aircraft are the complexity of manufacturing and variability required in the tooling and manufacturing process to support different products. Lastly, the O&M costs are the pilot incurred costs of using the aircraft. These include: fuel, batteries, maintenance, and insurance; the most significant, hourly operational cost is the fuel costs to operate the vehicle. Using this as a metric the aircraft design process focused on minimizing the overall LCC of the final design by focusing on lower O&M and flyaway costs.

4.6 Technology

To ensure the feasibility of an EIS date of 2028 and 2030 for the 4 and 6 seat variants, respectively, Hawken plans to implement a technology freeze date of 2024 to allow approximately 2 years for certification before beginning full scale production in 2026. These technologies will allow us to better meet the customer’s needs and desires.

Technology	2017 TRL	2024 Anticipated TRL	Implemented
Distributed Electric Propulsion	7	9	Yes
Brushless Motors	9	9	Yes
High Energy Density Lithium-Ion Batteries	4	9	Yes
Jet-A Turbocharged Piston Engines	8	9	Yes
General Aviation Autonomous Aircraft Systems	2	5	No*

Table 3: By 2024, TRL’s of all utilized technologies are anticipated to increase to feasible levels for GA application with the exception of autonomous flight

To fulfill the RFP’s requirement for hybrid system, Hawken investigated several future and current technologies to ensure the respective entry into service (EIS) dates for the 4 and 6 seat variants could be met. Table 3 compiles the technologies considered with their respective estimated technology readiness level (TRL). The TRL of a technology was approximated by using the NASA diagram shown in Figure 2.²⁸

The first technology studied was Distributed Electric Propulsion (DEP). The DEP system concept relies upon distributing several small propellers across the wing span, causing the wing to see higher local velocities than the free stream flow due to the propeller wash^{42, 43}. This provides several essential benefits to an aircraft. Higher local velocity

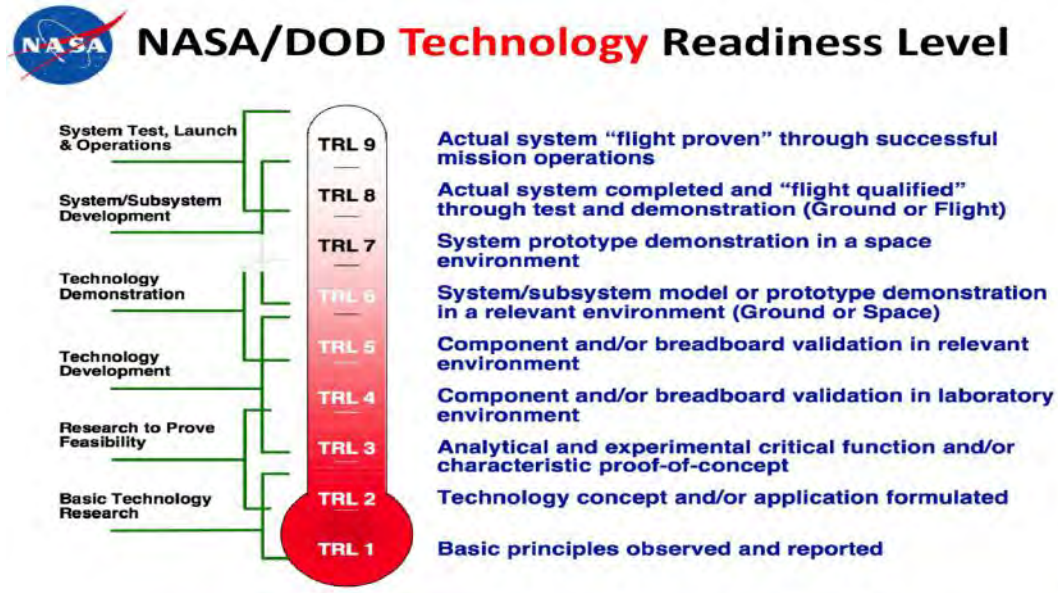


Figure 2: TRLs vary from 1 to 9 based upon a technology's implementation into industry²⁸

results in a higher dynamic pressure, allowing the wing area to be reduced yet still produce the same amount of lift as a larger wing without DEP. A smaller wing also increases both aspect ratio and wing loading. The higher aspect ratio reduces induced drag during cruise. The increased wing loading makes the aircraft less susceptible to displacement from wind gusts, improving overall ride quality for occupants. Additionally, the high-lift capabilities from the use of DEP result in short takeoff and landing performance.⁴³ Lastly, since the propellers utilized in a DEP system are relatively small, they can be easily folded back on the propeller hub to reduce drag when not in use. Figure 3 shows a DEP system that NASA Armstrong is currently testing:²⁹



Figure 3: NASA is currently investigating DEP on a test aircraft called the X-57 Maxwell²⁹

To provide mechanical power to the small propellers, a DEP system uses high power-to-weight ratio motors. In order to research motors applicable for DEP application, Hawken contacted Dr. Pat Jensen of General Electric to

expand Hawken’s understanding of the electric motor and battery market.⁴⁰ Industry experts, including Jensen, suggest that a major breakthrough in motor technology is unlikely to occur in the next decade; today’s high end motors provide good approximations of motor performance 10 years from now.

Table 4: Brushless Motors provide high power to weight ratios, ideal for application in the aerospace industry

Motor	Power (Continuous hp)	Weight (lbs)	hp/lb	Inverter weight (lbs)	Total weight (lbs)	Combined hp/lb
Siemens 260 KW Electric Engine	350	110.2	3.18	66.12	176.32	1.99
EMRAX208 Brushless AC	53	18.8	2.82	11.28	30.08	1.76
EMRAX268 Brushless AC	110	44.75	2.46	26.85	71.61	1.54
EMRAX348 Brushless AC	201.15	88.18	2.28	52.91	141.1	1.43
Joby motors S2	18.77	8.82	2.13	5.29	14.11	1.33
EMRAX228 Brushless AC	55	27.12	2.03	16.27	43.39	1.27
YASA-400 Brushless AC	93.87	52.91	1.77	31.75	84.66	1.11
Protean Drive Motor	72	68	1.06	0	68	1.06
Remy HVH250-115-POC3 Brushless DC	185	125.4	1.48	75.24	200.64	0.92
Sineton A30K016	40.23	34.83	1.15	20.9	55.73	0.72
Thin Gap TG715X	5.4	5.21	1.04	3.13	8.34	0.65

Table 4 presents current high power-to-weight ratio brushless motors available as commercial-off-the-shelf parts. The table accounts for the approximate weight of a motor controller required to convert DC battery power to usable AC power, as well as to control the operation of the motor, which is roughly 60% of the motor’s main weight.⁴⁰

Almost every competitor aircraft’s engine(s) consumes 100/100LL AvGas. According to the online aviation journal *Air Facts*, the use of 100LL AvGas is declining worldwide due to increasing cost and decreasing availability.⁷² Additionally, environmental policy pushes to shift away from the last leaded fuel promote the use of a commonly used alternative to AvGas: Jet-A. Unlike AvGas, Jet-A is readily available worldwide and has a relatively stable cost. In lieu of the disadvantages of AvGas, major GA engine manufacturers such as Continental Motors, Lycoming, and Raikhlin Aircraft Engine Developments (RED) are beginning to produce Jet-A fueled turbocharged piston engines.^{22,30,44} Thus, Hawken plans to implement Jet-A piston technology into the HEAT design.

In order to provide a source of electrical power to the system, Hawken has determined anticipated battery capac-

ity and performance metrics. Market projections of battery performance, including the additional weight of battery management systems (BMS), over the next 10 years for varying battery chemistry can be seen in Figure 4. Hawken obtained this data was obtained from a battery expert, Dr. Pat Jensen.⁴⁰

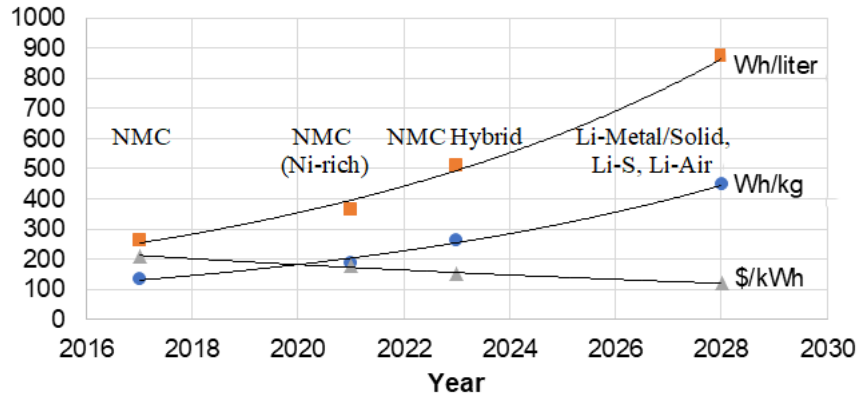


Figure 4: Battery energy density is anticipated to improve at an increasing rate over the next decade

The data in Figure 4 shows an increasing relationship in battery energy density vs time. These estimates are conservative, and will likely increase as the battery industry has historically outperformed market predictions over the last several decades.⁴¹ Thus, Hawken is confident that a 350 Wh/kg battery will be available on the market by 2024. It is worth noting here that battery density includes the density of the battery cell itself, and auxiliary support systems such as battery management system hardware, electronics, and cooling systems. Additionally, the price predictions seen in Figure 4 match the results of a study completed by Carnegie Mellon University in 2014,⁵ as shown in Figure 5. The study suggested that batteries would be priced between \$300/kWh and \$150/kWh by 2024.

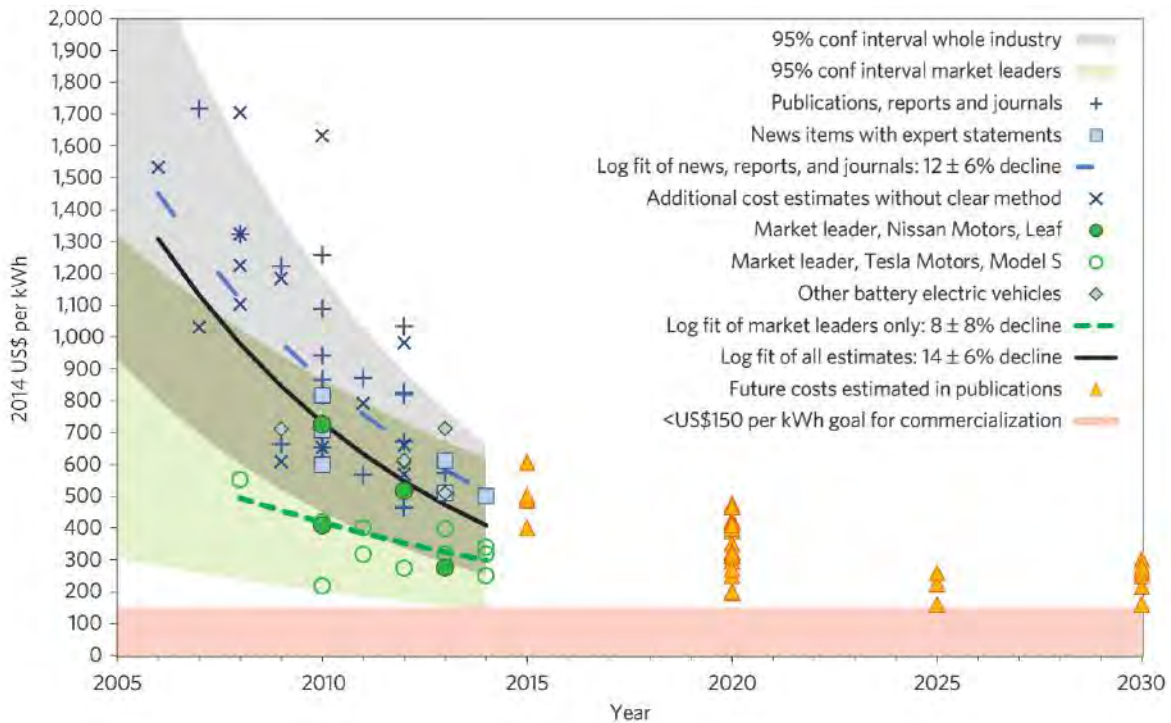


Figure 5: Research suggests lithium-ion battery prices will fall between \$300 and \$150/kWh by 2024⁵

The last technology Hawken researched to meet the RFP requirements was an autonomous system for the HEAT aircraft family. While some level of autonomy has been researched by government agencies like DARPA and NASA in the last few years, very little of that technology has made its way into the General Aviation sector. Levels of autonomy for civil general aviation aircraft have not yet been established; however, SAE automotive vehicle autonomy levels are comparable to a system that could be used to define GA autonomous systems.³⁷ SAE Level 2 autonomy is defined as system steering (changes in flight path) and acceleration/deceleration; these are functions that modern autopilots can already perform. SAE Level 5 autonomy indicates full automation in any environmental conditions, which exceeds current commercial capabilities. Additionally, research indicates that consumers are not expected to trust a fully autonomous aircraft by 2028.^{38,56} Currently, no FAR’s have been proposed to define the certification standards or process for general aviation aircraft autonomous systems. Hence, Hawken elected to design system architecture laying the groundwork for future implementation of autonomous capabilities, rather than incorporating it in the 2028 and 2030 EIS variants.

5 The HEAT Family

5.1 Conceptual Designs

Hawken’s final product, the Hybrid Electric Air Transport (HEAT) family, consists of a 4 seat variant, Prometheus, and 6 seat variant, Zeus. The initial sizing process for the HEAT family began with the preliminary designs, and will be discussed prior to detailed design features and decisions.

5.1.1 Initial Concepts

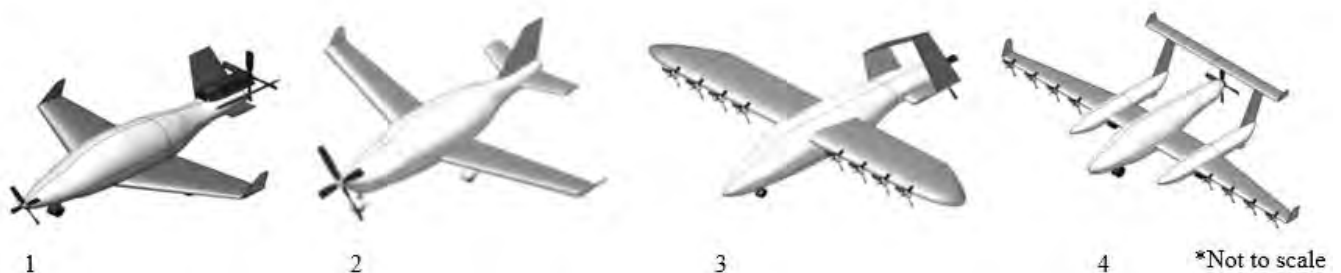


Figure 6: Initial aircraft concepts varied widely to flesh out a multitude of aircraft configurations

Figure 6 shows 4 preliminary design concepts intended to meet RFP requirements; design features from these concepts were iterated and shaped to create the final HEAT family. Each design offered unique solutions to meet the requirements and exemplified design objectives such as comparable maintenance, production and manufacturing costs, and reliability to that of competitor aircraft. The preliminary designs were evaluated with these objectives in mind to produce the best overall design for the customer. The Decision Matrix used in the evaluation is discussed in Section 5.1.2.

During design reviews of the four preliminary design concepts, the Hawken team unanimously determined DEP would be implemented in the final design. Such a hybrid configuration was thought to reap more benefits than either of the other two proposed propulsion systems seen in Figure 6. The justification of DEP’s use is provided in Section 5.6.1 Hybrid Systems Considered.

5.1.2 Pros/Cons Matrix

Table 5: A Pros/Cons matrix allowed Hawken to select the best initial concepts for the final aircraft design

Weighting Factors									
	Weighting Scales	Ability to Integrate with DEP	Stability Characteristics	Weight Reduction	Effect on Drag	Aesthetics	Maintenance Cost	Manufacturing Cost and Ease of Manufacturing	Total Score
Wing Vertical Placement	High	2	4	3	3	3	5	4	32
	Mid	4	4	4	4	3	5	5	39
	Low	4	4	5	4	5	5	5	42
Number of Fuselages	1	5	3	5	5	5	5	5	45
	3	3	5	2	2	3	2	2	24
Main Propeller Orientation	Push	2	4	4	4	3	4	5	34
	Tractor	4	3	5	3	4	5	5	40
Empennage	Diamond Tail	2	2	2	2	3	2	2	19
	V-Tail	3	3	4	3	4	3	3	31
	Conventional	4	4	5	3	4	5	5	40
Planform Shape	H-Tail	3	3	3	3	3	3	3	28
	Elliptical	2	2	4	5	3	3	3	30
	Tapered	5	4	4	3	5	4	4	39

Once the propulsion system was finalized, each of the preliminary designs in Figure 6 were evaluated in the decision matrix, Table 5. Design features were down-selected with weighting factors to best meet the RFP design objectives, the MoMs, and other desirable features. A 1 to 10 scale was applied for each weighting factor, where 1 and 10 were the least and most important factors, respectively. The leftmost column contains the design categories. Each category was determined using the preliminary design features and divided into specific configurations in the adjacent column. For instance, the 'Vertical wing placement' category contained high, mid, and low wing configurations. Design traits were scored on a 2 to 5 scale, ranging from poor to excellent, respectively, for their ability to meet the weighting factor criteria. Each score was normalized by 5 and then multiplied by the weighting scale under each factor.

The low wing configuration produces a pitch-up moment when the DEP system is running, whereas the high wing produces a pitch-down moment, creating difficulty on takeoff. The low wing design only requires a single wing spar, versus two separate spars and additional frame supports for the mid wing configuration. The single spar design of the low wing reduces the aircraft weight. In the fuselage category, a triple fuselage design was considered for extra storage of batteries and seat cargo. However, it was determined the space for the DEP motors on the wing leading edges would be limited, preventing the aircraft from using the optimal number of motors to keep minimize operating cost. Additionally, a single body fuselage has lower wetted area, decreasing parasite drag and production costs associated with fewer components and material. The reduction in drag causes a decrease in operating cost. These reasons render the low-wing configuration as the best suited design for the HEAT family.

Two propeller orientations were considered: push and tractor propellers. Due to turbulent flow in the DEP wake, it is more advantageous to keep the main propeller out of the wake to increase fatigue life, resulting in lower maintenance costs. The prop wash of the preferred tractor orientation will interfere with the inboard-most DEP propellers, but will have less fatigue effect on the DEP propellers considering their relative sizes. Varying propeller orientation in the preliminary designs resulted in different empennage configurations. To best meet customer needs and desires, the conventional tail was selected over T-tail, H-tail, and diamond tail configurations for its overall simplicity of control surface systems, low structural weight, reduced wetted area, and standard maintenance for conventional control surface configurations. Additionally, other configurations have significant safety issues, such as T-tail deep stall and locked-in deep stall problems at high angles of attack.

Finally, the planform shape of the wing was considered. While the elliptical wing is said to produce an elliptical

spanload, these aerodynamic benefits would be lost due to the physical interference from the DEP system nacelle structures. Additionally, an elliptical wing requires increased manufacturing requirements than other more simple geometries due to its complex shape, increasing production costs. A tapered wing was selected for simple integration with DEP and for its simplified manufacturing processes.

5.2 Mission Profile

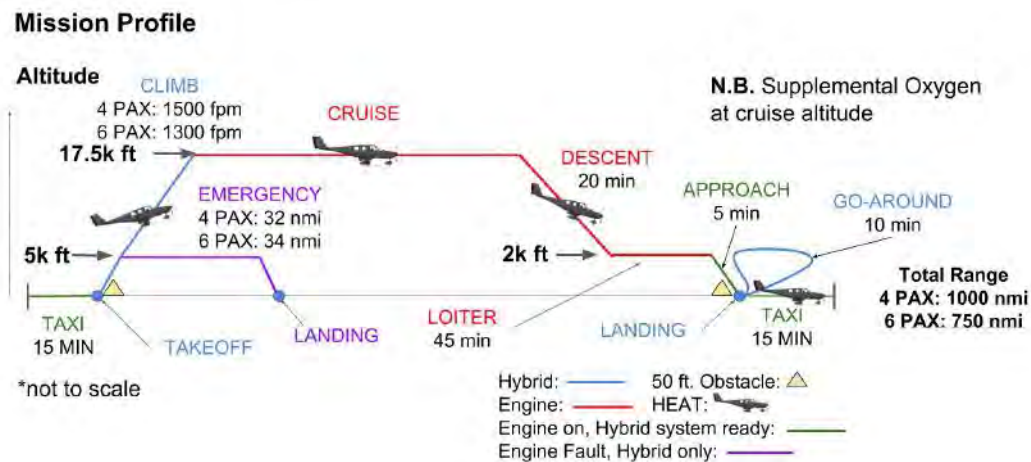


Figure 7: Hybrid propulsion allows for the HEAT family to meet RFP specified take-off and climb requirements, as well as extend an aircraft's emergency range at 5000 ft. altitude

Figure 7 shows a mission profile which conforms to the RFP requirements. The RFP specifies that the electric propulsion component of the hybrid system be used during takeoff, climb, and go-around. During engine-only phases, indicated by red segments, the DEP propellers will not be running and are folded back to reduce drag, minimizing operational cost. However, for the approach phase, the DEP propellers will be opened for stand-by in the event a full-power go-around is necessary. In preparation for a go-around upon reaching the pilot's final destination, the engine can trickle charge the batteries using an alternator, with a negligible effect on main engine performance. Additionally, the DEP system is able to provide reverse thrust after touchdown when landing to decrease landing distance. This phase of the mission is shown with green segments. The primary source of power during takeoff and climb is provided by the DEP to decrease fossil fuel consumption and operational costs. To satisfy the RFP requirement for engine failure at 5000 ft, the DEP system can fly Prometheus and Zeus 32 and 34 nmi, respectively, for an emergency landing; due to a high lift-to-drag ratio, the emergency range increases with altitude. With these battery-only emergency ranges, the pilot will have ample range to divert to another airport in the event of an in-flight emergency.

Prior to takeoff, preparing the aircraft for flight is necessary. One critical aspect of preflighting is charging the batteries. Charging can occur both on the ground and in the air. On the ground, it will take approximately 19-24 minutes using a 300 amp, 450V charging station or 9-11 hours using a 40 amp, 120V wall outlet.⁴⁰ For reference, modern day Tesla supercharging stations output 250 amps at 400V.⁵⁷ Although wall outlets are more readily available today, the increase in popularity of hybrid-electric and electric vehicles is paving the way for charging station infrastructure. Hawken envisions TeslaTM-style charging stations that could become commonplace in general aviation aircraft hangars. Thus, for faster recharge times, the HEAT family will use these charging stations.

By flying closer to the minimum cruise speed of 174 KIAS required by the RFP, it allowed a smaller, 6-cylinder engine to be used, increasing fuel efficiency and thus reducing fuel consumption. The 4 seat Prometheus and 6 seat Zeus variants cruise at average speeds of 181.5 KIAS and 178.5, respectively, exceeding the minimum cruise speed requirement while still flying at the optimal efficiency of the main engine. The angles of attack during cruise are -0.072° and 0.65° for Prometheus and Zeus respectively.

As previously stated, Hawken plans to market the HEAT family internationally, where Jet-A engines are more common than AvGas engines. Several factors contributed to cruise altitude selection of the Jet-A engine. While increasing cruise altitude reduces drag at a given cruise speed, Hawken wanted to ensure BasicMed pilots can fly the HEAT family, which prohibits pilots from flying in the FL (flight level) altitudes (above 18,000 ft).⁴ The popularity of BasicMed is increasing due to the less restrictive medical-physical requirements; including these pilots maximizes market potential. Furthermore, Jet-A engines have difficulties relighting above 18,000 ft pressure altitude. To keep the pilot's mind at ease, cruise altitudes of 17,500 ft eastbound and 16,500 ft westbound were chosen. This is below the BasicMed limit, but still minimizes drag and provides a slight altitude buffer before relighting difficulties.

5.3 Initial Sizing

5.3.1 Design Space

Given the mission profile from (Figure 7), the power requirements are shown in the design space (Figure 8). Here, the wing area and power required are shown for a given MTOW, meeting RFP takeoff, climb, cruise, and landing requirements, as well as the FAR 61 KIAS stall speed requirement. Assumptions for the constraint diagram in Figure 8 include (i) cruise altitude 17,500 ft pressure altitude, (ii) $C_{Lmax} = 1.7$ without DEP, (iii) aspect ratio (AR) = 14.4, (iv)

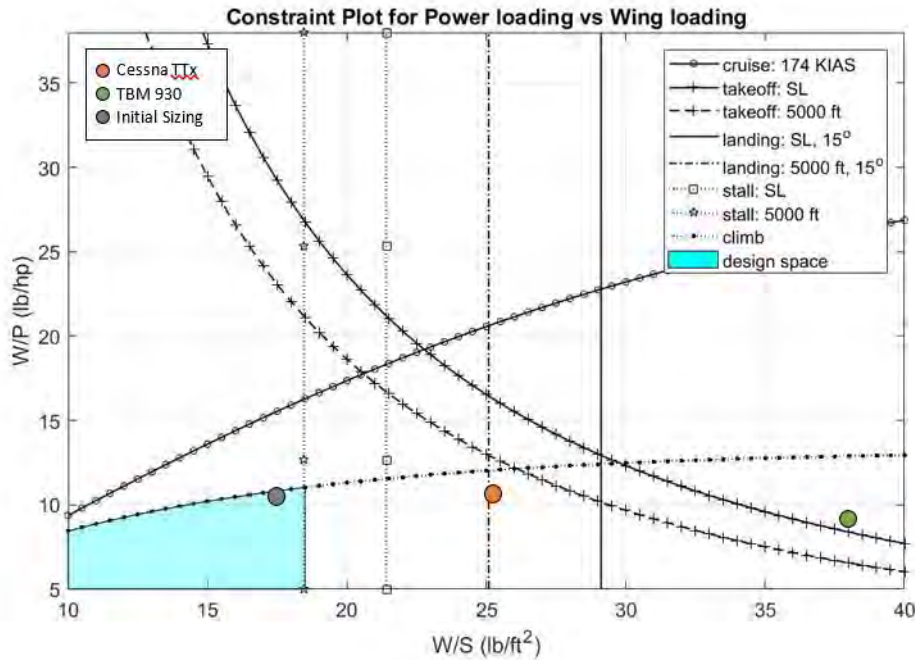


Figure 8: The design space for the HEAT family with the gray dot representing the design point

$CD_0 = 0.03$, (v) span efficiency = 0.8, and (vi) propeller efficiency = 0.9. As stated previously in the mission profile, aiming to meet the 174 KIAS cruise speed allows for a smaller, more economic engine to be used, setting up to reduce the operational costs. Also shown in Figure 8 are several of our competitor aircraft. Neither the Cessna TTx nor the TBM 930 meet the RFP’s requirements nor meet them optimally.^{16,34} The TBM 930 has much more power than necessary and is not even in the design space but meets the most RFP requirements of all our competitors as shown in the Section Market Research 4.3. The Cessna TTx also has more power, while utilizing a smaller wing than the TBM-930, and yet cannot meet all RFP requirements. However, by reducing the power required from these competitors, the HEAT family will save on operational cost.

Hawken identified the design space to be limited by climb requirements and $C_{L_{max}}$. Note, this results in a larger wing area that would not reap the full benefits for DEP. However, as will later be discussed in Section 5.3.2 Max Takeoff Weight Sizing, initial sizing methods are more widely used and accepted for non-hybrid aircraft sizing. Thus an initial, non-hybrid aircraft weight is necessary first before sizing a hybrid aircraft. To then take advantage of DEP, the wing area can be reduced by increasing the $C_{L_{max}}$, moving stall limits to the right in Figure 8. Additionally, the required power of the carbon engine can be reduced to decrease operational costs. The final constraints that will

size the hybrid-DEP system are the minimal wing area for supporting systems to fit in the wing to reduce drag during cruise, a powerful enough Jet-A engine to meet cruise requirements, and a large enough C_{Lmax} . All of these constraints are later elaborated on in the next section. Note, in both cases, both Prometheus and Zeus employed the same design spaces to ensure high weight commonality.

5.3.2 Max Takeoff Weight Sizing

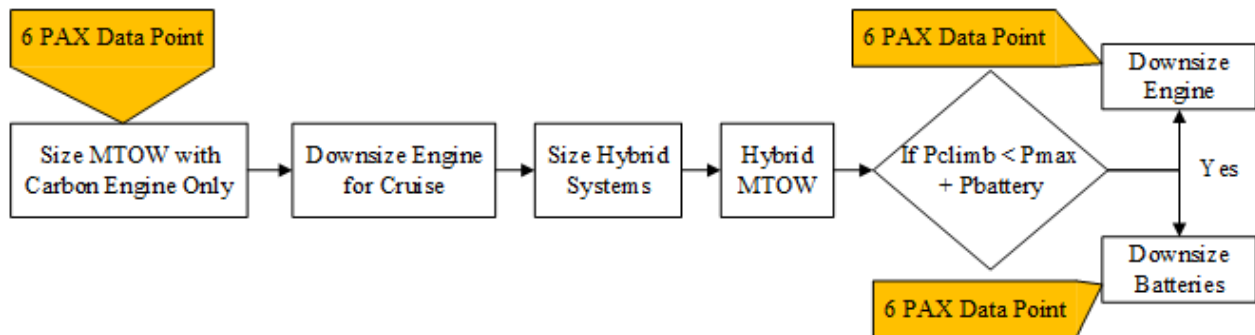


Figure 9: Hybrid MTOW sized by reducing engine size and adding DEP systems to TBM-930 MTOW estimation (meeting RFP requirements)

For initial Max Takeoff Weight (MTOW) estimation of a hybrid aircraft, conventional methods do not account for the constant weight of batteries during flight. Therefore, Hawken developed a process shown in Figure 9 to estimate MTOW of a hybrid electric aircraft. The TBM-930, an aircraft which met the most RFP requirements, was used to provide a starting point for the MTOW estimation process. This heavy aircraft provided an overestimate of MTOW, allowing for addition of a hybrid system to downsizing the MTOW estimate.

As previously seen in the market research, no competitor aircraft meet all RFP requirements. However, in the 6 seat category, the Daher TBM-930 is the closest competitor with respect to meeting but still exceeding some RFP requirements. Because the TBM-930 exceeds cruise speed, range, and climb rate requirements, using its parameters would give an overestimate of MTOW. This overestimate was found with the process described in Raymer,¹⁵ using the TBM-930's BSFC (0.583 lb/(hp*hr)) at 18,000 ft (with cruise speed of 284 KIAS¹). Additional assumptions provided by Raymer included: fuel fractions show in Table 6, an $(L/D)_{max}$ of 12 (an average for fixed gear propeller aircraft), a cruise L/D equal to $(L/D)_{max}$ and loiter L/D equal to 86.6% of $(L/D)_{max}$, and an ideal propeller efficiency of 0.9. When calculating the fuel weight's percentage of MTOW, total fuel weight also accounted for 1% of fuel trapped and 5% left in reserves. To ensure the accuracy of the MTOW estimate, competitor aircraft empty weights and MTOW's were

used to create the trendline shown in Figure 10. Thus with these assumptions and the TBM’s engine parameters, an oversized MTOW for a carbon engine was produced.

Table 6: Fuel fractions accurately account for fuel use of a carbon engine-only aircraft

	Warm-up/ Takeoff	Climb	Descent	Go-Around
After/Before Weight Ratio	.97	.985	.99	.99

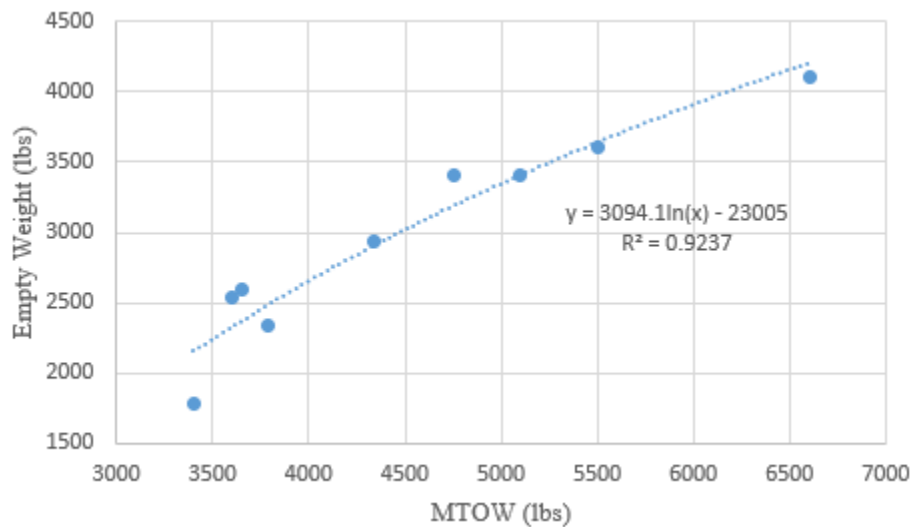


Figure 10: Empty weight trend line determined from 6 seat aircraft empty weights

Using the design space in Figure 8, power and wing loading requirements were estimated as: a W/S of 11 with cruise and climb W/P values of 11 and 17, respectively. Note, to keep weight commonality between the variants $\geq 75\%$, the 6 seat, Zeus, was sized to meet the climb power requirements of the 4 seat, Prometheus, so that the same engine and airframe could be used between the variants. To reduce the acquisition and operating costs from the overestimated MTOW, the engine weight had to be reduced to meet and not exceed RFP requirements. Downsizing from the TBM-930’s turboshaft to a smaller power, JetA RED A03 engine, the power deficit ($P_{\text{climb}} - P_{\text{max,engine}}$) was accounted for with a hybrid system. To estimate the hybrid aircraft MTOW, the carbon engine MTOW had its engine and fuel weight replaced with the smaller, JetA engine and required fuel weight (keeping the same payload). Using the previous discussion of batteries in Technology Section 4.6, batteries were sized for their end-of-life charge capacity to ensure the aircraft could still perform as required by the end of its operational life. The final component of the hybrid sizing was adding in the weight required for a DEP system. Using initial research from the X-57 Maxwell program,

12 DEP motors and controllers were used to estimate the hybrid propulsion weight.⁴² 12 motors were selected from initial experimental results in the program showed, for the propeller size, optimal performance with 12 motors for its given span (such details will later be discussed). The motors used by the program were Joby-S2 motors, weighing 9 lbs with controller weighing an additional 60% of the motor weights. With these considerations, a preliminary hybrid MTOW was calculated, as shown in Figure 9.

From the constraint plots and this hybrid MTOW, the inequality $P_{climb} < P_{battery} + P_{max,engine}$ was true. Thus, the acquisition and operating cost could further be reduced by downsizing either the engine or batteries. The batteries were downsized in the same manner as before, and a Lycoming IO-720-B1BD was used as the downsized engine design point. While the Lycoming is an AvGas engine and Hawken sought to use only JetA engines, it was used as a trade-off to show if a JetA engine of similar power ratings was made, the trade-off between downsizing the engine once more or the batteries was accounted for. Using these two design points, all non-common weights between the variants were subtracted to ensure high weight commonality. By keeping the same airframe structure and engines between the variants, manufacturing costs could be reduced from a manufacturing process producing different airframes. The non-common weights used to keep the same airframe included fuel, 2 PAX, 2 bags, 2 seats (60 lbs each), and the 6 seat battery weights. Following the same process as the 6 seat sizing, the fuel and battery weights were tabulated to meet the 4 seat mission requirements, providing final estimates for the 4 seat MTOW's.

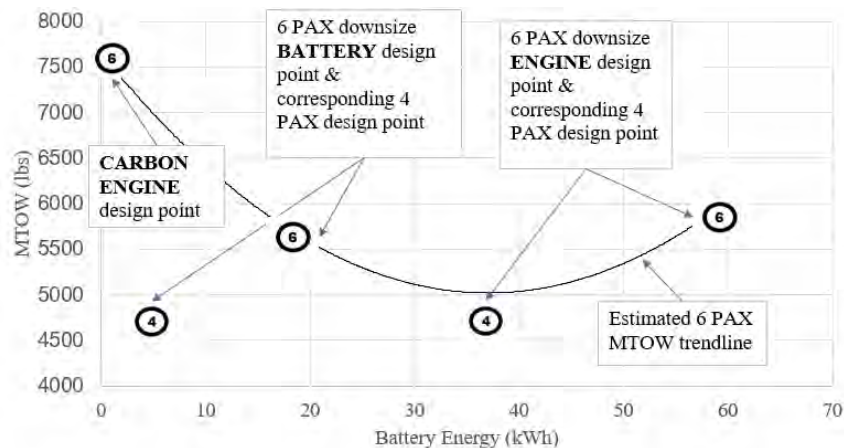


Figure 11: The minimum MTOW was determined to occur with the smallest battery weight

Figure 11 shows the results of this sizing process with MTOW plotted against battery energy required. Two sets of design points are shown: the downsized engine or batteries from the initial, hybrid MTOW with 6 and 4 representing the 6 and 4 seat data points, respectively. For the downsized battery design points, the Prometheus' and Zeus' MTOW's

were 4670 and 5700 lbs, respectively. For the downsized engine design points, the 4 and 6 seat MTOW's were 4680 and 5920 lbs, respectively. As can be seen in Figure 11, there is a minimum in the middle of the trend line. By choosing the smallest MTOW design point (the downsized battery design point), the best sizing estimate was made because it was near a minimum MTOW. With a near-minimum MTOW and using a common airframe between both variants, operational and manufacturing costs were preemptively reduced.

5.4 Configuration and Passenger Layout

Figure 12 shows the final designs from the initial sizing. Just as Prometheus was the Greek titan who first brought fire to man, the Prometheus aircraft will be the entry model into the new hybrid electric general aviation market. The aptly named Zeus shares its name with the Greek god of lightning; Zeus will take to the skies, outperforming the competition with its revolutionary propulsion technology.



Figure 12: Hawken is proud to present the HEAT Family Prometheus and Zeus

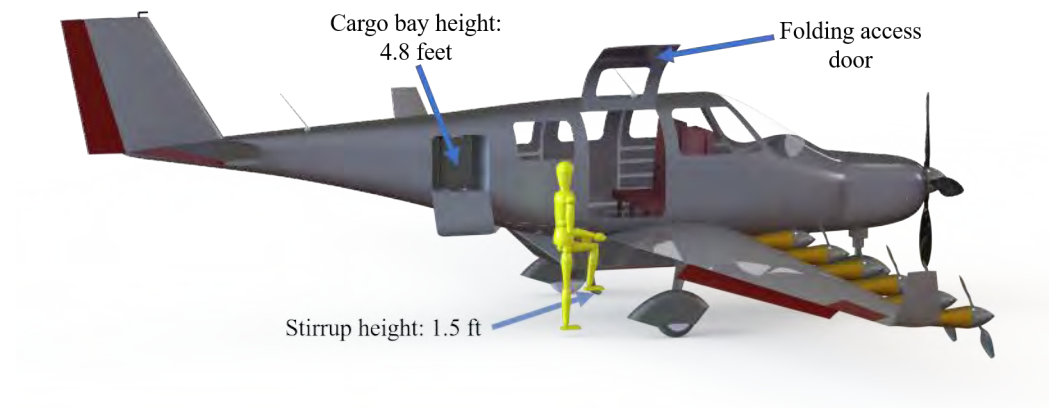


Figure 13: An average human can easily access both the aircraft’s cargo bay as well as the cabin

Aircraft entry and egress is performed by stepping on the wing via the stirrup and opening the main access door (Figure 13). The convenient stirrup is only 1.5 ft above the ground, allowing for comfortable access without the complexities and added weights of a folding staircase. The main cabin door is 3 ft wide and folds upwards, providing occupants plenty of space to climb in. A 10-inch wide aisle allows easy access to all areas of the plane. The back seat is a single double chair that is built into the fuselage. The two middle seats are removed to convert the Zeus into the Prometheus. The seat pitch between the second and third row is 45 inches, giving commercial first-class level legroom to the passengers, shown in Figure 14. At Hawken, pilot and passenger safety is the highest priority. The supporting seat mounts for the middle section of seats in the Prometheus variant are not included. This ensures the pilot cannot enter an area of undetermined CG loading cases if the customer purchases and installs 2 seats in Prometheus’ midsection.

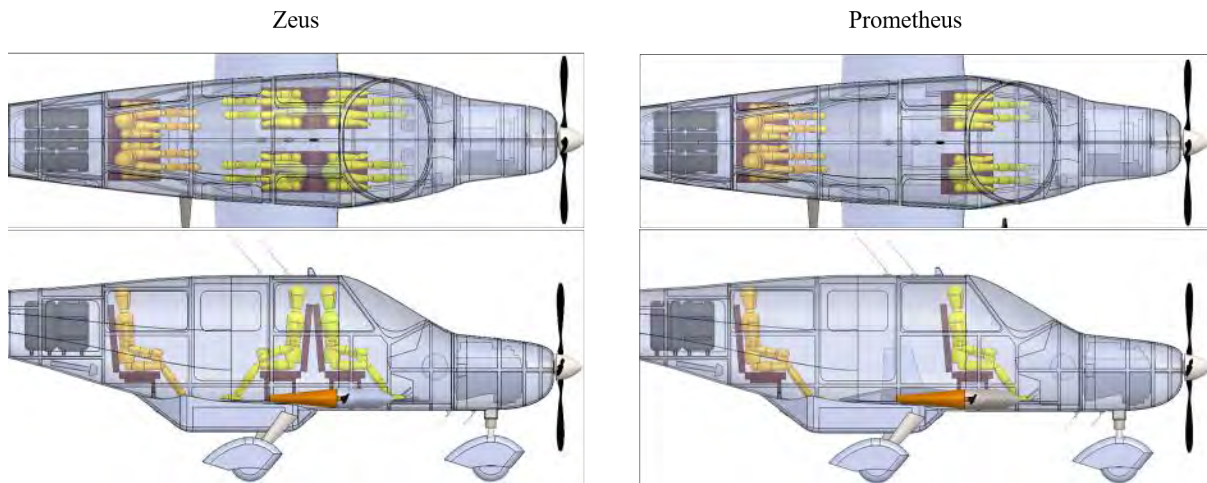


Figure 14: The seat pitch between the second and third row is 45 inches, giving commercial first-class level legroom to the passengers

The fuselage centerline diagrams show cross sections along the plane’s longitudinal axis. Note each human model is six ft tall showing the cabin will be comfortable for a majority of users. There is plenty of headroom and elbow room for all passengers and pilots. These diagrams also show the ample storage space in the cargo bay, shown in Figure 15.

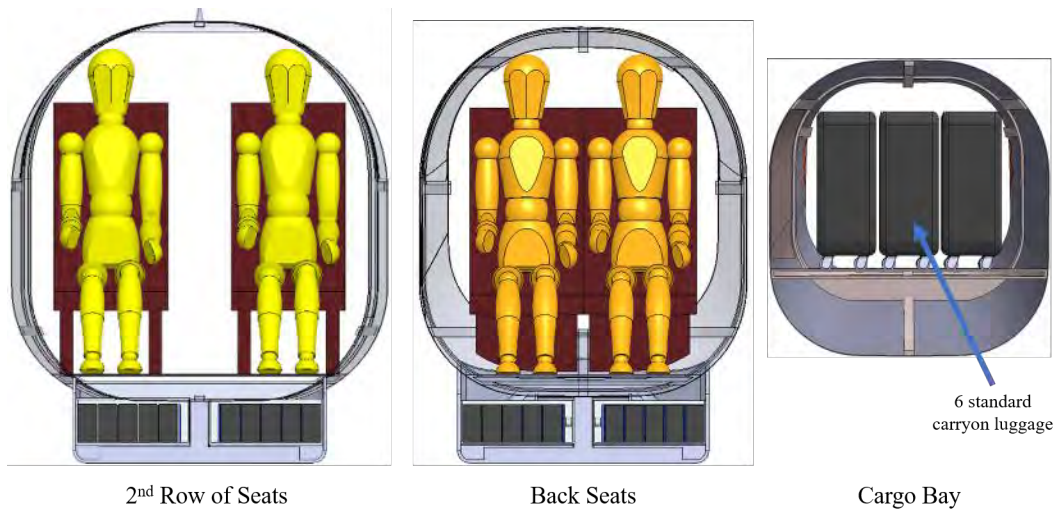


Figure 15: Location of passenger accommodations

The cargo bay is in the rear of the plane behind the back two passengers shown in Figure 16. This space is accessed from the outside by opening the cargo bay which is suspended 4.8 ft off the ground. 6 standard carry-on luggage can be easily stored in the cargo bay with room to spare. Extra storage is located underneath the passenger seats for laptop bags or briefcases. The total space in the cargo area is 23 ft³ and each seat contains an extra cubic foot of storage. The

total storage space adds to 27 ft³ for the Zeus and 25 ft³ for the Prometheus.

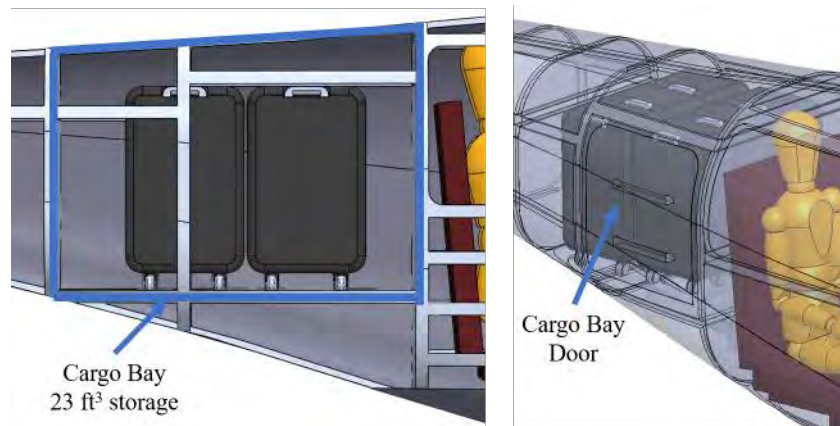


Figure 16: The easily accessible cargo bay provides ample storage for all passengers. Not pictured is a cargo net, which will prevent cargo from moving mid flight and disrupting the balance of the aircraft.

5.5 Aerodynamic Design and Analysis

In order to follow the Hybrid design philosophy established in Section 4.1 Genesis of the Problem, Hawken sized the wing for cruise and determined that the 4 seat Prometheus required a C_L of 0.43 and the 6 seat Zeus required a C_L of 0.5 during cruise.

5.5.1 Wing Design

Using the initial MTOW's for the Prometheus and Zeus, the main priority in the aerodynamic design was to minimize the drag on the aircraft to further reduce operating cost while providing sufficient lift. This goal was achieved by minimizing parasite drag and induced drag from the wing. With these considerations, the HEAT family aircraft were designed for optimal operation at an altitude of 17,500 ft. The 4 seat Prometheus model cruises between 180 and 183 KIAS and the 6 seat Zeus model cruises between 177 and 180 KIAS. Both the 4 seat Prometheus and 6 seat Zeus models share the same fuselage and wing to meet the commonality requirements as stated in the RFP. Knowing that increased aspect ratio would decrease induced drag and a reduced wing surface area would decrease parasitic drag, Hawken sought to maximize AR and minimize area. However, the wing area had to be large enough to fit all necessary components inside, and a span less than 50 ft. was desired to fit inside the Group 1 gatebox for increased flexibility in aircraft storage. Therefore, Hawken chose a wing area of 160 ft² and a span of 48 ft. A view of the wing planform is provided in Figure 17.

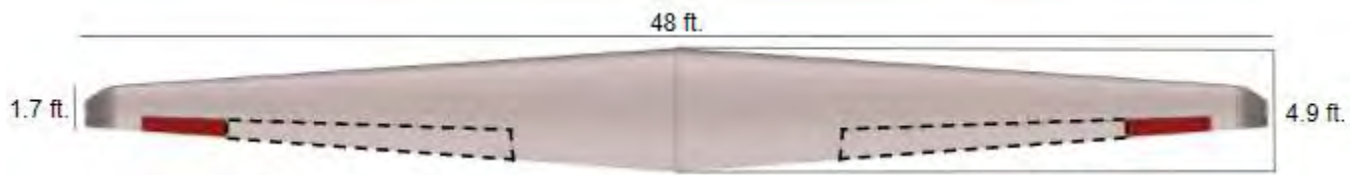


Figure 17: Top view of the wing planform. Split flaps, shown by dotted lines, provide additional lift during take-off and approach

To further reduce drag on the wing and improve aerodynamic efficiency, Hawken investigated the feasibility of using an elliptical wing because of its highly efficient elliptic spanload distribution. Since elliptical wings are difficult to manufacture and would drive up the cost of the aircraft, an alternative shape was selected: tapered wings. Hawken conducted research to determine if there was a taper ratio that could produce similar results to an elliptic wing. A taper ratio of 0.35 creates a nearly elliptical spanload distribution and was chosen for the wing.⁴⁷ As an alternative, the wing could have been twisted to produce an elliptical lift distribution. However, due to the complexity of manufacturing such a twist, whilst increasing weight, this option was quickly dismissed in order to reduce acquisition cost. Note, there is a minimal amount of twist of -0.5° in order to improve stall characteristics at the tip, giving the pilot more of a safety margin before stall. The wing is mounted at 0 degrees on both aircraft. However, the Prometheus model will fly at an angle of attack of -0.1° , and the Zeus model will fly at 0.7° in cruise as a result of their different MTOW values.

5.5.2 Airfoil Selection

After the wing shape was selected, Hawken researched optimal airfoils for distributed electric propulsion aircraft. Using a study describing the airfoil selection process for the X-57 Maxwell DEP aircraft, where three airfoils were examined: GAW-1, GAW-2, and GAW-215.³⁹ Hawken further analyzed these airfoils using XFOIL to determine which would be the most suitable.²⁰ The lift and drag coefficients were obtained for each airfoil over an angle of attack range of -15 to 15 degrees. The lift and drag coefficients were used to create a drag polar for each airfoil, shown below in Figure 18. The GAW-215 airfoil was selected for the wing based on its drag polar. Its drag bucket contains the lift coefficients of 0.43 and 0.50 at an altitude of 17,500 ft for both the 4 seat Prometheus and 6 seat Zeus models, respectively, minimizing the induced drag of the wing during cruise.

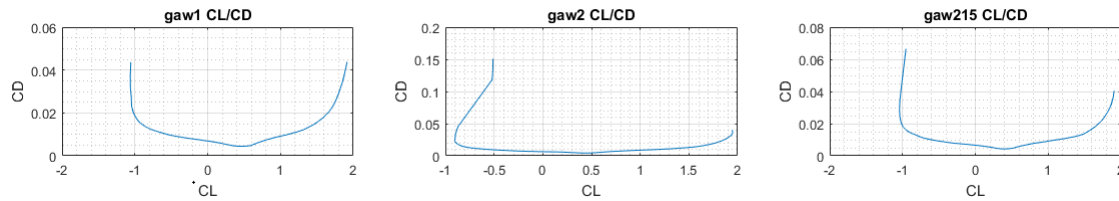


Figure 18: The GAW-215 was selected due to its superior drag polar

The tail airfoil was also designed with emphasis on minimizing drag. Hawken considered two airfoils: the NACA 0009 and NACA 0012. The drag polars for these airfoils are shown in Figure 19. The tail needed to produce a C_L of -0.159 for the Prometheus and -0.068 for the Zeus to meet stability criteria. These lift coefficients required a mounting angle of -1.5 degrees and -0.6 degrees for the Prometheus and Zeus, respectively. The NACA 0012 airfoil was thus selected for the tail because it minimizes drag at these angles.

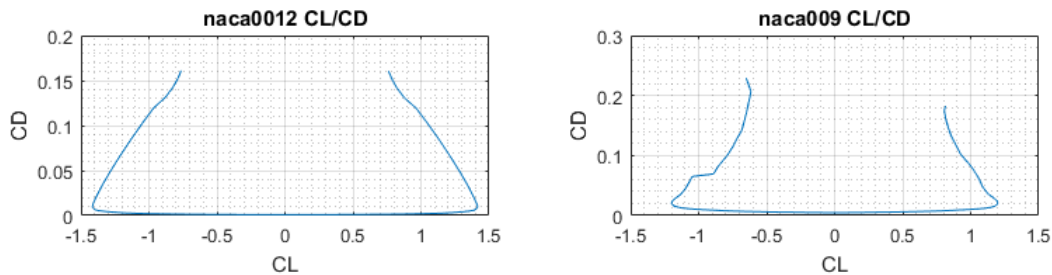


Figure 19: The NACA 0012 was selected due to its drag polar

Takeoff required a total C_L of 2.64 to meet RFP and FAR requirements. The DEP system creates an additional C_L of 0.84. With the wing able to provide a maximum C_L of 1.25, this means a C_L of 0.55 is required by flaps. During landing, the flaps must also produce a C_L of 0.55 because DEP will not be used (otherwise making it difficult for landing). Hawken selected split flaps for their reduced complexity and therefore low maintenance after analyzing other various configurations of flaps. The flaps were sized to be 0.3c long, recommended by Hoerner and Borst,³⁵ and span 11.6 ft of each wing (allowing space for flaperons on the outboard sections of the wing). In order to meet the necessary C_L for takeoff and landing, the flaps must deflect 15 degrees.

5.5.3 Drag Build-Up

In accordance with thrust and drag book-keeping, the drag build-up determined the parasite drag using the exposed area from each component, a method described by Sadraey.⁶⁰ Shown in Table 7 is the parasite drag on each component

Table 7: Total parasite drag for the HEAT family is .0357

Component	C_{D0} of Component	% of Total C_{D0}
Fuselage	0.0061	16.99
Wing	0.0110	30.79
Horizontal Tail	0.0009	2.51
Vertical Tail	0.0007	1.98
Landing Gear	0.0025	7.09
Distributed Propellers	0.0080	22.28
Miscellaneous Components	0.0063	17.58
Trim Drag	0.0003	0.77
Total C_{D0}	0.0357	100.00

and the total parasite drag at cruise conditions, which is 0.0357. For takeoff and landing, the flaps are deflected at 15°, increasing the parasite drag to 0.060.

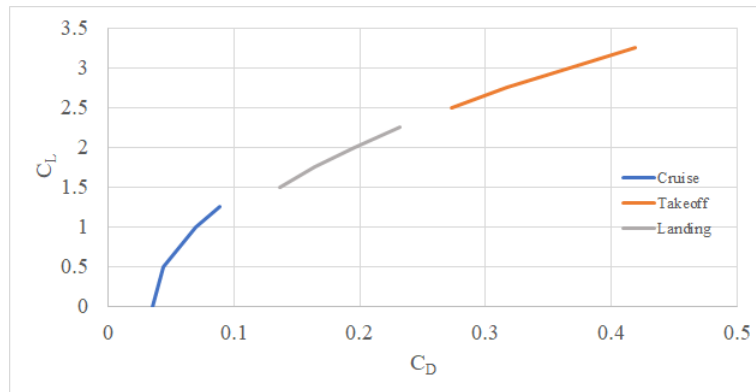


Figure 20: Drag Polar showing Cruise, Takeoff, and Landing Conditions

Figure 20 shows the drag polar for the HEAT Family during cruise, takeoff, and landing conditions. The takeoff and landing drag polars have a different C_{D0} than the cruise condition due to the deflection of the flaps required to produce sufficient lift.

5.5.4 VLM Analysis

Hawken utilized Tornado Vortex Lattice Method (VLM) as well as Siemens Star-CCM+ Computational Fluid Dynamics (CFD) to ensure that the required lift could be produced by the aircraft. Prometheus requires a C_L of 0.43 while the Zeus requires a C_L of 0.5. Both models were analyzed in Tornado VLM, using 5 chordwise panels and 50 spanwise panels, showing convergence and therefore validating the preceding discussion. The values obtained from

Tornado VLM were the C_L , C_{L0} , $C_{L\alpha}$, C_m , C_{m0} , $C_{m\alpha}$, aerodynamic center location, and static margin. These values for both the Prometheus and Zeus models are provided in Table 8 below.

Table 8: Results from Tornado VLM Analysis of wing and empennage

Value	Prometheus	Zeus
C_{L0}	0.444	0.451
$C_{Lcruise}$	0.437	0.515
$C_{L\alpha}$	0.099	0.099
C_{m0}	-0.212	-0.246
$C_{mcruise}$	-0.207	-0.289
$C_{m\alpha}$	-0.068	-0.067

The static margin and neutral point were also calculated in Tornado VLM for both the Prometheus and Zeus variants. While discussed in more detail in Section 5.11 Due to the high commonality by weight of the HEAT family of aircraft, Hawken aimed for a static margin of 15% in order to ensure stability if the static margin was slightly higher or lower. The wing was placed longitudinally on the Zeus model to obtain a 10% static margin. This longitudinal wing placement was kept common between the Zeus and Prometheus models, causing the Prometheus to have a 19% static margin.

5.5.5 CFD Analysis

While Hawken initially ran VLM to rapidly estimate aerodynamic values during the design process, Hawken then utilized Star CCM+ computational fluid dynamics (CFD) analysis to verify the VLM estimates and provide a more detailed model of the aircraft. Specifically, Hawken modeled aircraft body's lift using the models show in Table 9:

Table 9: Hawken CFD analysis used physics models representative of 3D incompressible flow

Physics	Model Type
Space	Three Dimensional
Time	Steady
Material	Gas
Flow	Segregated Flow
Equation of State	Constant Density
Viscous Regime	Turbulent
Reynolds-Averaged Turbulence	Spalart-Allmaras Turbulence

Hawken used the above models due to the fact that our aircraft flies in low-speed, incompressible, 3D flow during cruise. Additionally, Hawken attempted to model the aircraft as close as possible to cruise flow conditions, so a flow field of 65 ft x 65 ft x 885 ft was selected to allow ample space between the walls of the test section and the body of the aircraft.

When running CFD analysis, it is important to ensure that the mesh resolution is fine enough to capture a majority of the flow fields around a body for accurate analysis, but not complex enough to adversely affect computational time. Thus, Hawken set meshes around three primary fields of flow: body surface, near field, and far field. Hawken utilized a target mesh cell size of 0.5 in^3 around the surface of the aircraft, with some cells as fine as 0.08 in^3 . For flow occurring within one aircraft length in front of the plane and two aircraft lengths behind the plane (the near field), cell sizes of 1.8 in^3 were utilized, in order to provide a balance between resolution and computational time. For the far field flow regime, a mesh size of 19 inches^3 was used to decrease computational cost and allow the freestream flow to settle. Figure 21 shows a close-up view of the mesh size of the aircraft wing.

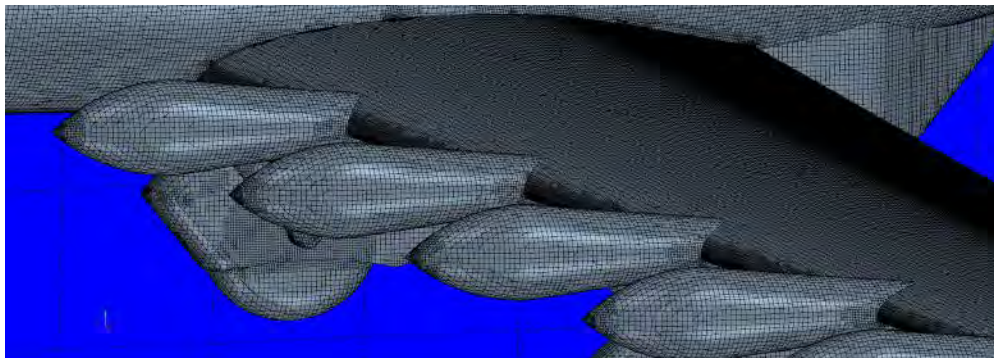


Figure 21: Surface mesh cells varied from 2 in^3 to 0.08 in^3 , with a target size of 0.5 in^3

The aircraft was run at several values of α and allowed time for total simulation convergence (between 1000 to 2000 simulation iterations). The aircraft's C_L with respect to α was then compared to that obtained by a VLM plot, as shown in Figure 22.

Figure 22 shows less than a 1% difference in VLM and CFD at α values less than 10° . This result affirmed the numbers Hawken utilized for earlier design computations and helps to add confidence in our performance predictions.

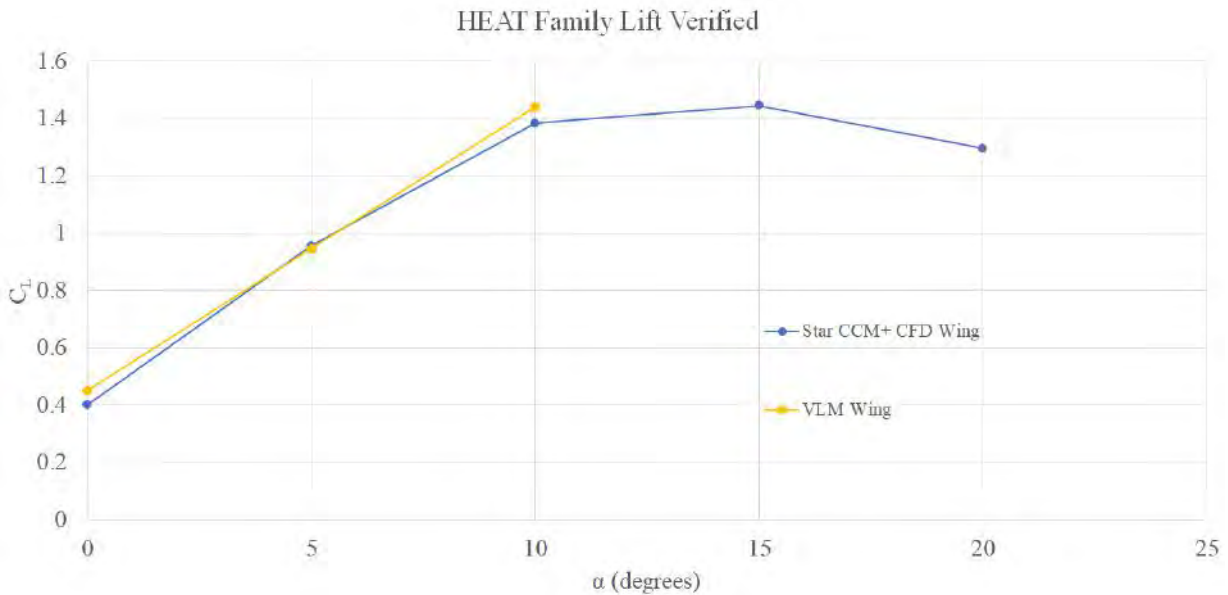


Figure 22: CFD and VLM predictions for lift varied by less than 1% at angles of attack less than 10°

5.6 Propulsion

5.6.1 Hybrid Systems Considered

As referred to in Section 4.1 Genesis of the Problem, a hybrid propulsion system allows for the aircraft’s engine to be sized appropriately for cruise, which is the longest portion of the mission profile. Thus, it makes sense to ensure that a hybrid system remains the most efficient during this extended period of the mission. Team Hawken considered three hybrid propulsion systems, illustrated below in Figure 23 and Table 10:

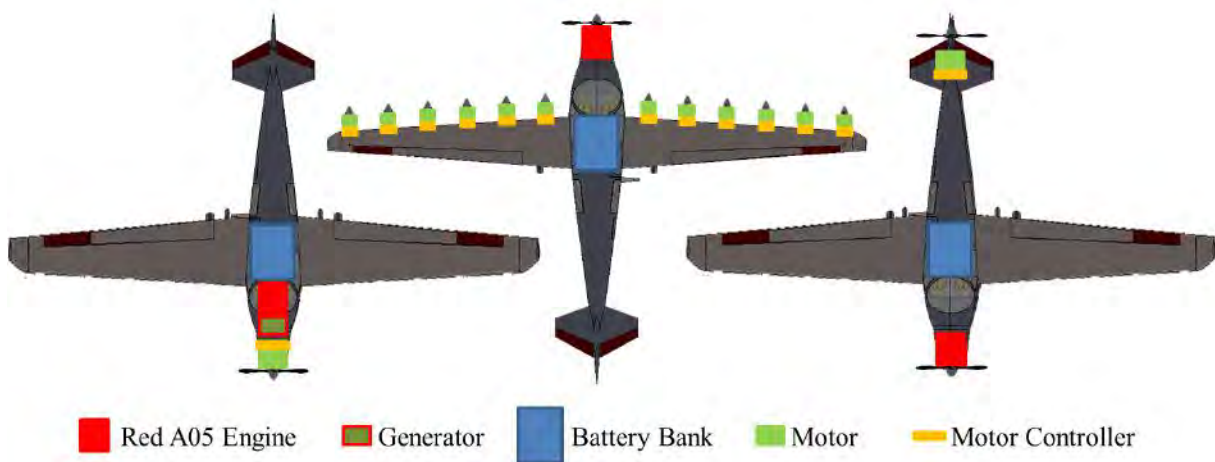


Figure 23: The Hawken team analyzed 3 hybrid propulsion systems

Table 10: The 3 hybrid systems analyzed by Hawken vary by cost, weight, efficiency, and performance

	Single Motor Propulsion	Distributed Electric Propulsion	Dual Engine/Motor Propulsion
Cost	\$215K	\$203K	\$185K
Weight	1012 lbs	1113 lbs	903 lbs
Efficiency	0.210 to 0.214	0.223 to 0.267	0.223 to 0.267
Pros	Simple	+C _L , Efficient, Smaller wing	Lighter, Efficient
Cons	Inefficient, bigger wing	Heavier, more advanced controls	Bigger wing, rear prop integration

Table 10 expresses conservative estimates of propulsion system metrics, based upon Hawken’s market research. Hawken found several important points from this trade study. First, all three hybrid systems were roughly comparable in price given the power requirements for our design. Second, the weights of the three systems were also quite comparable to one-another. A third, key point discovered from this trade study was that converting all of the engine’s power to electrical generation is inherently inefficient, and would result in a 5% reduction in efficiency during cruise. With Hawken’s goal to reduce operation costs, and fuel consumption directly contributing to operational costs, Hawken quickly disqualified this design. The two residual system designs have their internal combustion engines separate from the electric propulsion, thus they are not constrained by additional mechanical and electrical losses along the propulsion train during cruise when the motors are not in use. Ultimately, DEP was chosen from the two remaining designs as Hawken valued the lift performance benefits that the technology could offer over the slightly reduced cost and weight of the dual engine/motor design. Additionally, Hawken noted that the reduction in drag due to the smaller wing would further reduce operational costs.

5.6.2 DEP Sizing

As mentioned earlier in Section 5.5.1 Wing Design, Hawken optimized the wing to be as small as possible for cruise. As a byproduct of this, the small wing could not generate the 5300 lbs of lift required for the 1500 ft. takeoff distance specified by the RFP, so Hawken utilized DEP to increase the aircraft’s lift capabilities. Figure 24 shows the relationship between the flow velocity over the wing and the lift generated by the wing and simple flaps (orange line) as well as wing, flaps, and DEP (maroon line) at takeoff. Knowing that the aircraft wing needed an increase in flow velocity ranging from 50.6 KIAS to 73.8 KIAS, Hawken used actuator disk theory and DEP propeller sizing

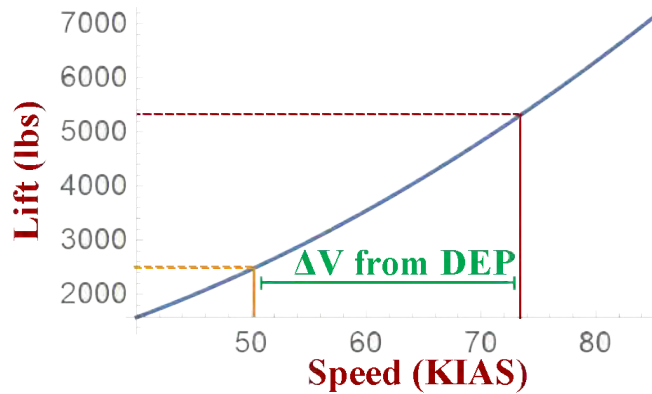


Figure 24: DEP closes the velocity gap required for take-off

methods from Patterson and Derlaga’s NASA technical paper.⁴² From this paper and actuator-disk analysis, Hawken determined that 12 sets of propellers with 3-foot diameters, spaced evenly along the wing, was the configuration required to generate the necessary flow over the wings to increase lift. Figure 25 shows this difference in lift.

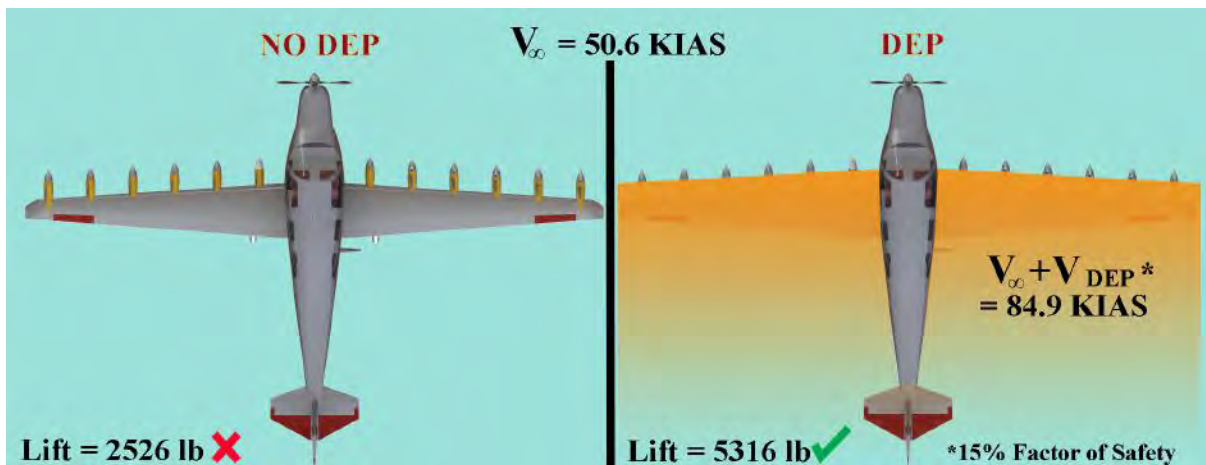


Figure 25: DEP more than double’s the aircraft’s lift capability upon take-off

In addition to the 3 ft propeller diameter, the NASA technical paper recommending placing the propeller blades 1.5 ft in front of the leading edge of the wing.⁴² This served two purposes. Firstly, it allowed for our propellers to fold back upon themselves to reduce drag when not in use. Secondly, it gave the design the largest β value, or equivalent propeller slipstream velocity, possible given the folding propeller constraint. This is due to the fact that a propeller slipstream tends to swirl as well as contract the further it travels from the disk. At a space of 1.5 ft in front of the wing’s leading edge, the slipstream’s axial velocity is 85% that of the velocity immediately after the disk,⁴² so Hawken up-sized the required velocity by 15% from 73.8 KIAS to 84.9 KIAS to account for this.

5.6.3 Hybrid Propulsion System Configuration

In order to increase commonality between the two aircraft in the HEAT family, Hawken sized the propulsion system for the more constraining of the two variants, the Zeus, then used the same propulsion system in the Prometheus. Figure 26 shows the system layout in the aircraft, and Table 11 displays the propulsion system’s key parameters.

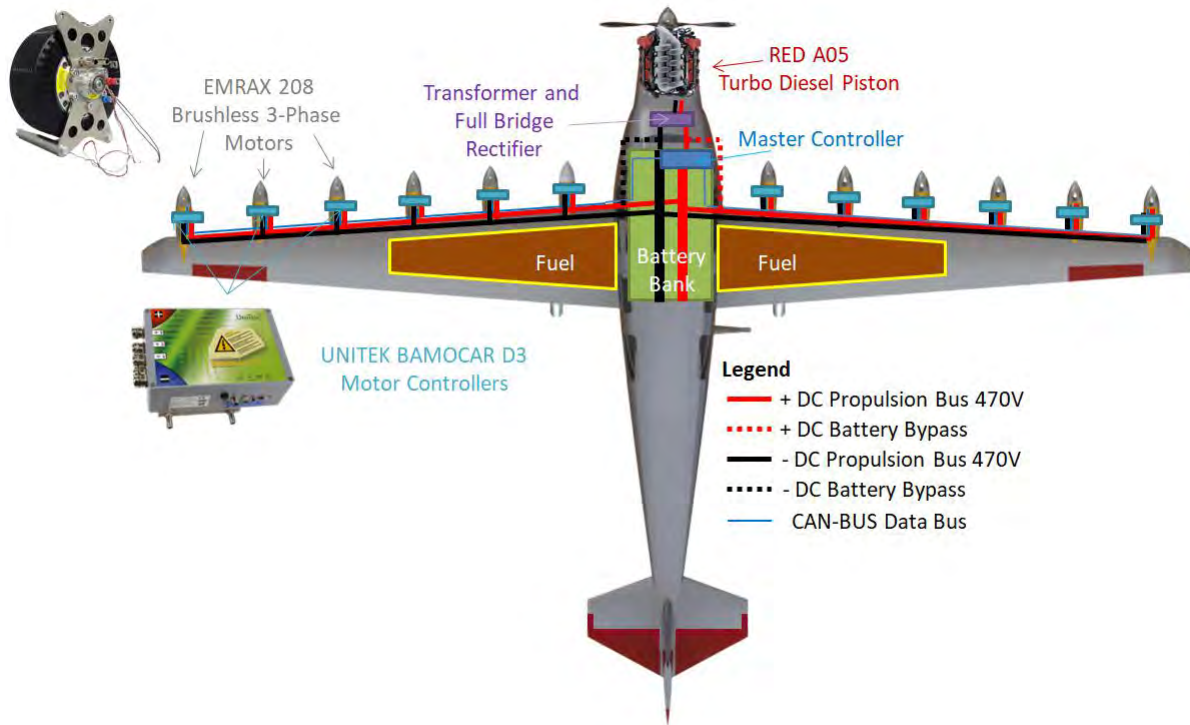


Figure 26: The propulsion system features 12 distributed motors and 1 primary internal combustion engine

Table 11: Hawken’s hybrid electric system’s components are expected to be in service by 2024, with TBO values equal to or greater than current aircraft in the industry

Component	Prometheus (4)	Zeus (6)	TBO	2017 TRL	2024 TRL
Red A05 - Turbo Diesel	270 hp	270 hp	2000 hrs	8	9
Lithium-Sulfur Battery Bank	41.7 kWh	53.9 kWh	~15k cycles	4	8
EMRAX 208mm Brushless 3-Phase Motor (x12)	53 hp (643 hp)	53 hp (643 hp)	15 years	9	9
Folding Propellers (sets)	12	12	2000 hrs	9	9
Propulsion Electrical Bus	DC	DC	15 years	9	9

Engine: Hawken chose a Jet-A/Diesel piston engine with the intent to sell this aircraft family globally. Since traditional AvGas is up to 5 times more expensive per gallon abroad, utilizing an engine that runs on universally available Jet-A will reduce fuel costs for the customer.⁴⁹ Moreover, AvGas is the last leaded fuel and its consumption is decreasing due to its environmental impacts. Hence, its implementation into the HEAT family aircraft design creates risk from both environmental²⁶ and economic perspectives. Thus, Hawken selected the Raikhlín Aircraft Engine Developments A05 turbocharged diesel piston aircraft engine, which is the only diesel engine in its class that met the aircraft’s cruise power requirements of >250hp continuous.^{22,30,44} Table 12 shows the A05’s performance parameters, provided by RED.¹⁸

Table 12: The RED A05 Engine performs well in all phases of flight

Engine Performance Data	Engine Speed RPM	Propeller Torque ft-lb	Shaft Power hp	BSFC lb/hp-hr
Take-off Sea Level	4000	730	300	0.364
Take-off 5000 feet	4000	730	300	0.38
Max continuous FL80	3750	657	270	0.355
Best Economy Sea Level	3500	584	240	0.339

Battery: Next, Hawken selected a lithium-sulfur chemistry for the HEAT family’s batteries. This battery chemistry was analyzed by our team to be the most likely chemistry to be available in 2024 and capable of meeting our 350 Wh/kg requirements, as endorsed by our expert Pat Jensen.⁴⁰ The batteries were designed to provide power exclusively for the propulsion system, and not additional auxiliary systems which are powered by the engine’s alternator. This allows battery weight to reduce by 30 pounds at the expense of roughly 2 knots cruise velocity due to less engine power available. While the batteries were not sized for auxiliary system power, the team implemented a bypass system to provide power to the auxiliary systems in the event of an engine out emergency. Total battery discharge time for both aircraft is 20 minutes, which provides 1 minute of power for take-off, 14 minutes of climb to 17,500 feet, and 5 minutes of residual for 2 go-around attempts. The batteries can also be charged in flight, adding an additional 1 minute of charge time per hour during cruise. The slow charge time was chosen by Hawken in effort to limit the performance impact to the main engine during cruise, and allow the aircraft to cruise about the minimum 174 KIAS threshold set by the RFP. The batteries for both aircraft are contained in a pod underneath the fuselage of the aircraft, shown in Figure 27.

The pod has cowl flaps that open and close to allow air circulation to cool the batteries. These flaps are automated

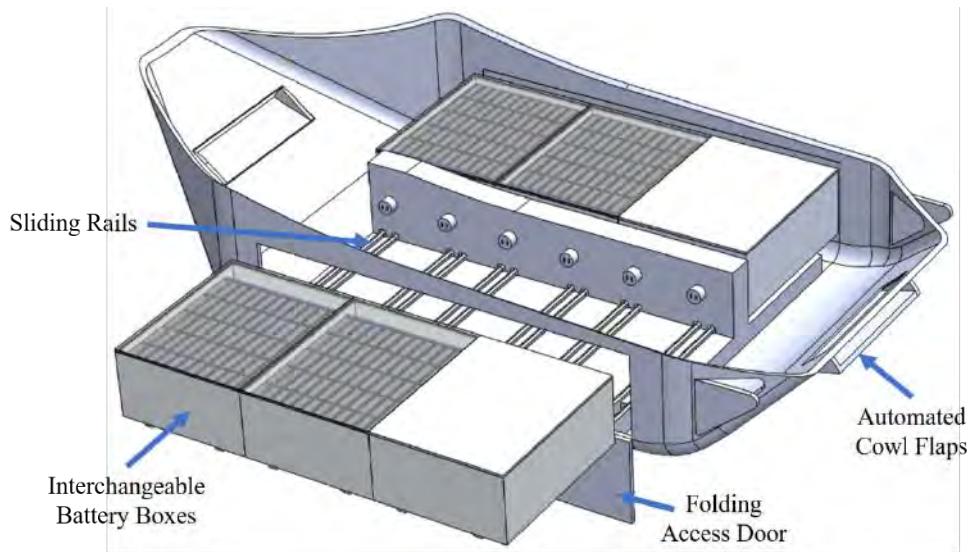


Figure 27: The battery attachment pod allows for easy access, maintenance, and upgrades to the batteries

and actuate based on battery temperature to keep the batteries at an optimal performance temperature of specified by the battery manufacturers, around 70 °F.⁴⁰ But with the HEAT family, the avionics software will be programmed such that the flaps do not open within 10 KIAS of stall speed to keep the pilot safe at low speed performance.

The side doors fold open 180° for easy access to the battery boxes. These boxes slide out on rails and can be interchanged with similar boxes. The top panel can be folded up and the batteries and cooling plates can be removed. The batteries are standard COTS (Commercial Off The Shelf) lithium-sulfur pouch cells that can be switched out (Figure 28). This allows the battery cells to be swapped out when near the end of their life or upgraded when battery density improves. The conduction plates help regulate the battery temperature by siphoning heat from the batteries into the freestream. This further helps to promote optimal battery temperatures during operations and aircraft performance by keeping the cowl flaps open for less time, minimizing the cowl flap drag penalty. The conduction plates can also be electrically heated in cold weather conditions ensuring the battery performance is not hindered by the weather. Two battery management systems are used for redundancy to ensure every cell in the battery pod is at an optimal state during the entire mission. The accessibility of the battery boxes and easy removal of the attachment pod allows for easy maintenance or replacement to ensure no extra workload is added for the pilot, when comparing a non-hybrid and hybrid aircraft.

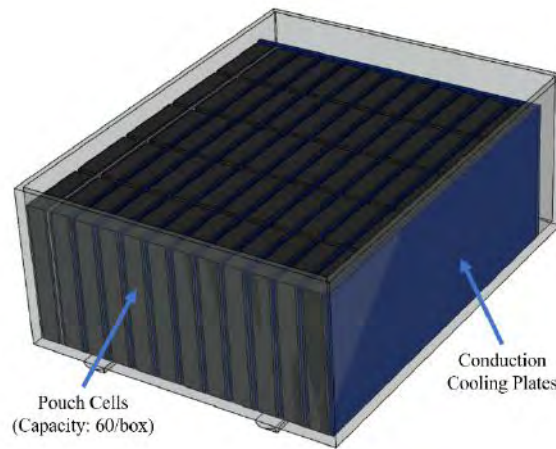


Figure 28: One of the six battery boxes located in the attachment pod

Motors: 12 EMRAX 208mm brushless 3-phase motors power the HEAT family DEP system and provide enough power to achieve the lift for takeoff, allowing for a reduced wing area for cruise. This further reduces drag and decreases fuel consumption. Additionally, these motors had best-in-class power to weight ratios and provided a comparable in-class price per pound of weight. These metrics are illustrated in Table 13.

Table 13: EMRAX 208mm brushless 3-phase motors have the best price per pound

Motor	Power (Continuous hp)	Weight (lbs)	hp/lb	Controller weight (lbs)	Total weight (lbs)	combined hp/lb	Price (\$USD)	Price/Weight (\$USD/lb)
Siemens 260 KW Electric Engine	350	110.2	3.18	66.12	176.32	1.99	50,000	283.58
EMRAX208 Brushless AC	53	18.8	2.82	11.28	30.08	1.76	7440.2	247.35
EMRAX228 Brushless AC	73.15	27.12	2.7	16.27	43.39	1.69	10478.2	241.51
EMRAX268 Brushless AC	110	44.75	2.46	26.85	71.61	1.54	17610.2	245.93
EMRAX348 Brushless AC	201.15	88.18	2.28	52.91	141.1	1.43	Not for sale	N/A
Joby motors S2	18.77	8.82	2.13	5.29	14.11	1.33	Not for sale	N/A
YASA-400 Brushless AC	93.87	52.91	1.77	31.75	84.66	1.11	17,028	201.14
Protean Drive Motor	72	68	1.06	0	68	1.06	15,000	220.59
Remy HVH250-115-POC3 Brushless DC	185	125.4	1.48	75.24	200.64	0.92	36,500	181.92
Sineton A30K016	40.23	34.83	1.15	20.9	55.73	0.72	Not for sale	N/A
Thin Gap TG715X	5.4	5.21	1.04	3.13	8.34	0.65	Not for sale	N/A

*Estimated cost, no easily accessible data for motor or controller

Propellers: The HEAT family uses these motors to drive the DEP propellers during take-off, climb, and go-around, but not for cruise. Thus to reduce drag in cruise, the HEAT family can fold its 3 foot diameter DEP propellers back.

This system is illustrated in Figure 29, showing the deployed and stowed configurations. Note, to reduce acquisition cost of the HEAT family, Hawken believes it will be more efficient to outsource this folding propeller design, with hopes to hit 85% DEP propeller efficiency. Additionally, Hawken will ensure that the folding propeller design has a locking mechanism to allow the propellers the ability to provide thrust in both the forward and reverse direction.

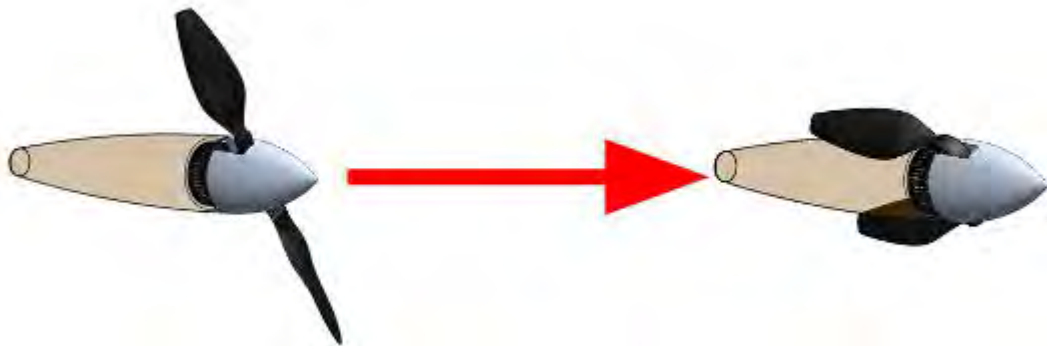


Figure 29: Folding propellers will allow the aircraft to reduce drag when DEP is not in use

For the main tractor propeller of the aircraft, the HEAT family uses a 6 foot diameter constant speed propeller to generate 1200 lbs of static thrust. While a fixed pitch propeller reduces production and maintenance costs by roughly \$20,000 when compared to a constant speed propeller,⁵³⁵² its propeller efficiency can only be optimized for one particular engine setting and flight altitude. Every competitor aircraft listed in the RFP utilizes a constant speed propeller to reap upwards of 85% propeller efficiency in all phases of flight, helping to reduce fuel consumption and decrease operating costs.^{3,6-8,11,13,14,33,45,50,51,68-70} As detailed propeller blade design is out of the scope of a conceptual design, Hawken will work with a propeller blade manufacturer like McCauley to develop an efficient yet economical propeller.

Propulsion Electrical Bus: The last component needed to connect all of these propulsion components is the electrical system. Hawken chose a DC bus for the motor power lines since an AC bus was estimated by Hawken to be up to 5 times heavier due to the excess weight from transformers. It was also determined that an AC bus would induce extra electrical noise in the avionics systems due to signal oscillations. Despite Hawken’s implementation of a lower noise DC propulsion bus, Hawken took extra steps to prevent noise interference from the motors with the avionics systems by isolating the propulsion bus from the avionics bus. In order to minimize weight of the DC propulsion bus, Hawken took guidance from Dr. Pat Jensen of General Electric to individually wire each motor.⁴⁰ It should be noted that

doing this requires different sized wires, as the 100 amp current draw from each EMRAX 208mm motor experiences different wire resistance values over different distances. Sizing was done in accordance to Figure 30 shows the relative sizes of the wire, and Table 14 shows the lengths, weights, and size of each wire run per wing.¹² Hawken computed these values of wire lengths traveling from the battery bank to the motor controllers and back again, adding a 15% factor of safety to account for any additional wire required to bypass the structures in the wing.

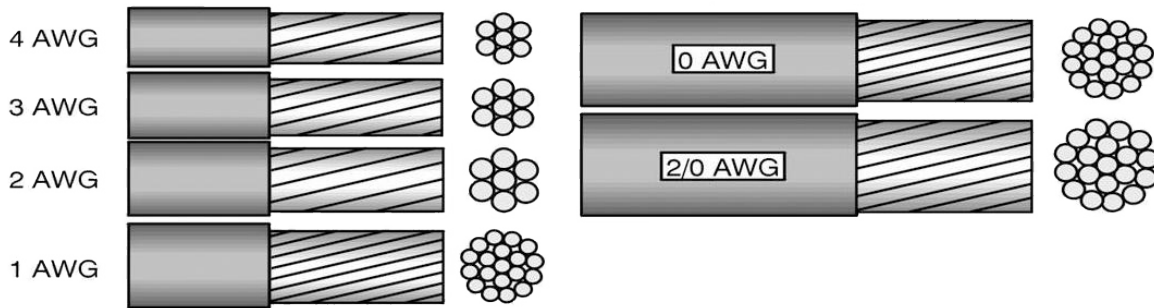


Figure 30: The American Wire Gauge is a standard sizing methods for electrical wires

Table 14: The further the DEP motor on the wing, the larger and heavier the wiring becomes

	Inboard → Outboard						
Motor Number	1	2	3	4	5	6	Totals
American Wire Gauge	4	3	2	1	0	2/0	
Diameter (in)	0.2043	0.2294	0.2576	0.2893	0.3249	0.3648	N/A
Length per wing (ft)	6.5	13.5	20.5	27.5	34.5	41.5	144
Weight per wing (lbs)	0.82	2.71	4.12	6.97	11.02	16.72	42.36

Efficiency: Hawken’s propulsion system is efficient. Table 15 shows how Hawken’s design compares with a traditional aircraft in the major phases of flight.

While Hawken’s hybrid system can be less mechanically efficient than that of a traditional aircraft due to the pilot’s capability to charge batteries in cruise, charged batteries increase mission flexibility and safety by increasing emergency range and go-around time. Should a pilot wish to reap maximum efficiency, he simply would charge the batteries exclusively on the ground and not in cruise, and can achieve identical efficiency’s as that of a traditionally powered aircraft.

Table 15: Hawken’s hybrid propulsion system provides comparative propulsion efficiency to that of a traditionally powered aircraft, but increases mission flexibility and safety by allowing for battery charge in cruise

Component	HAWKEN'S Hybrid Aircraft				Traditional Gas-only Aircraft		
	Takeoff η	Climb/Go-Around η	Charge Batteries in Cruise η	Don't charge in Cruise η	Takeoff η	Climb/Go-Around η	Cruise η
Red A05	0.35	0.35	0.35	0.35	0.3	0.3	0.35
Alternator	N/A	N/A	0.95	N/A	N/A	N/A	N/A
Transformer/Full Bridge Rect.			0.99				
Charge Battery			0.95				
Discharge Battery			0.95				
Electrical Bus	0.99	0.99	N/A	N/A	N/A	N/A	
UNITEK Controller	0.99	0.99					
EMRAX 208 Motors	0.94	0.96					
Propellers	0.85	0.85	0.85	0.85	0.85	0.85	0.85
TOTAL	0.260	0.266	0.267	0.298	0.255	0.255	0.298

5.7 Structural Design and Material Selection

5.7.1 V-n Diagrams

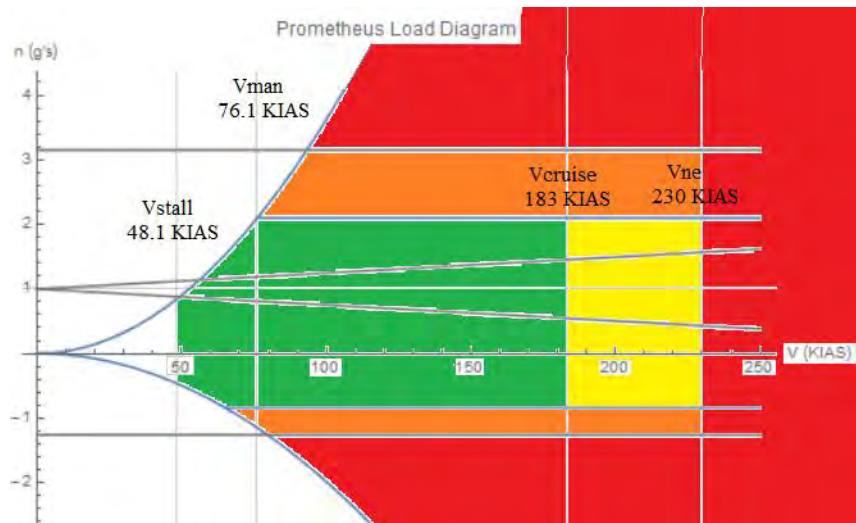


Figure 31: The 4 seat Prometheus’ final loading for the full mission profile

Pictured in Figure 31 is the V-n diagram for the 4 seat Prometheus. It exhibits a stall speed of 48.1 KIAS, a maneuvering speed of 76.1 KIAS, and a cruise speed of 183 KIAS. The 6 seat Zeus V-n diagram may be seen in Figure 32. It features at 50.6 KIAS stall speed, a maneuvering speed of 84.1 KIAS, and a cruise speed of 180 KIAS. It is important to note that both the Zeus and Prometheus have the same dive, and ultimately, never exceed speed: 230 KIAS. This is due to both aircraft sharing the same wing spar for higher weight commonality, which bears the

highest structural loading. The increased weight commonality between the Prometheus and Zeus helps to reduce manufacturing costs due to the necessity of only producing one specific spar.

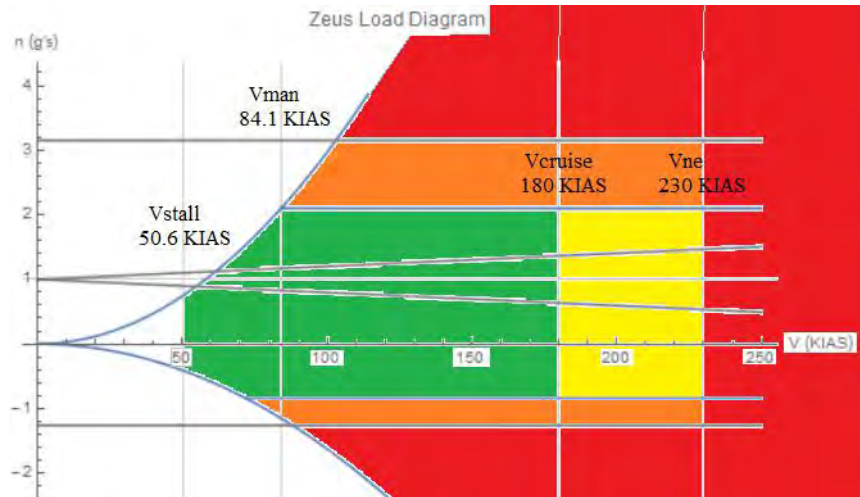


Figure 32: The 6 seat Zeus' final loading for the full mission profile

While the green in the diagrams indicates the flight envelope, the yellow region indicates speeds at which structural failure may occur due to gusts or turbulence. The orange region indicates the flight profile that will begin to cause the structure of the aircraft to yield, and the red indicates the regions at which structural failure will occur.

With the set propulsion system and aerodynamic requirements, the HEAT family have a structure to meet the unique requirements of a high-thrust DEP system as well as all FAR requirements. Several materials were considered for this design and can be seen in Table 16.

5.7.2 Materials Selection

For the wing spar, aluminum alloy 2024-T3 was selected for preliminary analysis and then finalized through trade studies (discussed later in this section). This material was chosen primarily for its light weight, but it also proved to provide sufficient structural stability. This material has high tensile strength with a high fracture toughness and slow crack growth. These qualities will improve the lifespan of the wing spar, further reducing overall maintenance costs through reduced repairs. For the skin, alloy Al 7075-T6 was chosen due to its high tensile modulus and low density.

Both vertical and horizontal tail spars were made of the same materials as the wing, which is Aluminum 2024-T3. This material boasts a higher fracture toughness and slower crack growth in comparison to other aluminum alloys, and meets the budgeted weight requirements. The empennage skin, made out of Al 7075-T6 alloy, proved to be the best

Table 16: Materials and Weights Table for Structurally Designed Components

Materials and Weights Table		
Component	Material	Weight (lbs)
Wing Spar	Al 2024-T3	644.0
Horizontal Tail Spar	Al 2024-T3	15.0
Vertical Tail Spar	Al 2024-T3	9.1
Fuselage	Al 7075-T6	442.0
Main Landing Gear	Al 7075-T6	140.0
Nose Landing Gear	Al 7075-T6	97.0
Wing and Tail Skin	Al 7075-T6	162.2

material choice for its low density and high tensile modulus.

The fuselage longerons and skin were manufactured out of the Aluminum 7075-T6 alloy for its high tensile modulus. The skin of the fuselage was chosen to be Aluminum 2024-T3 for good fatigue life, balanced tensile strength, and high fracture toughness. Like the longerons, the fuselage frames were made of Aluminum 7075-T6. This allowed for the higher stress frames, such as those near the windows or doors, to be better reinforced in their structure, securing the integrity and safety of the flight.

To save on weight, the thinnest skin thickness for these selected materials was desired. Comparing the skin thicknesses for transport aircraft recommended by Niu⁴⁸ and Nicolai,⁴⁶ a common, minimal skin thickness was found to be 0.1 inch thick aluminum alloy's. Thus, skin thickness is minimized using common aviation design practices.

When Hawken designed the structure, we designed to an individual owner-operator and not a corporation with financial capabilities for a repair infrastructure. With this in mind, it was decided by using an alloyed material or metal rather than a composite, one is able to save on the expensive repair costs that result from composite materials. While required infrequently, composite material repairs are typically very expensive compared to the cost of repairs of metal alloys.³¹ The use of common metals in our design benefits the consumer since his or her local airport will likely have a maintenance facility with experienced, metalworking mechanics at a cheaper rate than going to a commercial aircraft composite repair facility. Furthermore, using lighter materials such as aluminum and titanium alloys still allowed the

HEAT family to finish with acceptable MTOW's as discussed the Weights section 5.10.

With the material selection summarized above, the trade studies to support these decisions will be discussed, starting with the wing's material selection and design.

5.7.3 Wing

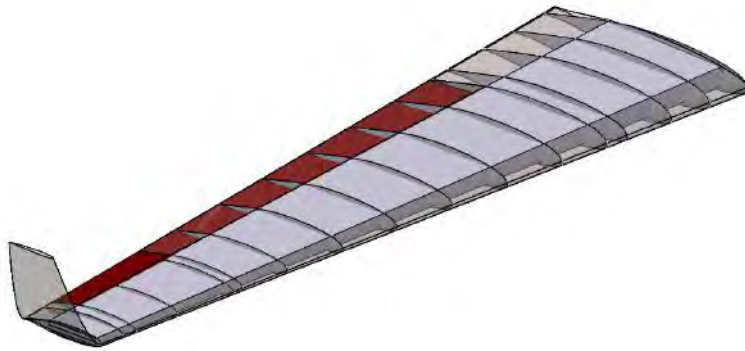


Figure 33: Wing spar is linearly tapering box beam which reduces weight and provides enough structural support for all phases of flight

A layout of the HEAT family wing spar may be found in Figure 33. The same spar is used for the 4 seat Prometheus as the 6 seat Zeus in order to maintain higher commonality by weight, with one exception; the fuel tank in the Prometheus' spar is 10.09 ft long (5.045 feet per wing, giving a total volume of 93 gallons of fuel) and the fuel tank in Zeus' spar is 7.82 ft long (3.91 feet per wing, for 78 gallons of fuel). Additionally, the wing bears the weight of the wires (49 lbs per wing), motors (120 lbs per wing) and controllers (60 lbs per wing) for the DEP system.

To design the wing spar, 5 loading cases were chosen and tested on an initial hollow, linearly tapering box beam to find the lightest weight spar that would still meet relevant FAR's. These 5 cases were the takeoff case (DEP system on), cruise (DEP system off), landing (DEP system on with reverse thrust), and rough landing (DEP system on with reverse thrust), and a static/stationary loading case for the when the plane is in the hangar. The resulting bending stresses for these 5 loading cases on the box beam may be found in Table 17. Here, it can be seen that the highest stresses occur during the takeoff loading case, and because of this, the takeoff loading case was used to design the spar.

Since bending stress dominates stresses (over shear stress), the bending stress during takeoff was the main factor used to design further iterations of the wing spar, as seen in Table 18, which shows a comparison of bending stresses to shear stress. After determining that the main source of stress was due to the thrust of the DEP system, two flanges

Table 17: Takeoff was the most restrictive case with additional thrust from DEP system operations

Bending Stress for Loading Cases on Box Beam			
Loading Case	Variant	Horizontal Bending Stress (ksi)	Vertical Bending Stress (ksi)
Cruise	4PAX	20.14	5.10
	6PAX	31.74	6.88
Rough Landing	4PAX	11.39	2.45
	6PAX	16.81	2.60
Takeoff	4PAX	36.25	2.14
	6PAX	45.69	3.50
Static	4PAX	0	1.92
	6PAX	0	2.39
Landing	4PAX	11.39	2.45
	6PAX	17.01	2.60

Table 18: Bending stress is dominant during takeoff

2-Flange Box Beam Stresses During Takeoff	
Stress	Magnitude (ksi)
Horizontal Bending	12.85
Vertical Bending	4.24
Shear	0.02

were added to the cross section in order to improve bending resistance. However, these two flanges ultimately over-designed the wing spar; they increased the factor of safety from 0.21 to 5.33, vastly exceeding the FAR requirement of 1.5. To save on the spar weight, by designing towards the 1.5 factor of safety, a flange was removed and the remaining one was centered on the cross section.

This redesign reduced the factor of safety to 2.05, and decreased the overall weight of the wing spar. A progression of these cross sections, as well as their factors of safety and stresses can be found in Figure 34 below. The final wing spar tapers linearly along the span of the wing, allowing for the maximum workspace possible to reduce stress and optimize performance with a lighter spar weight. The taper ratio of the final beam design is the same of that of the wing: 0.35.

To select the material for the wing spar, a study of 4 materials was conducted. Each of these materials, the resulting

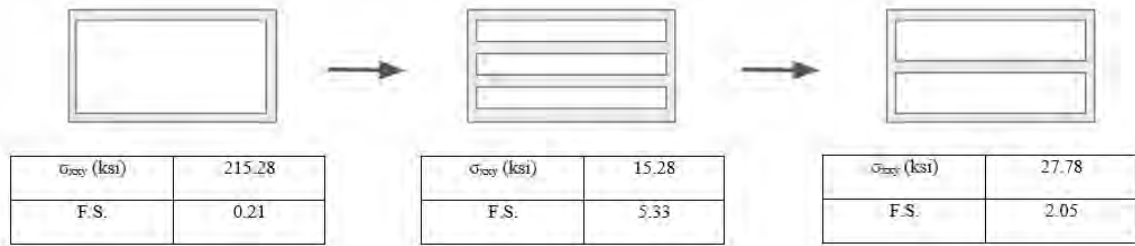


Figure 34: A design progression of wing spar cross-section designs was completed to find the lightest design for Aluminum 2024-T3

Table 19: Aluminum 2024-T3 for its crack resistance and weight reduction

2 Flange Takeoff Material Comparison			
Material	Von Mises Stress (ksi)	Weight (lbs)	F.S.
Al 2024-T3	13.61	616.4	3.45
Ti-6Al-4V	13.54	986.2	9.66
AISI 4130	13.44	1744.4	16.14
Ti-6Al-6VSn	13.54	1010.8	12.91

weight of the wing, and the factor of safety of the spar can be found in Table 19. The aluminum alloy 2024-T3 was selected due to its balance of both weight and tensile strength, all while providing a reasonably designed factor of safety. Additionally, this alloy has high resistance to cracking,³¹ meaning fewer repairs on the spar. For the skin, the aluminum alloy 7075-T6 was chosen due to its lighter weight and higher tensile strength, which allowed for the wing to meet weight budget requirements. Both the 4 seat Prometheus and 6 seat Zeus utilize the same wing spar and design to maintain a higher percent weight commonality, reducing manufacturing costs for the HEAT family. Ensuring the volume requirements for systems in the wing, a scale image of the cross section found at the root of the wing is shown in Figure 35.

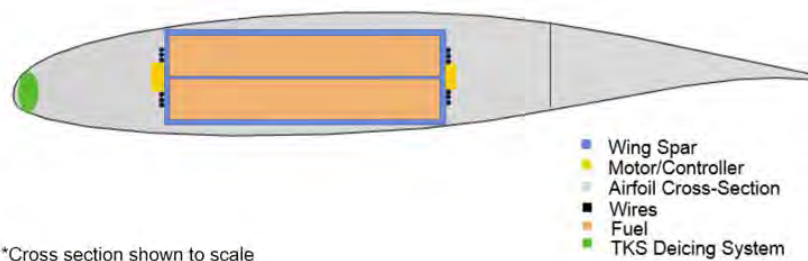


Figure 35: Final cross section shown to illustrate all volume requirements are met

5.7.4 Fuselage

A structural layout of the HEAT family may be seen in Figure 36. Note, both fuselages have the same structural layout except for the seat mount structure in the center of the Prometheus. Additionally, the frames shown in Figure 36 have been stationed around high-stress areas. These include windows, the front windshield, empennage and wing spars, doors, and the connecting points for the nose landing gear (carrying up to 20% the aircraft weight) and engine mounts. However, to ensure low weight, such high-stress areas were stationed close to one another to reduce the number of frames required to distribute these loads.

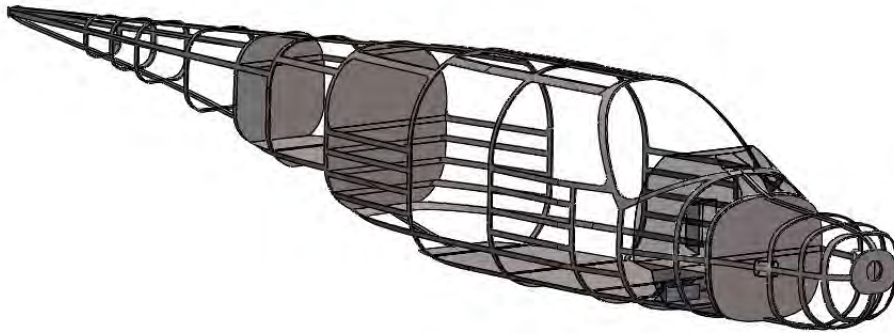


Figure 36: A common fuselage structure is used for the HEAT family

5.7.5 Empennage

Table 20: Fuselage structure specifications determined using plate buckling analysis of the skin

Fuselage Structure	
Number of Longerons	38
Longeron Spacing (ft)	0.58
Frame Spacing (ft)	2

A description of the structures used in the fuselage may be found in Table 20. To design the fuselage structure and meet all load cases, the most constraining moment (occurring at takeoff), acting at the root of the wing, determined longeron and frame spacing. This moment sized these dimensions by treating the skin of the fuselage as simply supported plate and determining the critical buckling length. As a result of this analysis, the fuselage has 38, 0.192-inch radius longerons made of Al 7075-T6 each spaced 0.58 ft apart. The use of this material for the longerons allowed

for a reduction in the number of longerons and subsequently their contribution to their overall weight of the aircraft due to this material’s strength. The carbon engine is mounted in the nose of both aircraft, which is separated from the cabin by a 0.015” stainless steel sheet in order to meet fire safety codes.

Both the horizontal and vertical tail spars are made of the same material: aluminum alloy 2024-T3. This material was chosen for the same reasons as the wing spar; the aluminum alloy allowed for increased crack resistance, reducing maintenance costs due to its increased lifespan. The empennage utilizes two hollow box beams that taper linearly, along the span of the two tails, shown in Figure 37. The thickness of these tails taper linearly, in accordance with their dimensions. This taper ratio is the same as the wing at 0.35. The empennage also uses the same skin as the wing: Al 7075-T6. This alloy was once again chosen due to its light weight and high tensile strength, allowing for increased performance while meeting weight requirements. A table of the Von Mises stresses acting on the empennage may be found in Table ??, along with their respective factors of safety. Both vertical and horizontal spars feature factors of safety greater than 5.0, exceeding FAR requirements.



Figure 37: A common empennage structure is used for the HEAT family

Stress Characteristics			
	Yield Strength (psf)	Von Mises Stress (psf)	Factor of Safety
Horizontal	6.77E+06	7753	5.0+
Vertical	6.77E+06	572	5.0+

Table 21: The empennage is adequately sized for all phases of flight

5.8 Acoustics

5.8.1 Community Airport Noise

Total community noise production is a combination of both airframe and propulsion noise. In order to meet Federal Aviation Regulations on noise generation the HEAT family aircraft shall produce no more than 80 dB in order to receive U.S. certification.^{23,24} The International Civil Aviation Organization (ICAO) also has noise certification requirements in terms of cumulative Effective Perceived Noise level (EPN) limits. ICAO takes the summation of fly-over noise at 6.5 km, sideline noise at 450 m and approach at 2 km and for the HEAT family aircraft, states the cumulative value at these three points can be no greater than 280 EPNdB.¹⁹ However, Stage 5 (ICAO Chapter 14) standards are predicted for implementation for the HEAT family aircraft class starting in 2021, requiring the aircraft to produce less than 250 EPNdB total. The ICAO requirements also dictate that a propeller aircraft of HEAT family weight class must meet Chapter 10 requirements. These regulations state that during the take-off portion of flight the aircraft cannot generate more than 85 dB at 1000m away at any point in its mission.

Noise estimates for the HEAT family aircraft were attempted to be modeled using NASA's Airframe Noise Prediction Program (ANOPP). The ANOPP model selected utilizes Munson and Fink Airframe Noise Estimation model to estimate takeoff, flyover, and sideline noise. This model accounts for flap trailing edge noise as well as noise due to landing gear, however, for flyover noise the model was set to have no flaps to simulate a non-landing configuration of the HEAT family aircraft. This is done to approximate noise produced by the airframe in the ICAO required phases of flight, substituting the higher takeoff noise for the approach value. From the ANOPP software, several acoustic suites are available for propeller and jet engine simulation. However due to the close proximity of the wing mounted propellers an exact estimate could not be generated, but instead only crude estimate made using typical wing engine spacing. Once awarded the contract, Hawken will with NASA to produce a predictive suite that can account for the complex interactions produced by the DEP design based on spanwise engine placement. But for the time being, to approximate the DEP acoustic performance, Hawken consulted the tilt-wing, DEP aircraft, the Greased Lightning.

In Figure 38²¹ the Greased Lightning's acoustic performance was recorded in a wind tunnel, echo chamber acoustic. The Greased Lightning tests were performed with three bladed 16X8 propellers. However, with any wind tunnel testing, there always differences between the lab and real-world conditions. Thus, the HEAT family two-bladed propellers are assumed to have similar performance, despite the difference in the number of propellers per motor hub.

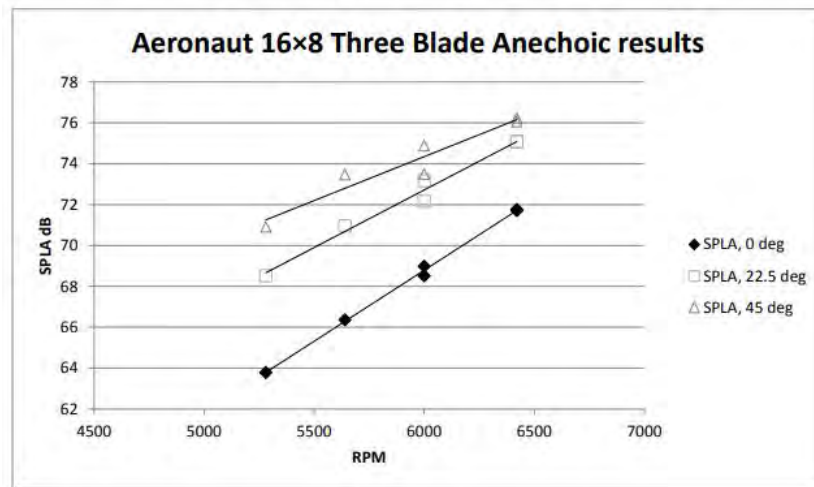


Figure 38: Anechoic chamber Aeronaut 16x8 three blade acoustic data at varying angles

Given the HEAT family will be operating well below 6500 rpm, and will not exceed an angle of attack greater than 15°, the HEAT family easily meet the current Stage 4 noise certification, as seen in Figure 38. Additionally, using preliminary estimates from ANOPP the airframe is able to meet Stage 5 noise values, shown in Table 22.

Table 22: ANOPP results for airframe noise for ICAO chapter 14 requirements

Component	Approach (EPNL)	Sideline (EPNL)	Flyover (EPNL)	Total (EPNL)
Airframe	59.4	72.4	49.2	181
Stage 5 (Chapter 14)	93	88	81	251

Furthermore, the HEAT airframe easily meets Chapter 10 requirements for the low weight, propeller class aircraft seen in Table 23.

Table 23: HEAT family noise for ICAO chapter 10 requirements

Component	Takeoff (dB)
Airframe	59.4
DEP	77
Chapter 10	85

Cabin Noise: The wing mounted motors and propellers will be the most significant source of cabin noise. In order to ensure a comfortable in-flight experience for passengers, if the new noise approximations from ANOPP indicate a

need, active noise canceling systems will be implemented in the cabin. These systems work by producing out-of-phase pressure waves to cancel noise propagation entering the cabin. However, since the majority of the noise will only be present during short, initial periods of the flight, should the motor noise be manageable, no active noise canceling systems will be implemented for systems and manufacturing cost savings.

5.9 Systems

The aircraft systems were designed with four objectives: reduce pilot workload without sacrificing safety, improve pilot capabilities, proper integration of the DEP system with other relevant aircraft systems, and maximize value by keeping cost low. The result is that the HEAT family variants are outfitted with next-generation aircraft systems, making flying easier for pilots, improving ride quality and overall passenger experience, while providing best in class aircraft performance.

5.9.1 Landing Gear

The HEAT family feature a conventional fixed gear tricycle gear configuration, with leaf spring style main gear and hydraulic damped nose gear. This design has a lower maintenance cost, system complexity, weight, and overall greater reliability than a retractable gear configuration. Each gear only harnesses a single wheel. To place the landing gear, the wheel locations were determined using the geometric method outlined by Gudmundsson,³² based around the CG's forward and aft limit, discussed later in Section 5.10 Weights and Center of Gravity. The nose landing gear has neutral static stability and neutral dynamic stability and does not require a shimmy damper. While the nose gear is perpendicular to the ground, the main gear struts are aft-canted 24° , and canted 30° toward the fuselage. All three gear assemblies feature wheel boots to minimize profile drag; the C_{D0} for the landing gear is only 0.0021. The nose gear carries a maximum of 20% of the aircraft load at the Zeus' MTOW, and no less than 10% of the Prometheus' MTOW, allowing the HEAT family to have common longitudinal and lateral landing gear placement. An overturn angle of 33.5° and 34.5° for the 4 and 6 passenger variants confirms an acceptable wheel track of 5.18 ft.

A tail strike angle of 18° ensures proper tip-back clearance during takeoff rotation. The maximum tip-over angle from the main gear to the wingtip, when the outboard-most propeller is folded, is 9.7° to ensure clearance for a slip maneuver in a crosswind takeoff or landing condition. The tire pressure was sized by determining the pressure required

to ensure that the takeoff speed, V_{TO} , is less than or equal to the hydroplaning speed, V_{aqua} (EASA AMC 25.1591). The acceptable tire pressure range is a minimum of 46 PSI, and a maximum of 70 PSI; this provides the HEAT family with the capability to take off and land from paved and unpaved runways, in wet or dry conditions, and minimizes the probability of puncture that high pressure tires experience in unpaved grass fields. Additionally, single-disk braking with hydraulic pressurization provides strong braking performance while maintaining a low maintenance cost.

5.9.2 Pneumatic/Fluid

The HEAT family utilizes dual vacuum pumps for vacuum system pressurization and instrument air systems. In order to reduce aircraft weight, cost, and system complexity, the main cabin is unpressurized with supplemental oxygen provided for all occupants as required by 14 CFR 91.211 at or above cabin pressure altitudes of 12,500 ft MSL. A single 6 lb/person supplemental oxygen tank can supply up to 7 hours and 30 minutes of oxygen using a constant flow regulator cannula.

5.9.3 De-Icing and Anti-Icing

During flight, the aircraft can experience Flight Into Known Icing conditions (FIKI). Tecalemit Kilfrost Sheepbridge Stokes (TKS) ice protection system utilizes an ethylene-glycol based fluid that can perform both anti-ice and de-ice functions; the technology has been in use for over 60 years. Hawken's TKS system is shown Figure 39 and disperses de-icing liquid on the leading edges of wings and tails.³⁶

A total of 6 gallons of the fluid is contained in 8 reservoirs, 4 on each of the main wings. Fluid lines connect the main wing reservoirs with the tail surface leading edge dispersal pumps. Fluid is pumped from the reservoirs using a 28 volt pump, drawing a maximum of 55 Watts of power during operation from the engine's alternator. The fluid is dispersed through porous 0.08 mm thick laser-perforated titanium plates on the front cockpit windshield and leading edges of the main wing, vertical tail, horizontal tail. Each hole on the titanium plates is 0.0025 inches in diameter. The fluid reduces the freezing point of super-cooled water in the free-stream flow, allowing it to pass over the aircraft without freezing. TKS's significant advantage over other icing systems is that it can be used for both anti-icing and de-icing. Ice accumulations on the leading edge are chemically broken down on the layer closest to the surface when exposed to the fluid, allowing the local airflow to force the ice off the wing. This capability gives the HEAT versatility

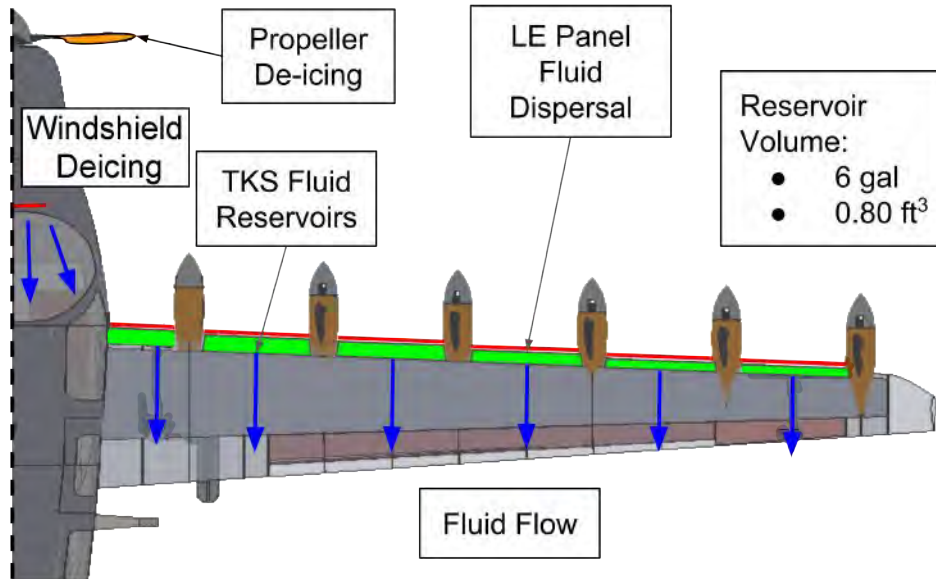


Figure 39: Diagram of the HEAT family's TKS de-ice and anti-ice system³⁶

in icing conditions; it can act as a preventative anti-ice protection measure or as a method of removing ice buildup along the wing leading edge. While the system is highly acclaimed for its strong performance for FIKI, it is still the pilot's responsibility to monitor weather patterns to determine when icing conditions are imminent using weather radar, as discussed in this section. Since the TKS plates are coincident with the leading edge of the wing, located between the wing skin and a reservoir backplate, they must be manufactured together. To ensure lower manufacturing costs and the highest quality standards, Hawken plans to manufacture these laser-perforated titanium sheets in-house, as opposed to outsourcing the manufacturing of the HEAT's wing leading edge.

The last system components required to ensure the HEAT family can fly in known icing conditions without compromising safety, are the pitot probe electric heating elements for the tail-mounted probe. A 35-watt heater is mounted under the aft pressure chamber and a 100-watt heater mounted aft of the probe's ram air inlet. Additionally, the propellers utilize embedded resistive heating circuits, which act as electric heating elements.

5.9.4 Fuel System and Hydraulics

The fuel system is comprised of two fuel tanks, located in the single wing spar, as well as fuel lines running from the wing tank to the forward gas engine. The same spar is used for the 4 seat Prometheus as the 6 seat Zeus in order to maintain higher commonality by weight, with one exception; the fuel tanks in the Prometheus' spar extend 5.045 feet

from the root of each wing (giving a total volume of 93 gallons of fuel) and the fuel tank in Zeus' spar extends 3.91 feet per wing (for 78 gallons of fuel). The fuel system schematic can be seen in Figure 40.

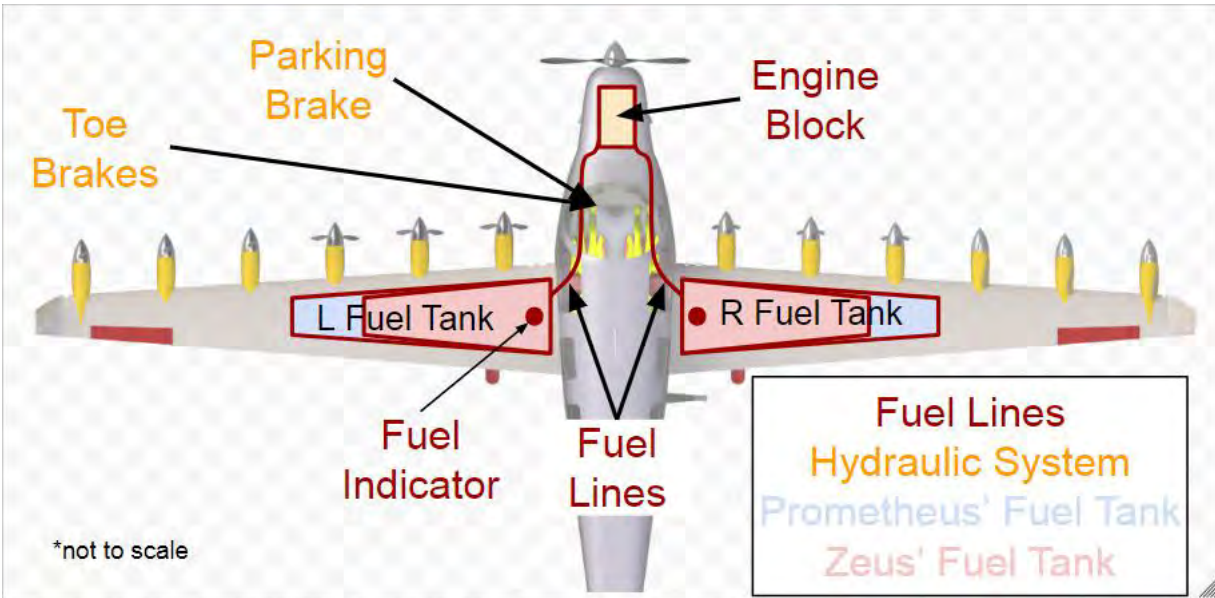


Figure 40: Fuel system features two wing tanks with fuel lines to the main engine

A backup wing fuel pump supplies fuel pressure if there is a failure or loss of the primary engine-driven fuel pump.⁵⁴ Electronic capacitance (IR-density compensated) type fuel indicators are used, as opposed to traditional float type fuel indicators, which are notoriously unreliable at low quantities of fuel and generally less accurate due to aircraft motion. Capacitance fuel indicators are specifically designed for environments with significant vibration or electrical noise.⁶⁷ These adverse problems caused by the DEP system make capacitance indicators best suited for the HEAT family. Additionally, the capacitance indicators can run on the same 28-volt system as the de-icing system, mentioned later in this section.

5.9.5 Fire and Heat Protection

To avoid overheating, the battery cell temperatures in the fuselage belly battery box are monitored by the battery management system developed by Hawken to provide air-cooled during takeoff and landing by automatically deploying cowl flaps. This is talked about in greater detail in Section 5.6.3 Hybrid Propulsion System Configuration.

Although the FADEC system automatically monitors fuel-air mixture to regulate engine temperature within normal operating limits, a Garmin G600 TXi EIS provides engine temperature information, guiding the pilot with engine

temperature and rate-of-temperature rise data to choose to shut down the engine should an emergency arise. The engine firewall attached to the engine mount is a 0.015-inch-thick stainless-steel sheet, preventing fire and significant heat transfer to the cabin in the event of an emergency.

5.9.6 Conventional Sensors

A tail-mounted pitot probe and static port placed just aft of the engine cowling provide pitot-static pressure measurements, which are used as the secondary analog airspeed indicator, vertical speed indicator, and altimeter. The GPS utilized in the avionics system provides primary data of ground speed, vertical speed, and altitude; this redundancy allows for safe flight in the event of either a pitot probe or GPS failure. The utilization of a squat switch in conjunction with airspeed allows for the FADEC system to automatically determine what phase of flight the aircraft is in, in order to choose the optimal distribution of power between DEP and the main engine.

5.9.7 Avionics

Figure 41 below shows the HEAT SkyVision Flight Deck is a fully integrated avionics flight deck with Garmin general aviation avionics components.



Figure 41: HEAT Family SkyVision Flight Deck is fully capable of VFR, IFR, and operating in all airspace classes

Selecting a reputable company with commercial-off-the-shelf availability reduces aircraft cost. The SkyVision Flight Deck instrument panel features a left seat G600 TXi primary flight display (PDF) and center G600 TXi 6-cylinder Engine Information System (EIS), a GTN 750 GPS/NAV/COMM/MFD, and an optional lower right seat GTN 725 GPS/MFD. Backup analog instruments include an altimeter, airspeed indicator, and heading indicator.

A GTX-345 ADS-B transponder -centered on the top of the instrument panel- allows for tablet and mobile app integration, reducing pilot workload during flight by centralizing flight plan information, as well as implying pre-flight planning. Dual Garmin GWX 70 radars provide a total of 210° of forward and lateral color doppler weather radar, compatible with the PDF and MFD to reduce pilot workload and reliably aid in real-time navigation. A GMA 35 3-comm integrated audio panel -centered on top of the instrument panel- allow the pilot to monitor multiple frequencies simultaneously, increasing pilot safety. Hawken will work with Garmin to integrate the sensors with a GFC 600 Digital Autopilot, which serves to reduce pilot workload throughout the climb, cruise, and descent phases of flight. The Garmin EIS TXi provides 6-cylinder engine monitoring and management on a 10.2-inch touchscreen, displaying engine temperature, fuel, oil, electrical, and other sensor data. Data is automatically logged and stored on pilot mobile devices. The unit features a lean assistance mode, which is incorporated into the Full Authority Digital Engine Control (FADEC) system. Additionally, the unit fully monitors the aircraft's electrical system, critical to the operation and integration of the DEP system. The DEP integrates with the FADEC system, condensing control of both propulsion systems into a single throttle control. This configuration not only reduces pilot workload, increases safety, but also enables the aircraft to be certified as a single engine land (SEL) GA aircraft.

A series of switches that control aircraft lighting, cabin environmental control system (ECS) for air conditioning and cabin heating, are located on the lower portion of the instrument panel for easy access for the pilot in command (PIC). The cockpit features two primary flight control sidesticks and rudder pedals, along with secondary flight control toggles, trim wheel, and throttle.⁶⁶ All systems operate using fly-by-wire (FBW) actuation and control, with the exception of toe braking, which is a hydraulic system. Mechanical control, although traditionally common amongst general aviation, is heavy and outdated; digital FBW systems without redundant mechanical actuation was first used in the 1970's and is common amongst modern commercial transports. By using FBW, mechanical cables and control rods are replaced with electronic components, reducing overall weight.⁶⁷ The full glass instrumentation enables more seamless integration of FBW into the control scheme of the HEAT family. The overall function of the FBW system is shown below in Figure 42.

Fly-by-wire enables more precise control of the aircraft while reducing physical pilot workload. Additionally, due to the high accident rate within general aviation, FBW is a push for safer flying; the flight control laws governing the HEAT's FBW system will be programmed to stay within the aircraft's flight envelope, mitigating the risk of stall.⁵⁸

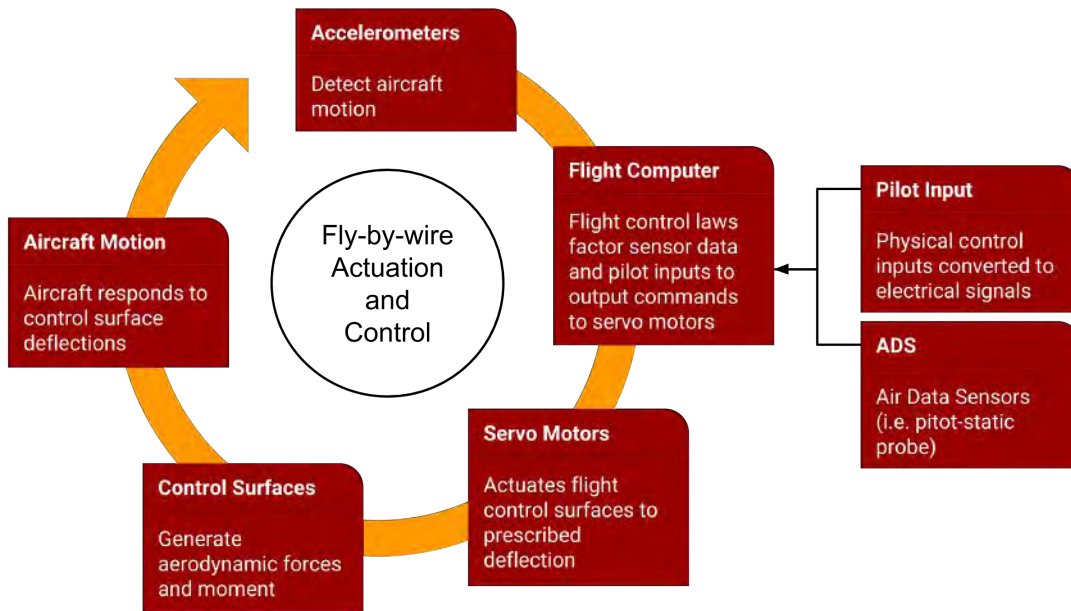


Figure 42: Fly-by-wire Actuation and Control Closed-loop Control System (with feedback)

Fly-by-wire can act passively as a stability augmentation, assisting the pilot with control inputs without taking control of the aircraft.

5.9.8 Communication

Communication is vital to the successful operation of an aircraft manually or autonomously. The antennas in Table 24 are specifically designed for general aviation aircraft, and are a balanced selection based on aerodynamics for appendage drag, performance, and cost. The antennae cover the VHF, UHF, L, and X frequency bands.

Together, the communication and instrumentation suite in the SkyVision Flight Deck make the HEAT aircraft fully VFR and IFR capable and include the necessary equipment to operate in all classes of airspace.

5.9.9 Autonomous Systems Architecture

Hawken has chosen not to implement autonomous systems due to certification challenges and complexity of the system integration. However, Hawken meets the RFP’s requirement for implementation of “an architecture capable of autonomous flight” by our utilization of glass avionics, onboard radar, FADEC, and electrically controlled flight control surfaces, all of which only require the addition of autonomous software updates and the future installation of additional, autonomous sensors.

Type	Device	Location on Aircraft	Function
VHF Antenna	Comant CI 109	Top of the fuselage	VHF Air Traffic Communication / CTAF
	Comant CI 122	Bottom of the fuselage	VOR Navigation
UHF/DME Transponder	Comant CI 105-3	Fuselage belly, away from other antennas	ATC Interrogation
			Distance Measuring Equipment
			Active GPS
ELT	Comant CI 317	Tail section	Emergency Locator Transmitter
Radiophone / Communication	Comant CI 200	Top of fuselage	UHF Air Traffic Communication Interrogation

Table 24: The HEAT family aircraft are equipped with communication systems required for all phases of flight

The paramount benefit of autonomous aircraft is combating pilot error and exhaustion. According to D. Kenny’s report “Aviation Accidents in 2014”, pilot error consistently is the primary cause of 75% of all general aviation accidents.¹⁷ Accidents in autonomous vehicles related to system logic error can be directly attributed to design errors, not operational errors. Ideally, a properly designed autonomous aircraft should have a substantial reduction likelihood of accidents and incidents. However, it is important to note that autonomous systems do not have an inherent aversion to risk or sacrifice, making the role of the pilot still important to safely operating an autonomous aircraft. A major challenge of implementing autonomous capabilities is working with the FAA to certify autonomous flight for civilian aircraft. If the FAA allows certification, Hawken will work closely with a third party to design the necessary software and flight control laws. The HEAT family’s as-designed flight control system lays the foundation required for autonomous architecture. The combination of a fully digital cockpit, FADEC, autopilot, and fly-by-wire actuation and controls allow for a flight computer to act upon information already provided by onboard sensors, instead of pilot input.

The addition of autonomous capabilities would remove the pilot input from the feedback loop, add additional sensors, require more computational power, as well as utilize more sophisticated flight control laws. The HEAT family will not incorporate autonomous features due to strong uncertainty in FAA certification, the drive to minimize cost, and high system complexity, the following section will discuss the hardware choices and process required for autonomous flight.

An autonomous system could perform millions of mathematical and logical calculations throughout all phases of flight -far surpassing that of a human pilot. Additionally, the avionics systems used are upgradable, with groundbreaking features typically added every decade. The ability to transfer data during flight enables weather information, AIRMETS, SIGMETS, NOTAMS, and PIREPS are factored into the flight route decision making, in real time. Since an autonomous system must operate in all environments, optical sensors can distinguish objects, anything from geese to Boeing 747's, at distances up to 4 times the VFR requirement for Class B airspace. Ultrasonic sensors can be employed to provide immediate proximity object detection or avoidance. Other sensors, such as short-wave infrared camera systems designed specifically for navigation, can provide augmented optics. Mid-wave and long-wave sensors distinguish objects using temperature differential between the heat emissions of objects in close proximity. Additionally, topographic LiDAR can be employed to provide near-infrared laser mapping of the surrounding geography, for terrain detection and avoidance. Acoustic sensors placed on the aircraft could detect rough engine noise, and other exterior sounds, critical to flight operations, extending past the limits of the human ear's frequency ranges (0.02 - 20 kHz). Communication procedures for transmissions between autonomous aircraft and manned aircraft should be dictated by the FAA, but the capability to use current line-of-sight and satellite radio frequency transmissions would be standard. Such equipment is already standard on general aviation aircraft, and artificial voice, such as text to speech, could easily be implemented. With the advent of machine learning, autonomous systems will soon be able to go beyond reacting from programmed only operations and will be able to use learned decision-making skills. As technology advances, these capabilities will only become faster, more sophisticated, more reliable, and more cost-effective.

5.10 Weights and Center of Gravity

Hawken's weights assessment incorporates all previously discussed component weights from structures, systems, and propulsion to provide the final center of gravity (CG) location and limits for safe flight. Figure 43 represents these limits with the nominal CG locations for both HEAT family labeled. Note, as was previously discussed, there is only one diagram represented for the HEAT family because the same airframe and propulsion system is used between both variants. The CG loading limits are defined by 2 constraints to ensure the stability of the aircraft. The forward limit is defined by the CG location when the elevator is unable to trim the aircraft. The aft limit is defined by the neutral point, where if the CG passes this point, the aircraft is statically unstable. By remaining within these limits, both stability

and performance capabilities are guaranteed.

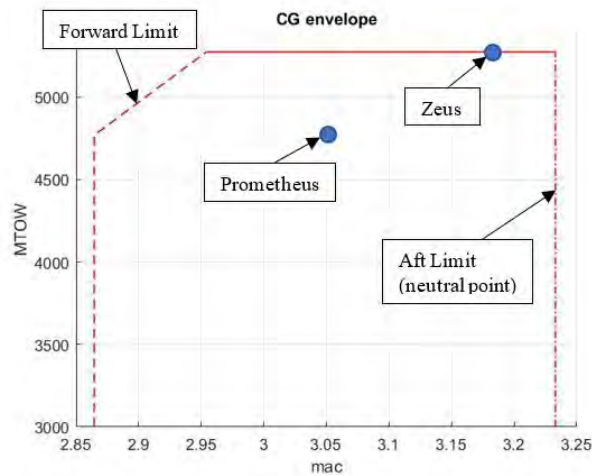


Figure 43: The boxed region depicts the safe positions for CG travel with both HEAT family aircraft plotted

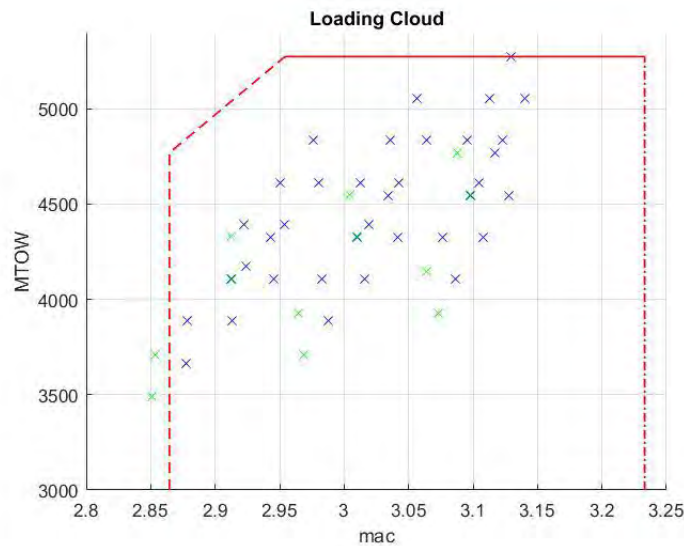


Figure 44: The boxed region depicts the safe position for CG travel for the Zeus and Prometheus (shown in blue and green respectively)

The feasible loading combinations with respect to these aforementioned limits are shown in Figure 44. All combinations of loading Zeus place CG within the envelope. 10 of the loading combinations for Prometheus also are within the envelope; however, 2 are in front of the forward limit. This occurs with one pilot, with or without a front passenger, their baggage, full batteries, and zero fuel. It should be noted here that almost every general aviation aircraft on the market today experiences a few unique loading conditions, and does not necessarily indicate a poor design.

These two unique loading cases for the Prometheus can occur on the ground as well as at the end of a long mission

when all fuel has been burned. For the pilot’s safety, specifications in the Pilot Operating Handbook will detail the installation of an additional 25-pound weight in the aft section of the luggage compartment. Because this loading case is very easily remedied, once the pilot has spent the necessary time studying the operator’s handbook, this loading case will not be an issue.

Table 25: The weight breakdown for the Prometheus and Zeus, showing both the common and differing weights

Component Weights			
	Prometheus (lbs)	Zeus (lbs)	Moment Arms (ft, '+ve' is aft of CG)
Wing	771		0.40
Horizontal Tail	35		17.09
Vertical Tail	26		18.36
Fuselage	442.0		1.22
Main Landing Gear	132.5		1.25
Nose Landing Gear	79.5		-7.72
Fuel System	41.5	36.5	0.40
Control System	71.6	79.5	-5.12
Avionics	115.0		-5.12
Electrical System	100.0		0.40
Anti-icing	30.0		0.91
Instruments	40.0		-5.12
Pilot Furnishings	80.0		-2.27
Middle Furnishings	0.0	80.0	0.27
Back Furnishings	80.0		5.67
Tray Tables and Cup holders	6.0		1.22
Installed Engine	484.0		-7.66
Motor	381.0		-2.27
Step Ladder	7.0		8.20
Battery	319.0	413.0	1.86
Empty Weight	3241.7	3418.7	
Fuel	654.0	541.0	0.40
Pilots	380.0		-2.27
Middle Passengers	0.0	380	0.27
Back Passengers	380.0		5.67
Baggage	120.0	180.0	8.20
Total	4776	5280	

The nominal CG locations were calculated using the component weights listed in Table 25. Empty weight is the sum of the weights above the empty weight section of the table, while MTOW additionally includes fuel, people, and baggage. To reduce manufacturing and maintenance costs for a family of aircraft, commonality was an important driver in the design process in addition to being an RFP requirement. The common weights between Prometheus and Zeus, are shown in the merged cells of Table 25. The RFP set a minimum of 75% commonality by weight for the airframe and propulsion system. The HEAT family has final a commonality of 94.8%. This is significantly more than the RFP requirement, but ensures a decrease in manufacturing and maintenance costs over a 75% weight commonality. Using the same structures between both family aircraft made this weight commonality possible, designing for the

most constraining load case found with Zeus. However, commonality drove Hawken to use the same structure for both aircraft, which slightly increases Prometheus' MTOW. The same engine and motors are used for both aircraft as well. Because of the high structural commonality, the empty weights are only 177 lbs different, despite a 500 lbs difference in MTOWs. This table data is categorized and displayed in a graphical format in Figure 45.

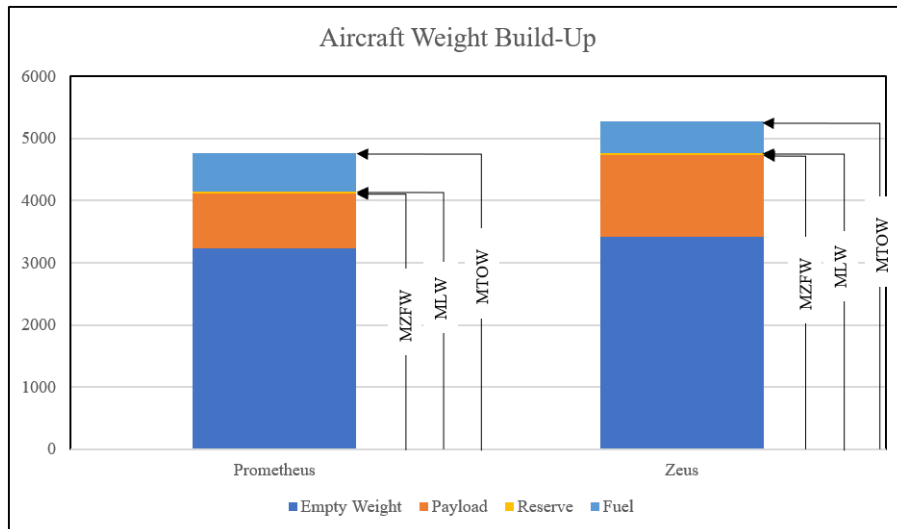


Figure 45: The weight build-up from zero fuel weight (MZFW) to max landing weight (MLW) to max takeoff weight (MTOW). Reserve fuel includes 45 minutes of additional flight²⁵

To provide a physical representation of these CG locations, limits, and contributions, are Figure 46 and Figure 47. The first figure locates the CG of all the major components, while the second figure displays the aircraft CG and the forward and aft limits.

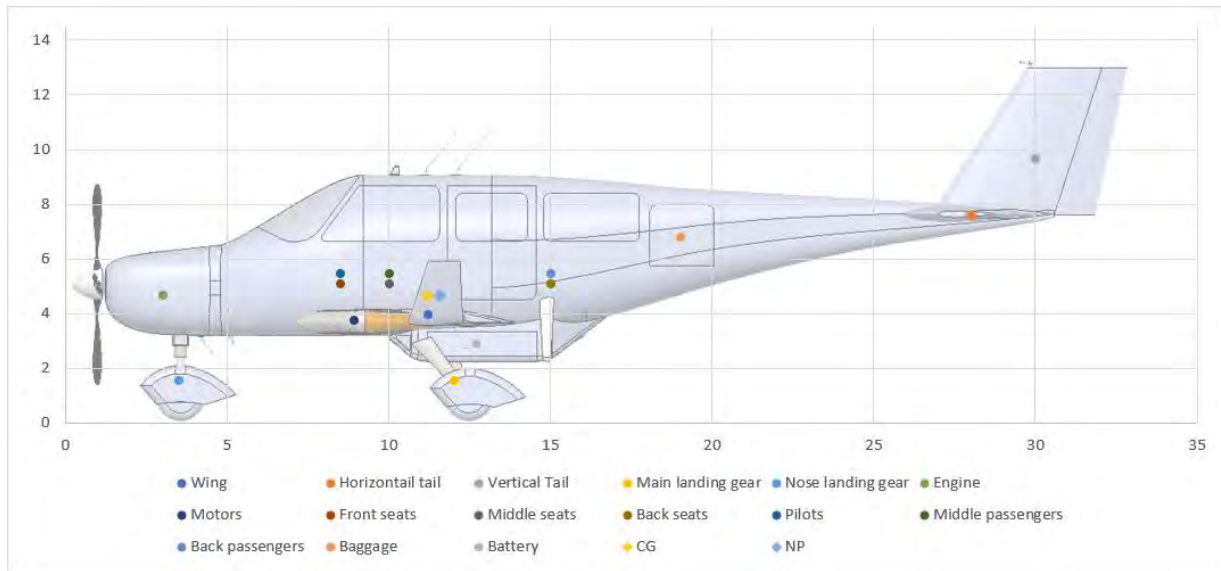


Figure 46: To scale CG travel limits shown to give a better, physical representation of these limits

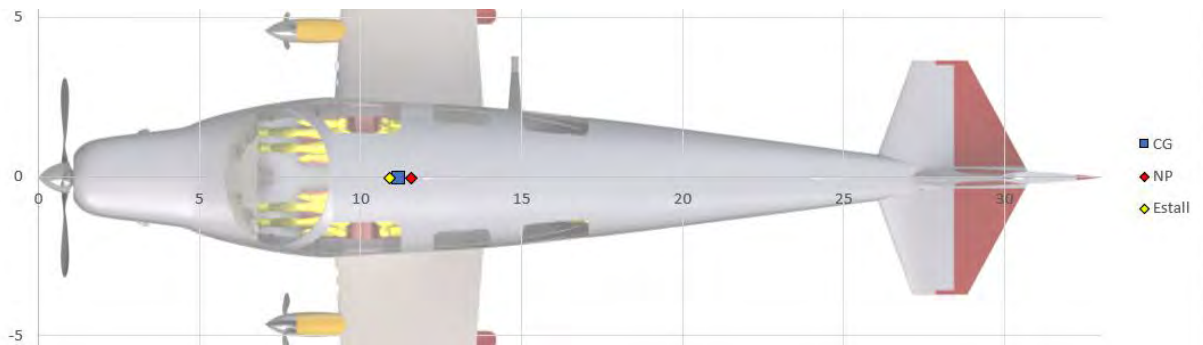


Figure 47: The aft limit is defined by the neutral point represented in orange. The forward limit, the green diamond, is set by the elevator moment. In between these is the CG with a blue square

5.11 Stability and Control

For stability and control, this process involved iterating the wing and tail placements until the desired static margins were achieved. With the finalized CG limits presented in Section 5.10 Weights and Center of Gravity, the finalized stability and control analysis for the HEAT family aircraft are presented in the proceeding sections. This describes empennage design, static stability, control surface sizing, DEP incorporation, and dynamic stability analysis.

5.11.1 Empennage

The empennage configuration on HEAT family aircraft was selected based on wing placement and FAR static stability requirements. The 3 empennage designs considered were a T-tail, cruciform tail, and conventional tail. The major constraint on configuration selection was having low drag during cruise with a secondary constraint being the interaction of the DEP propeller wake. Note, this secondary constraint was set to reduce the likelihood of flutter experienced by the horizontal tail. Using these constraints, Hawken sought to reduce operating cost and give the pilot full control authority with DEP systems running. The configurations to best meet these constraints were the T- and conventional tails. The T-tail was considered initially to ensure the horizontal stabilizer would be placed entirely out of the prop-wash from the DEP propellers. However, the significant drawbacks of increased weight and structural complexity ruled out this configuration to operating costs with a lighter aircraft. A conventional tail provides the least complexity and structural weight but the horizontal stabilizer would experience brief interactions with the DEP wake. Final analysis indicated, for the small section of flight DEP is running, the conventional tail would save manufacturing costs from reduced complexity and save on operating costs with less weight to fly. With the reduction in cost from Hawken's measures of merit and the uncertainty of flutter without proper testing, the conventional tail was selected. But it is worth noting, once awarded the contract, Hawken will perform the necessary wind tunnel and flight testing to ensure the pilot maintains full control of the aircraft with the DEP system running.

5.11.2 Static Stability

With the conventional tail configuration selected, the empennage was for static stability using methods defined in Raymer as well as Gudmundsson.^{32,55} The first step in sizing for static stability was selecting horizontal tail volume ratio, V_{ht} . Using competitor aircraft, V_{ht} 's as references for feasibility, a value of 0.7 was selected based on the wingspan and weight of the Zeus.⁶¹ The next step was constraining the tail moment arm to model long-coupled stability characteristics, a minimum of 3 MAC. Long-coupled tail placement was chosen for favorable stability characteristics, enabling a smaller empennage for a reduced wetted area and therefore drag. While having a shorter moment arm gives greater maneuverability, this did not outweigh the goal of reducing operating costs. Thus, to reduce operating costs, the V_h of 0.7 was incorporated with the Gudmundsson³² optimization process to minimize wetted area. The method resulted in tail location being the wing AC, l_h , of 19.5 ft with an area, S_h , of 18 ft². This process

is shown in the graph depicted in Figure 48. Using this as a starting point Hawken conducted further trade studies between l_h and S_h to find an optimal reduction in drag. By shifting the tail forward to 17.5 ft, with an S_h of 23 ft², C_{D0} was reduced by .001 from the preliminary optimization results. This final l_h value is equivalent to 4.9 MAC, ensuring the HEAT family aircraft perform as long-coupled aircraft.

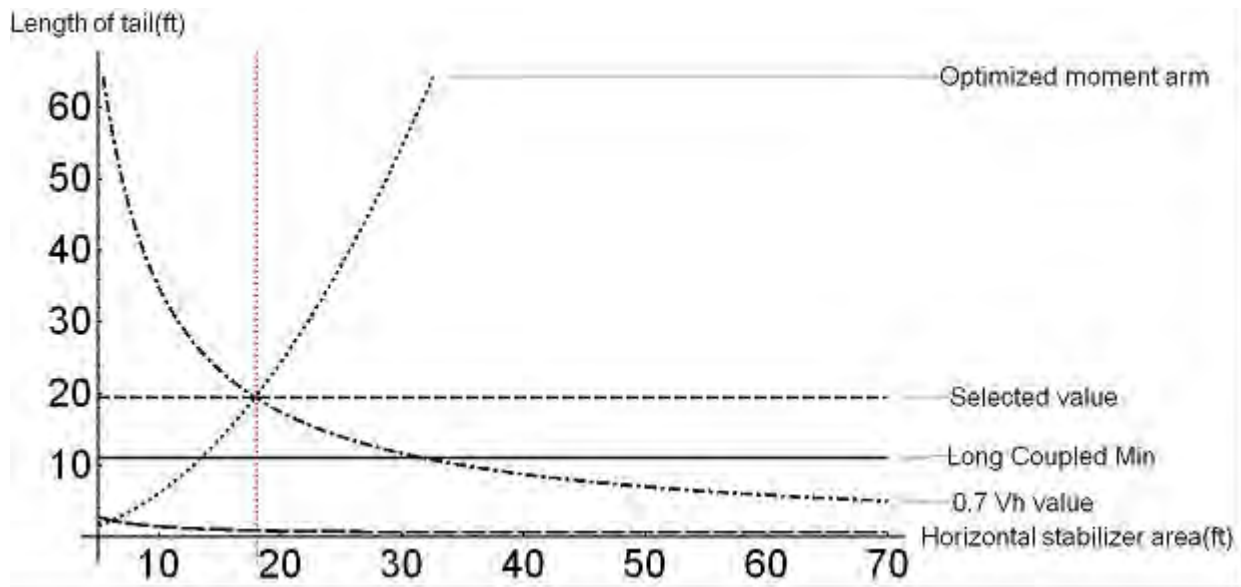


Figure 48: Graph depicting optimal moment arm for the horizontal tail in terms of the length of the tail and horizontal stabilizer area

Static stability was initially sized to ensure a static margin of at least 15%, a typical value for small GA aircraft.⁵⁹ Utilizing a moment balance the C_l from the horizontal tail was determined to be -0.071. This C_l was achieved using a NACA 0012 with an incidence angle of -0.65° . This design results in a C_{m0} value for the entire aircraft of 0.01383 and a static margin of 10.9%. Therefore the Zeus aircraft demonstrates static stability while reducing drag created by the tail and the aft fuselage length.

In an effort to maintain low manufacturing cost for the HEAT family aircraft as well as meet RFP requirements for commonality, the same tail sizing and airfoil were utilized. Applying the same moment balance to the Prometheus variant, the horizontal tail C_l becomes -0.18 due to the difference in weight and flight speeds. Therefore, utilizing the same NACA 0012, the horizontal stabilizer would be mounted at -1.5° . This design results in a C_{m0} value for the entire aircraft of 0.011 and a static margin of 19%. The Cessna 172 is the most produced aircraft in the world. It has a 19% static margin,⁹ providing good maneuverability to the pilot. From this sizing the process the final stability derivatives are found below in Table 26.

Table 26: Stability derivatives for the HEAT family

Stability Measure	Prometheus	Zeus
Static margin (% MAC)	19	10.3
$C_{l\beta}$	-0.04	-0.04
C_{lp}	-0.7	-0.7
C_{lr}	0.15	0.15
C_{mq}	-0.1	-0.1
$C_{n\beta}$	0.21	0.21
C_{np}	-0.08	-0.08
C_{nr}	-0.25	-0.25
$C_{y\beta}$	-0.74	-0.74
C_{yp}	-0.06	-0.06
C_{yr}	0.6	0.6
$C_{Z\alpha}$	-5.67	-5.67
C_{Zq}	-0.02	-0.02
C_{Zu}	-0.03	-0.03

5.11.3 Dynamic Stability Analysis

To provide a suitable, traveling work environment for business people and for general comfort of the pilot and passengers, a high level of dynamic stability was desired. Additionally, for newer pilots, a higher level of stability would ensure an easier to operate aircraft. The stability of the aircraft was compared to the Mil-spec 8785C criteria for Class I aircraft to provide an additional factor of safety above the FAR's. This was done to give the pilot peace of mind when flying a revolutionary aircraft design. In order to calculate the mass moments of inertia, approximate point masses were assigned to the HEAT family Solid Works model with the CG manually assigned to match finalized CG locations. The calculated dynamic stability values for both the Zeus and Prometheus can be seen in Table 27.

From Table 27, the Prometheus can be seen to meet all requirements for Level 1 stability whereas the Zeus meets all criteria except short period damping. However, the Zeus easily meets the 0.2 required for Level 2 stability in short period and has a time to half amplitude nearly identical to the Prometheus, 3.05 seconds. Therefore, in an effort to maintain the sizing compatibility between aircraft, if flight testing and certification indicated greater dampening is required a basic stability augmentation system can be implemented using the skeletal systems for autonomous systems.

Table 27: The HEAT family meet all but spiral Mil-spec dynamic stability requirements

Mode	Mil-spec 8785 C Level 1	Zeus	Prometheus
Short Period	$0.3 < \zeta < 2.0$	0.28	0.3
Phugoid	$\zeta > 0.04$	0.06	0.06
Dutch Roll	$\zeta > 0.08$	0.19	0.2
Roll	$T < 1.4s$	0.19 s	0.17 s
Spiral	$T < 20s$	28.06 s	27.84 s

5.11.4 Control Surface Sizing

Continuing the minimization of manufacturing cost, for control surfaces, requires the same size surfaces between aircraft to ensure interoperability for the HEAT family. Due to the large C_L requirements for the HEAT family wing, the ailerons will also function as flaperons for take-off and landing phases of flight. The ailerons were initially sized to ensure compliance with Mil-spec 8785C Level 1 roll rate requirements for the same reasoning stated above. To begin sizing, the chord was chosen to match the chord of the dedicated flap system to ensure similar flight characteristics along the wing when the ailerons are being utilized as flaps. Utilizing methods found in Sadraey the minimum size for the ailerons to achieve Level 1 made the ailerons encroach on the area of the wing dedicated for flaps.⁶¹ Therefore, to minimize the size of the ailerons and maximize the available space for flaps, while still providing a greater factor than FAR's, Mil-Spec 8785-C level 2 was used. The ailerons were placed to end at 95% of the span with the resulting wing control surface sizing found below in Table 28 and Figure 49.

Table 28: Aileron size and location in ft and % span of the wing

Inner location ft (% span)	Outer Location ft (% span)	Length ft (% span)
16.8 (80%)	19.95 (95%)	3.15 (15%)

Based on the above sizing, the following roll rates were calculated for both the Zeus and Prometheus. These roll rates are found compared to level 1 requirements in Table 29. From Table 29, both aircraft fail the Mil-spec roll requirements; however both aircraft easily exceed FAR roll requirements of 30° in 5 seconds.

Due to the unique abilities presented by DEP, traditional sizing methods for the rudder are no longer effective. Despite having 12 wing-mounted engines the HEAT family aircraft will not be sized as a multi-engine aircraft. This

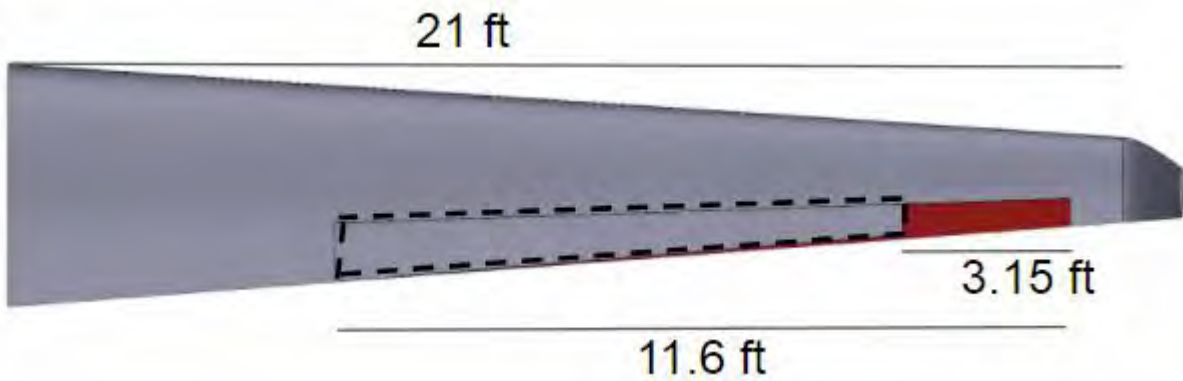


Figure 49: The ailerons are sized to meet both Mil-Spec and FAR roll requirements for enhanced maneuverability

Table 29: Mil-spec and FAR roll requirements for the HEAT family aircraft provide enhanced safety and roll performance

Mode	Mil-spec 8785 C Level 1	FAR Part 23	Zeus	Prometheus
Cruise	Bank angle 45o (1.7s)	4.62s	2.22s	2.13s
Take off	Bank angle 30o (1.3s)	3.77s	1.81s	1.74s

is the result of asymmetric lift that results from an engine out condition, except, with electrical buses, there is a possibility that an entire wing of motors fail. Therefore, instead of sizing a rudder to counter asymmetric thrust of one failed motor the rudder would need to be sized to counter the asymmetric thrust of an entire wing of failed motors. However, the nature of DEP propulsion results in a greater roll moment caused by asymmetric lift compared to the smaller yaw moment caused by the asymmetric thrust. In an effort to combat this roll, the DEP system will have failsafe mechanisms in place to shut down mirroring motors on the opposite wing, removing asymmetric thrust and lift. This system will negate the need to certify the HEAT family aircraft as multiengine as well as the rudder sizing requirement for asymmetric thrust.

Additionally, the DEP system allows the vertical tail to be placed closer to the CG location, shortening the aircraft’s total length. Traditionally, the vertical tail and rudder must be placed such that at least 33% of the rudder area is outside of the vertical space above the horizontal tail, in order to enable sufficient flow in a flat spin, visualized in Figure 50.⁶³ However, with a DEP aircraft design, the wing mounted propellers provide almost instantaneous airflow of the wings once turned on. Harnessing counter-rotational asymmetric thrust, as well as the instantaneous airflow, provided by DEP, spin recovery can be achieved with minimal rudder input. This benefit places the vertical tail 3 ft closer to the CG location, shortening the overall aircraft length (decreasing CD0) and decreasing structural weight. The only

constraint left for sizing the vertical tail was a crosswind landing scenario. In accordance with FAR's for crosswind landings, the rudder was sized to be a constant chord of 25% of the vertical tail for the entire vertical span, as seen in Figure 51.⁶¹

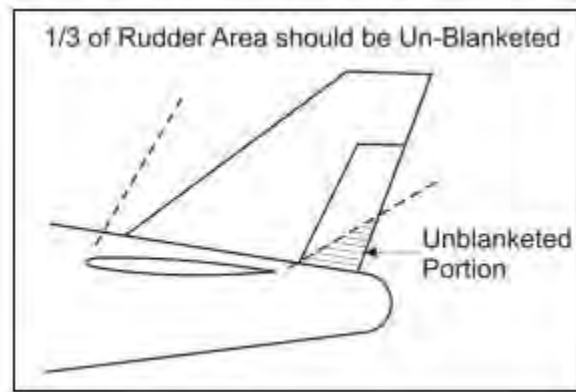


Figure 50: Influence of the empennage design on the spin recovery characteristics⁵⁵

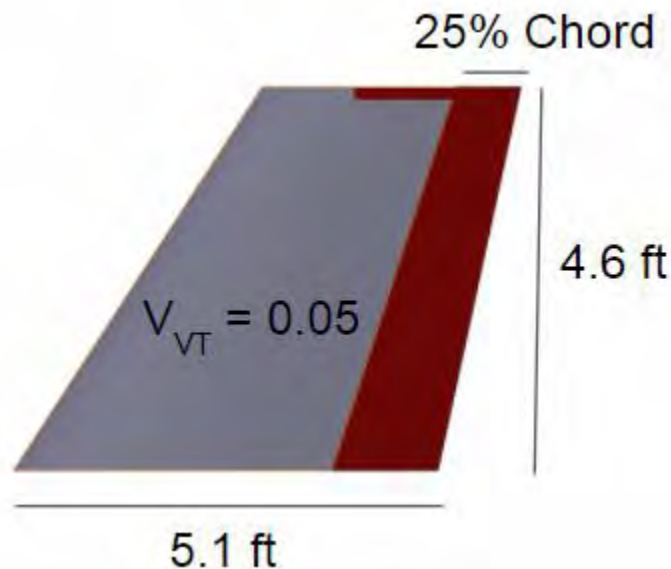


Figure 51: Dimensioned vertical tail for the HEAT family aircraft

DEP also has an effect on traditional elevator sizing methods. Instead of sizing the elevator to provide a sufficient pitch moment to enable rotation, the elevator is sized to ensure the aircraft does not over rotate due to the pitch moment produced by the DEP motors. The additional 2500 ft-lb pitch up moment produced by the DEP motors allows for a 7% chord ratio decrease for elevator sizing over traditional methods; however, since the motors will be utilized for the climb portions of flight the elevator must be deflected to counter the pitch moment to ensure a steady climb angle.⁶¹

For the HEAT family aircraft, the DEP produces 2300 lbs of thrust resulting in a slight decrease to the overall size of the elevator as documented in Table 30. Therefore, the final elevator sizing was determined to be 25% chord of the tail as seen in Figure 52. However, in order to simplify the actuation method for the elevator, the design was modified from a constant chord the entire span to a leading edge perpendicular to the centerline of the aircraft as seen in Figure 53. Additionally, to prevent flutter, counterbalances are internally stationed at the tip hinges for the empennage control surfaces.

Table 30: Elevator sizing based on DEP use cases

DEP condition	Elevator chord ratio	% change
None	0.29	0
Only take off	0.22	-7
Take-off climb	0.25	-4

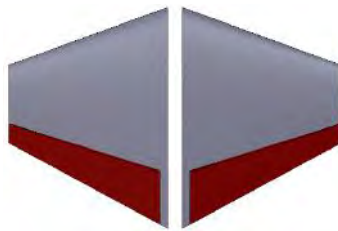


Figure 52: 7 Initial layout for the elevator on the horizontal stabilizer

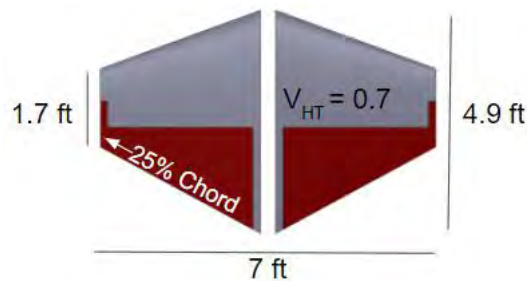


Figure 53: Dimensioned horizontal stabilizer with elevator shaded red

It is important to note that all of the control surface sizings were done on the most constraining aircraft model, the Zeus. In order to lower production and maintenance costs and increase commonality by weight as per the RFP requirements, the same control surface sizes will be used for the smaller Prometheus aircraft. This will result in a more agile aircraft should the pilot decide to utilize the aircraft to the limits of its design. Additionally, should the

pilot desire more fuel economy, the control surfaces will deflect less in traditional flight allowing for lower drag and increased efficiency.

With numerous design features set to reduce the operating and acquisition cost of the HEAT family, the family’s performance will be discussed below.

5.12 Aircraft Performance

In the takeoff configuration, the HEAT family utilize DEP as the primary source of propulsive power, while the main engine is at idle in case of DEP failure. The takeoff flap setting is extended to 15°. The required takeoff thrust required is prescribed by the minimum DEP thrust to achieve the C_L for a corresponding V_{TO} . For the HEAT family, this required thrust is 1979 lbs, achieved at 83.4% max static thrust from the DEP system. By using less than the absolute maximum available thrust from the DEP system, wear and tear are reduced yielding reduced maintenance costs.

In the landing configuration, both variants utilize the RED A05 engine as the primary source of power. The main engine produces idle thrust on approach, while the DEP system remains on standby with its props unfolded, ready for full takeoff and go around (TOGA) power. Combined with the main engine, the total available static thrust for the HEAT family is 3272 lbs. After a successful touchdown, the electric motors provide a reverse thrust of up to 30% of max continuous power, allowing for significant reduction in landing ground roll, as seen in Table 31.

Table 31: The HEAT family greatly exceed the take-off and landing distance requirements set by the RFP

Takeoff and Landing Performance, Sea Level (ISA +0)						
Configuration	Thrust (% Max Static Thrust)	Static Thrust, DEP System (lbs.)	Static Thrust, Gas Engine (lbs.)	Distance Over 50' Obstacle (ft.)	Ground Run (ft.)	Total Landing Distance (ft.)
6 PAX Takeoff, MTOW	83.4	1779	200 (idle)	488	476	964
6 PAX Landing, MLW	6.1	0 (idle)	200 (idle)	1013	598	1611
4 PAX Takeoff, MTOW	83.4	1779	200 (idle)	476	394	870
4 PAX Landing, MLW	6.1	0 (idle)	200 (idle)	1013	433	1446 (10% rev. thrust)

In the event of engine failure at 5000 ft above ground level (AGL), the electric-only emergency range for the 4 and 6 seat variants is 32 and 34 nmi, respectively. This allows either aircraft to return to their origin airports or to

an alternate airport within this emergency range. Although Hawken plans for single-engine aircraft certification with the FAA, the HEAT variants boast multi-engine performance characteristics. After V_1 speed with a propulsion system failure, the aircraft is able to continue climbing with either the main engine or DEP system inoperative.

Table 32: The Heat family take-off and landing performance is also great at 5000 ft AGL

Takeoff and Landing Performance, 5,000 ft (ISA +18 deg F)				
Configuration	Thrust (% Max Static Thrust)	Static Thrust, DEP System (lbs.)	Static Thrust, Gas Engine (lbs.)	Total Landing Distance (ft.)
6 PAX Takeoff, MTOW	83.4	1779	200 (idle)	1049
6 PAX Landing, MLW	6.1	0 (idle)	200 (idle)	1622
4 PAX Takeoff, MTOW	83.4	1779	200 (idle)	938
4 PAX Landing, MLW	6.1	0 (idle)	200 (idle)	1457 (10% rev. thrust)

The takeoff and landing calculations assumed a descent rate of 5.7 ft/s for the 4 seat variant, and 6.1 ft/s for the 6 seat variant. The DEP system is capable of producing up to 30% of max continuous power as reverse thrust. The full utilization of reverse thrust decreases the shown 4 seat landing distance by approximately 120 ft. If the landing distance is increased, the descent rate can decrease.

Table 33: Hawken’s DEP system allows for the option to use reverse thrust, further improving landing distances

6 PAX Reverse Thrust Landing Distances, MLW (ISA +0)		
% Max Static Thrust	Static Thrust (lbs.)	Total Distance Over 50' Obstacle (ft.)
8.4*	200 (idle)	1611
-10	-237.2	1446
-30	-711.6	1414

*standard landing condition, no reverse thrust

**negative values indicate reverse thrust

Table 34: Ground effect was considered in take-off and landing distance calculations

Parameter	Definition	Value
Kg	In-ground-effect induced drag parameter	0.0135

The HEAT family not only meets the RFP requirements for range, it boasts best-in-class performance. At MTOW, the Prometheus has a max range of 1338 nmi, and the Zeus has a max range of 1126 nmi. These ranges with required RFP payloads are shown in the HEAT family payload range charts, Figure 54. To show how incredible this range is,

Table 35: Hawken’s aircraft offer excellent low speed performance

V Speeds (ISA + 18 deg F)				
Parameter	Definition	Configuration	4 PAX Speed (KIAS)	6 PAX Speed (KIAS)
V _{SO}	Stall Speed	Takeoff	48.1	50.6
V _{TO}	Takeoff Speed	Takeoff	57.8	60.7
V _{SO}	Stall Speed	Landing	53.2	56.6
V _{TD}	Touchdown Speed	Landing	69.2	73.6
V _{APP}	Approach Speed	Landing	74.5	79.3
V _{AQUA}	Aquaplaning Speed	Takeoff and Landing	60.7	60.7

a sample route from Virginia Tech Montgomery Executive Airport to Stevens Field Airport in Pagosa Springs, CO, is shown Figure 55. At MTOW, no competitor is able to achieve such a feat.

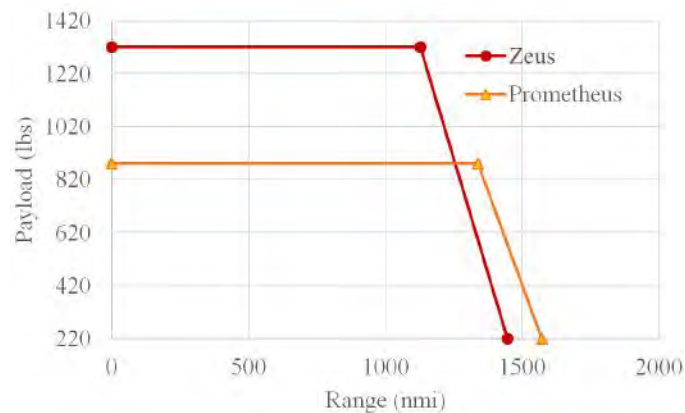


Figure 54: Hawken’s aircraft meet the range requirements of the RFP at MTOW

As can be seen these ranges exceed RFP range requirements. However, Hawken believes these extended ranges provide two benefits. Firstly, later stages of aircraft development after contract award could result in additional weight added due to detailed design work. A larger fuel capacity and fuel weight give some design oversight protection to the aircraft, ensuring that it will still meet the RFP range requirements. This will prepare the HEAT family for these possible design changes, saving in costly design amendments later in the manufacturing process. However, when adding these weights for an extended range, Hawken did not want to make significant contributions to MTOW to save on acquisition cost. With these considerations, 3% in fuel weight of MTOW was added to the Prometheus and Zeus,

respectively. The second benefit to increasing the total fuel weight was providing mission flexibility to the pilot. The pilot has the option to utilize the 3% extra MTOW for increased useful load of 140 pounds or a range increase of 40% from 750 to 1126 nmi or 1000 nmi to 1338 nmi for the 4 seat Prometheus and 6 seat Zeus respectively.

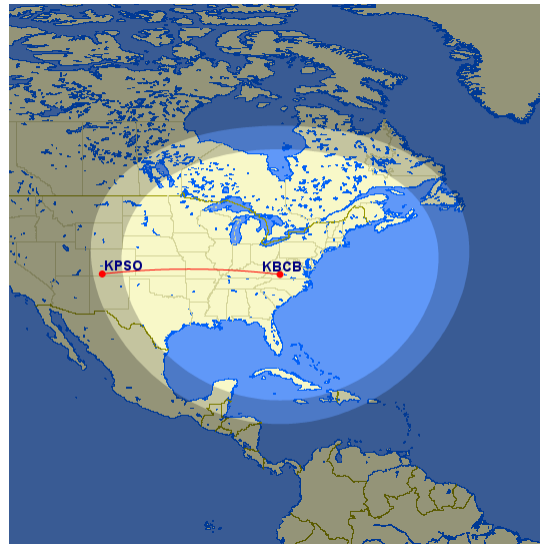


Figure 55: The 4 seat Prometheus can travel all the way from Virginia Tech To Pagosa Springs, CO at MTOW

However, even with the HEAT family out-performing competitor aircraft, Hawken was not satisfied with our payload capabilities. As battery technology improves in the next 20 years, higher energy density batteries of 450 Wh/kg and greater will be available as noted in the Technology subsection 4.6. Using our swappable battery feature, upgrading batteries in the years to come is possible. As shown in Figure 56, when batteries are upgraded payload capacity can be increased by a minimum of 7%.

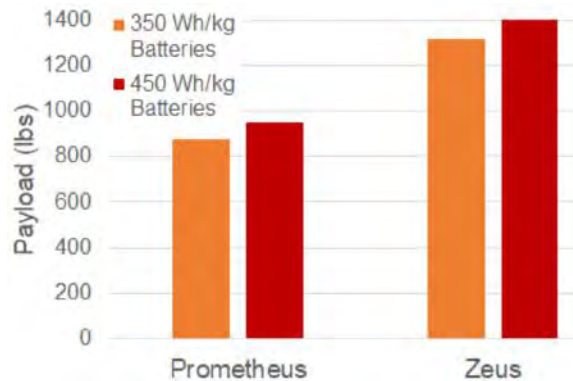


Figure 56: As battery densities improve in the future, Hawken’s payload capacity will continue to improve as well

5.13 Maintenance and Reliability

Hawken has utilized a number of design features which allow the team to offer equal to or better maintenance and reliability than that of comparable aircraft. Firstly, the RED A05 engine and its propeller both have TBO values of 2000 hours, comparable to the Cessna TTX's TSIO 550 engine with a TBO of roughly 1800 hours.⁶⁸ Since the other components of the HEAT family's propulsion system are electronic with little to no moving parts, they exhibit TBO values of approximately 15 years.⁴⁰ The battery bank features ease of access, due to its under-fuselage location on the aircraft as well as utilization of 6 individual boxes which are easily transported by an able-bodied person. Hawken's decision to utilize aluminum alloys allows for less costly structure maintenance than that of composites. Additionally, a completely aluminum structure does not suffer from galvanic corrosion interaction with composites, further reducing maintenance costs. Fixed landing gears feature no moving parts, and are inherently cheaper to maintain than that of their retracting counterparts. Lastly, the team's use of electric actuators to adjust control surfaces does not require the same level of maintenance as a hydraulic system, which may leak.

The RFP also requires that the team's design have reliability equal or better than that of comparable aircraft. The selected communication antennas are specifically designed for harsh environmental conditions, making them equally or more reliable than competitor aircraft. An astounding 34.6% of the landing gear system failures between 1993 and 2008 were attributed to landing gear retraction failure.⁷¹ HEAT's fixed tricycle gear configuration will prove to be more reliable than aircraft with retractable gear. Electronic capacitance density-compensated type fuel indicators increase the accuracy and precision of fuel level measurements, surpassing the reliability of traditional float type indicators. The SkyVision avionics suite featuring full digital instruments makes for an incredibly reliable instrumentation system. The use of dual electronic and analog instrumentation increases reliability and safety over conventional aircraft.

The reliability and maintenance improvements made for the HEAT family not only increase safety, decrease pilot workload, but reduce operational cost.

5.14 Cost

5.14.1 Eastlake Model Assumptions

To estimate the cost of the HEAT aircraft family, the Eastlake model was used.³¹ This model utilized several assumptions in order to arrive at a final number for the total cost and manufacturing of the aircraft. These assumptions

include CFR certification, an unpressurized fuselage, no composite materials used on the airframe, simple flaps and ailerons, a tapered wing, and one prototype. In addition to these assumptions, the structural weight of the airframe, as well as its maximum velocity were used. One drawback of the Eastlake model is that it uses cost in reference to the consumer price index (CPI) in 2012. To tailor the numbers to the CPI of 2017, the ratio of 1.814 was used, which is the ratio of CPI in 2017 to that of 2012. In order to accommodate the off the shelf parts and technologies used for the DEP technology, as well as an avionics suite capable of supporting autonomous architecture, these costs were added to the overall price of the aircraft. The cost of the avionics suite was given to be \$200,000. Additionally, the pay rates of engineering jobs, tooling jobs, and manufacturing jobs were retrieved from Engineersalary.com,⁶² which uses empirical data to estimate the current pay rates of employees in the aerospace industry. Using this resource, these pay rates were determined to be \$92/hr, \$52/hr, and \$52/hr respectively. A quality discount factor was also used to account for the industry experience of the employees. An experience effectiveness of anywhere above 80% can be assumed for this part of the model. In order to avoid a brash claim of being too experienced, but also the unlikely chance that the engineers would have too little experience, an effectiveness of 85% was assumed. This model also uses the number of planes produced over 5 years based on a monthly production rate. An analysis of the monthly production rate ranging from 4-10 may be found below.

5.14.2 Market Analysis

As the market for general aviation aircraft has increased within recent years, likewise has the desire for a more reliable, hybrid aircraft. Similarly to many other forms of transportation, a cheaper and greener alternative has been desired since the implementation of electricity into hybrid cars. The HEAT family hopes to fill this role, meeting the hybrid fervor and far exceeding it. Through the use of the cutting edge DEP technology, to mitigate both the fossil fuel emissions of traditional aircraft, as well as the high price of that same fossil fuel itself, the HEAT family is able to drastically reduce the overall operating cost from anywhere within the range of 50-80%, proving not only to be a market competitor, but a strong one as noted later in this section. In addition to providing cost reduction through the introduction of a hybrid system, other cost mitigation tactics have been utilized to lower manufacturing cost. Through the exclusive use of aluminum alloys, the cost of fabricating composites as well as costly composite repairs has been avoided. Additionally, the desire for general aviation aircraft has grown outside of America; China has also seen a

similar, if not stronger growth within the civil GA industry as noted in the Market Research section 2.3. The AVIC (Aviation Industry of Corporate China) has purchased Cirrus Aircraft manufacturer, Continental Motors', and also partnered with Cessna between 2009 and 2012. This evidence suggests a surge in interest for general aviation not just in the states, but also abroad. More recently, a 25% growth for the general aviation market has been projected by the US-China Aviation Cooperation Program, and due to the FAA China Bilateral Aviation Safety Agreement, certifying via the FARs also guarantees certification under China's aviation laws as well.⁶⁵ This indicates an untapped market potential, one in which the HEAT family looks forward to finding success.

5.14.3 Production Cost

The non-recurring costs of engineering, FAA certification, production tooling, and labor, as well as the overall cost of the aircraft were determined through the use of the Eastlake model. Assumptions are cited above, and these values include the prices of the off-the-shelf parts of the RED AO5 engine, DEP system, and avionics suite capable of supporting autonomy. With this in mind, the costs of engineering, FAA certification, production, tooling, and labor may be found in Table 36 for the Prometheus and Table 37 for the Zeus. These tables include the flyaway cost of the HEAT family, specifically \$804k for the Prometheus and \$806k for the Zeus. Based off these numbers for flyaway cost, the prices in order to net 15% profit are \$925k and \$927k appropriately. These values are marked by green boxes in Table 36 and Table 37. Note that these prices include the use of a quality discount factor and that due to the 94.8% empty weight commonality, both aircraft are very close in price.

Table 36: Cost components for the Prometheus' final production or fly-away cost

Prometheus Cost Breakdown		
		Total Hours
Engineering Hours		83,937
Tooling Hours		75,938
Manufacturing Labor Hours		762,340
		Total Cost
		Cost Per Unit
Total Engineering Cost	\$ 29,383,109.28	\$ 48,971.85
Total Development Support Cost	\$ 902,554.35	\$ 1,504.26
Total Flight Test Ops Cost	\$ 65,395.47	\$ 108.99
Total Tooling Cost	\$ 15,025,151.70	\$ 25,041.92
Certification Cost	\$ 45,376,210.79	\$ 75,627.02
Total Manufacturing Labor Cost	\$ 150,836,526.26	\$ 251,394.21
Total Cost of Quality Control	\$ 19,608,748.41	\$ 32,681.25
Total Cost of Materials	\$ 21,247,863.02	\$ 35,413.11
Quality Discount Factor		0.22
		Without QDF
		With QDF
Fixed Landing Gear Discount	\$ (7,500.00)	\$ (1,673.71)
Engine	\$ 110,000.00	\$ 110,000.00
Electric Propulsion System	\$ 92,000.00	\$ 92,000.00
Main Prop	\$ 5,706.86	\$ 1,273.55
DEP Props	\$ 34,241.19	\$ 7,641.29
Avionics	\$ 200,000.00	\$ 200,000.00
Fly Away Cost	\$ 829,563.64	\$ 804,356.71
Price for 15% Profit	\$ 953,998.18	\$ 925,010.22

Table 37: Cost components for the Zeus' final production or fly-away cost

Zeus Cost Breakdown		
		Total Hours
Engineering Hours		69,211
Tooling Hours		59,829
Manufacturing Labor Hours		762,340
		Total Cost
		Cost Per Unit
Total Engineering Cost	\$ 28,651,227.30	\$ 47,752.05
Total Development Support Cost	\$ 874,794.08	\$ 1,457.99
Total Flight Test Ops Cost	\$ 63,929.32	\$ 106.55
Total Tooling Cost	\$ 14,803,531.02	\$ 24,672.55
Certification Cost	\$ 44,393,481.72	\$ 73,989.14
Total Manufacturing Labor Cost	\$ 150,836,526.26	\$ 251,394.21
Total Cost of Quality Control	\$ 19,608,748.41	\$ 32,681.25
Total Cost of Materials	\$ 21,029,832.87	\$ 35,049.72
Quality Discount Factor		0.22
		Without QDF
		With QDF
Fixed Landing Gear Discount	\$ (7,500.00)	\$ (1,673.71)
Engine	\$ 110,000.00	\$ 110,000.00
Electric Propulsion System	\$ 96,000.00	\$ 96,000.00
Main Prop	\$ 5,706.86	\$ 1,273.55
DEP Props	\$ 34,241.19	\$ 7,641.29
Avionics	\$ 200,000.00	\$ 200,000.00
Fly Away Cost	\$ 831,562.37	\$ 806,355.45
Price for 15% Profit	\$ 956,296.73	\$ 927,308.76

5.14.4 Production Rate and Final Costs

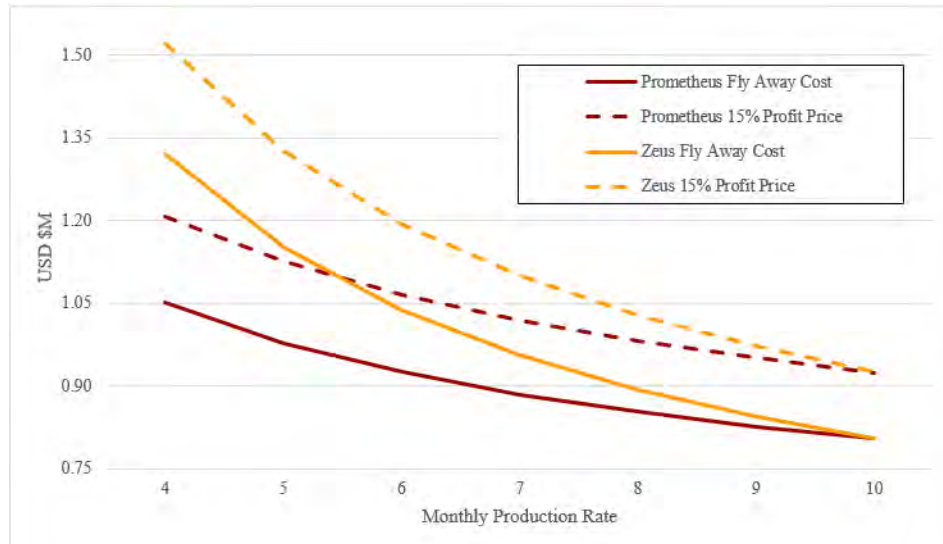


Figure 57: Each HEAT family is to be produced at 10 aircraft per month, and will be sold at \$925k and \$927k for the Prometheus and Zeus, respectively

As can be seen in Figure 57, a study was performed in order to determine the rate at which aircraft should be produced between 4 and 10 aircraft a month, as per RFP guidance. On this graph, one will find that the minimum values for flyaway cost, and subsequently 15% profit price, occur at 10 aircraft being produced per month. This production rate was selected to ensure competitive pricing on the market for these classes of aircraft. A comparison of these prices may be found in Table 38 and Table 39, which show the RFP’s market comparators for the 4 and 6 seat variants, respectively. It can be observed that the HEAT family remains competitive through its price, as well as vastly outperforming current GA aircraft through the operating costs. Calculated at \$58.50 and \$57.00 per hour for the Prometheus and Zeus, the HEAT family’s operating cost reduces that of current market competitors up to 80%, as seen in the stark contrast between the operating costs of the TBM 930 and Zeus. As previously mentioned, these values for cost were evaluated through the use of the Eastlake model, as well as the prices of off-the-shelf parts used in producing the aircraft.

Table 38: The Prometheus significantly reduces operating costs to \$58.50 per flight hour

4PAX Variant Cost		
Aircraft	Cost (USD)	Operating Cost (USD per flight hour)
Cessna TTX	\$734K	\$85.50
Cirrus SR22	\$790K	\$81.50
Cirrus SR22T	\$890K	\$100
Mooney Acclaim Ultra	\$769K	\$115.50
HEAT Prometheus	\$925K	\$58.50

Table 39: The Zeus also significantly reduces from the competition to operating costs to \$57 per flight hour

6PAX Variant Cost		
Aircraft	Cost (USD)	Operating Cost (USD per flight hour)
Beechcraft Baron	\$1.38M	\$190
Piper Matrix	\$940K	\$165
Daher TBM 930	\$4.26M	\$330
HEAT Zeus	\$927K	\$57

6 Project Plans and Risks

To ensure that Hawken’s HEAT family meet the EIS dates of 2028 and 2030, the has created a project development plan to detail the major phases of HEAT family production. Hawken has also identified major risks in the design and set out to mitigate them, to improve end-user safety.

6.1 Future Plans Through EIS

If awarded the contract, Hawken has laid out a schedule in Figure 58 for how we will meet the respective EIS for the Prometheus and Zeus. In addition to conforming the schedule to meet the EIS, the technology freeze date, 2024, was incorporated, allowing for an adequate time to certify future battery technology. Similarly to the Cessna 337,

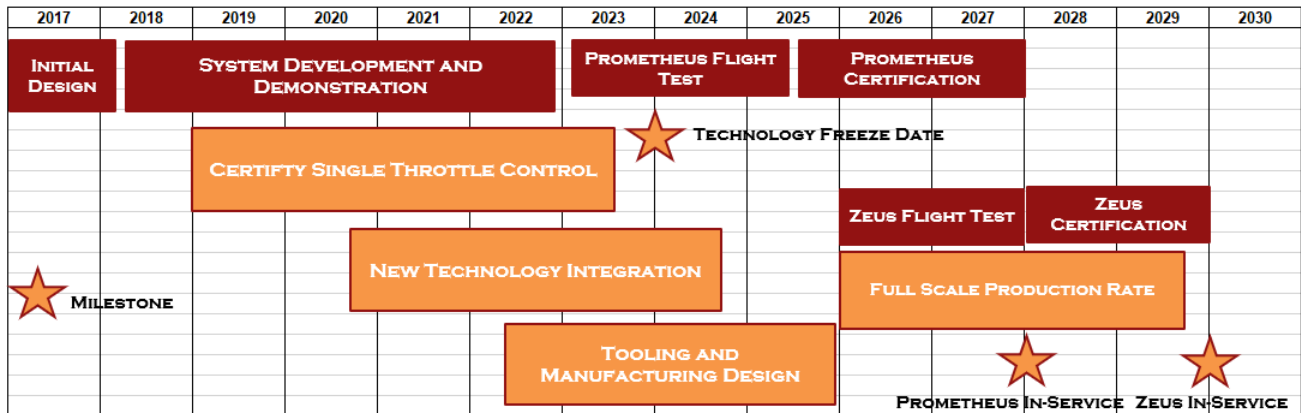


Figure 58: Adequate time has been designated to certify the HEAT family as a single engine aircraft

the HEAT family plans to use a single throttle control for its entire propulsion system.¹⁰ After working closely with the FAA, the HEAT family will be certified as a single-engine aircraft, restricting fewer pilots from flying the HEAT family whilst reducing certification costs. To ensure the HEAT family can be certified by the FAA as single engine aircraft, over 4 years have been allocated for the certification process.

6.2 Risk Assessment

Like any engineering project, Hawken’s design involved some degree of risk. Since customer safety is Hawken’s number one priority, Hawken has utilized a risk assessment process to identify and mitigate design risks. Risks are categorized based on severity and probability. The risk assessment matrix and its supporting tables are shown in Table 40, Table 41, and Table 42:

Table 40: Risks identified by Hawken vary from High, Serious, Medium, and Low based upon severity and probability

		Severity			
		Catastrophic (1)	Critical (2)	Marginal (3)	Negligible (4)
Probability	Frequent (A)	High	High	Serious	Medium
	Probable (B)	High	High	Serious	Medium
	Occasional (C)	High	Serious	Medium	Low
	Remote (D)	Serious	Medium	Medium	Low
	Improbable (E)	Medium	Medium	Low	Low

The design risks Hawken considered were battery failure, fossil fuel engine failure, wing icing, DEP propeller strike upon touchdown, and DEP adverse yaw. Hawken determined the consequences of each risk then assigned each

Table 41: Likelihood of risk was developed based upon probability

Likelihood					
Rating	Frequent (A)	Probable (B)	Occasional (C)	Remote (D)	Improbable (E)
Probability	>10%	10% to 5%	5% to 1%	1% to 0.5%	< 0.5%

Table 42: Severity of risk was based upon potential harm and cost to the aircraft and its occupants

Severity				
Rating	Catastrophic (1)	Critical (2)	3	4
Impact	Possible loss of human life; unsalvageable damage to aircraft.	Major human injury; substantial damage to aircraft.	Minor human injury; moderate damage to aircraft.	No human injury; minimal damage to aircraft.
Cost	> \$500K	\$500K to \$50k	\$50K to \$1K	< \$1K

risk a severity and a probability based on the previous figures. Using the severity and probability, a risk level was determined. Hawken then looked at mitigation tactics to reduce the risk level, as shown in the rightmost four columns in both risk matrices. Thus, the process of risk analysis and risk mitigation ultimately reduce the probability of such a risk occurring and make the aircraft safer for the customer. The risk matrix for design risks is shown in Table 43.

Table 43: The 5 major risks that Hawken identified were mitigated to acceptable levels

Risk Number	Risk	Consequence	Severity	Probability	Risk Level	Mitigation	New Severity	New Probability	New Risk Level
1	Battery Failure	DEP system won't have power and won't be able to provide the necessary flight characteristics during take off, climb, or go-around. Aircraft could crash.	Catastrophic (1)	Remote (D)	Serious (1D)	Link the carbon engine's alternator to allow for power distribution to the electrical bus, so that the main engine can provide direct power as well	Catastrophic (1)	Eliminated (F)	Medium (1F)
2	Carbon Engine Failure	Main engine no longer provide necessary power for cruise, meaning the airplane would no longer be able to complete its mission	Critical (2)	Remote (D)	Medium (2D)	DEP system turns on, extends glide slope to emergency airport	Marginal (3)	Remote (D)	Medium (3D)
3	Aircraft Icing	Ice on the aircraft would cause an increase in drag and decrease in lift, therefore reducing flight performance. The ice could also freeze the propellers and the plane would not be able to operate. The additional weight and unequal formation of the ice could unbalance the aircraft, making it hard to control.	Critical (2)	Remote (D)	Medium (2D)	Install a de-icing system on the wings, propellers, and pitot system to prevent the buildup of ice	Critical (2)	Eliminated (F)	Medium (2F)
4	Prop Strike upon landing	Outboard 3 DEP propellers strike ground, destroy propellers, could injure passengers and critically damage airframe	Critical (2)	Probable (B)	High (3B)	Disable the 3 outboard propellers upon landing and use three innermost DEP props for the 10% reverse thrust	Critical (2)	Improbable (E)	Medium (2E)
5	Wing-out DEP emergency case	If one wing of DEP were to suddenly fail at full throttle, the combined roll and yaw moment from the functional wing would spiral the aircraft out of control	Catastrophic (1)	Remote (D)	Serious (1D)	Have electronic system implemented in flight controls to automatically disable symmetric motors to counter adverse yaw and roll effects. Additionally, install manual override in cockpit to cut all DEP system power in event of automatic system failure.	Catastrophic (1)	Improbable (E)	Medium (1E)

References

- ¹ European Aviation Safety Agency. *EASA Type-Certificate Data Sheet Number: IM.E.008, Issue: 4, Type: Pratt & Whitney Canada PT6A-67 Series Engine*, 20 December 2007.
- ² B. AIN Online, ABACE Convection News. Carey. *China Buying Into World GA Market, Says Rand*, April 16, 2014 (accessed Feb 20, 2018). <https://www.flyingmag.com/general-aviation-in-china#page-6>.
- ³ Cirrus Aircraft. *Cirrus Aircraft SR22*, (accessed: Feb 20, 2018). <http://cirrusaircraft.com/aircraft/sr22/>.
- ⁴ AOPA. *Third Class Airman Medical Reform: Basic Med and AOPA's Fit to Fly*, 2018. <https://www.aopa.org/advocacy/pilots/medical/third-class-airman-medical-reform>.
- ⁵ Erica R.H. Fuchs Jay F. Whitacre Apurba Sakti, Jeremy J. Michalek. *A techno-economic analysis and optimization of Li-ion batteries for light-duty passenger vehicle electrification*, 2014. <https://www.cmu.edu/me/ddl/publications/2014-JPS-Sakti-et-al-Techno-Economic-EV-Battery.pdf>.
- ⁶ Avex. *Operating Costs*, (accessed: Feb 20, 2018). <https://www.newavex.com/tbm-learning-center/operating-costs/>.
- ⁷ Beechcraft Textron Aviation. *Baron G58*, (accessed: Nov 30, 2017). <http://beechcraft.txtav.com/en/baron-g58>.
- ⁸ Beechcraft Textron Aviation. *Baron G58*, (accessed: Nov 30, 2017). http://www.beechcraft.com/customer_support/technical_publications/docs/technical/58-590000-67_Section205.pdf.
- ⁹ Steven A. Brandt. *Introduction to Aeronautics Design Perspective*. American Institute of Aeronautics and Astronautics, 2015.
- ¹⁰ Cessna. *Super Skymaster Owner's Manual*, (accessed April 26, 2018). <http://jasonblair.net/wp-content/uploads/2015/06/Cessna-1971-Super-Skymaster-337-POH.pdf>.
- ¹¹ Cessna. *Cessna TTx*, (accessed: Feb 20, 2018). <http://cessna.txtav.com/en/piston/cessna-ttx>.
- ¹² Fence Wire Gauge Size Chart. *Common Wire Sizes*, 2017. <http://keyboard-keys.info/fence-wire-gauge-size-chart#>.
- ¹³ Cirrus. *CIRRUS SR22/SR22T GTS VS. CESSNA TTx*, (accessed: Nov 30, 2017). <http://whycirrus.com/compare/pdf/SR22GTS and SR22TGTS and Cessna Corvalis TTx.pdf>.
- ¹⁴ Cessna Aircraft Company. *Cessna Corvalis TT compared to the Cirrus SR22T GTS*, (accessed: Feb 20, 2018). <http://www.leggataviation.com/Corvalis%20vs%20SR22.pdf>.
- ¹⁵ Ch.3 p.11-31 D. Raymer. *Aircraft Design: A Conceptual Approach*. AIAA Education Series, Wright-Patterson Air Force Base, Ohio, 1989.
- ¹⁶ TBM Daher. *TBM 930*, (accessed April 15, 2018). <http://www.tbm.aero/products/tbm-930>.
- ¹⁷ Cirrus Design Corporation d/b/a Cirrus Aircraft. *ELECTRONIC STABILITY & PROTECTION*, 2018 (accessed April 19, 2018). <https://cirrusaircraft.com/innovation/esp-by-garmin/>.
- ¹⁸ Raiklin Aircraft Engine Developments. *RED A05 performance specifications*, 2017. <https://www.red-aircraft.com/wp-content/uploads/2012/04/RED-A05.pdf>.
- ¹⁹ Neil Dickson. *Aircraft Noise Technology and International Noise Standards*, 2015 (accessed April 3, 2018). https://www.icao.int/Meetings/EnvironmentalWorkshops/Documents/2015-Warsaw/3_2_Aircraft-Noise-Technology-and-International-Noise-Standards.pdf.
- ²⁰ Mark Drela. *XFOIL: Subsonic Airfoil Development System*, 2013. <http://web.mit.edu/drela/Public/web/xfoil/>.
- ²¹ Brian Edward Duvall. *Development and Implementation of a Propeller Test Capability for G1-10 'Greased Lightning' Propeller Design*, 2016 (accessed April 25, 2018). https://digitalcommons.odu.edu/cgi/viewcontent.cgi?referer=https://www.google.com/&httpsredir=1&article=1011&context=mae_etd.
- ²² L. Engines. *Lycoming Diesel Engines*, 2016. <https://www.lycoming.com/engines/del-120#>.

- ²³ FAA. *14 CFR Appendix F to Part 36*, 1988 (accessed March 20, 2018).
https://www.law.cornell.edu/cfr/text/14/appendix-F_to_part_36.
- ²⁴ FAA. *14 CFR Appendix G to Part 36*, 2006 (accessed March 20, 2018).
https://www.law.cornell.edu/cfr/text/14/appendix-G_to_part_36.
- ²⁵ FAA. *Air Traffic Bulletin*, 2012.
<https://www.aopa.org/news-and-media/all-news/2017/february/pilot/ttx-prime-performer>.
- ²⁶ Federal Aviation Administration (FAA). *About Aviation Gasoline*, July 25, 2017 (accessed April 30, 2018).
<https://www.faa.gov/about/initiatives/avgas/>.
- ²⁷ U.S. Department of Transportation Federal Aviation Administration. *FAA Enhances China Aviation Safety Partnership*, Oct. 27, 2017 (accessed Feb 22, 2018).
https://www.faa.gov/news/updates/?newsId=89010&omniRss=news_updatesAoc&cid=101_N_U.
- ²⁸ FedTech. *The challenge related to Technology Readiness Levels (TRL)*, 2016 (accessed November 29, 2017).
<http://www.fed-tech.org/single-post/2016/10/05/The-challenge-related-to-Technology-Readiness-Levels-TRL>.
- ²⁹ Yvonne Gibbs. *NASA Begins Endurance Testing on Cruise Motors for All-Electric X-Plane*, Jan 2018. <https://www.nasa.gov/centers/armstrong/feature/All-electric-X-57-CruiseMotors-Begin-Testing.html>.
- ³⁰ R. GmbH. *RED Aircraft Engines*, 2014. <https://red-aircraft.com/engines/general/?lang=en>.
- ³¹ S. Gudmundsson. *General Aviation Aircraft Design*. Butterworth-Heinemann, 2013.
- ³² Snorri Gudmundsson. *General Aviation Aircraft Design: Applied Methods and Procedures*. Butterworth-Heinemann, 2013.
- ³³ T. Haines. *Cirrus SR22T: More of a good thing-AOPA*, (accessed: Feb 20, 2018).
<https://www.aopa.org/news-and-media/all-news/2013/may/pilot/cirrus-sr22t-more-of-a-good-thing>.
- ³⁴ Thomas A. Horne. *Cessna TTx Prime Performer*, (accessed April 15, 2018).
<https://www.aopa.org/news-and-media/all-news/2017/february/pilot/ttx-prime-performer>.
- ³⁵ R. J. Huston. *Book Review: Fluid-Dynamic Lift, by Dr. Ing S. F. Hoerner, co-author and editor, Henry V. Borst*. Journal of the American Helicopter Society, 1978.
- ³⁶ CAV Ice Protection Inc. *About TKS Ice Protection Systems*, 2018 (accessed April 29, 2018).
<https://www.caviceprotection.com/content/about-tks-ice-protection-systems>.
- ³⁷ SAE International. *AUTOMATED DRIVING*, 2017 (accessed April 23, 2018).
<https://web.archive.org/web/20170903105244/>.
- ³⁸ N. Baggioni J. Bouchard. *As Airlines Aim For Autonomous Flight, Near-Term Revolution Will Be Going Single Pilot*, 2017. <https://www.forbes.com/sites/oliverwyman/2017/10/25/single-pilot-commercial-flights-are-not-far-off-even-if-fully-autonomous-flight-is/#389308e83b17>.
- ³⁹ Karen A. Deere Jeffrey K. Viken, Sally Viken and Melissa Carter. *Design of the Cruise and Flap Airfoil for the X-57 Maxwell Distributed Electric Propulsion Aircraft*, 2017 (accessed April 27, 2018).
<https://doi.org/10.2514/6.2017-3922>.
- ⁴⁰ P. Jensen. *A discussion on the Future of Batteries*, 2017. Interview.
- ⁴¹ C.-X. Zu. H. Li. *Thermodynamic analysis on energy densities of batteries*. Energy & Environmental Science, 2011.
- ⁴² N. Borer M. Patterson, J. Derlaga. *High-Lift Propeller System Configuration Selection for NASA's SCEPTOR Distributed Electric Propulsion Flight Demonstrator*. NASA Langly Research Center, 2016.
- ⁴³ M. Moore. *Distributed Electric Propulsion Research*. NASA Langly Research Center, 2015.

- ⁴⁴ C. Motors. *Continental Diesel*, 2017. <http://www.continentaldiesel.com/typo3/index.php?id=2&L=1>.
- ⁴⁵ Continental Motors. *550 Series*, (accessed: Nov 30, 2017). <http://continentalmotors.aero/uploadedFiles/Content/xImages/550Series-SpecSheet-WEB.pdf>.
- ⁴⁶ Grant Nicolai, Leleand M. (Leland Malcolm); Carichner. *Fundamentals of Aircraft and Airship Design*. American Institute of Aeronautics and Astronautics, 2010.
- ⁴⁷ Leland M. Nicolai and Grant Carichner. *Fundamentals of Aircraft and Airship Design*. American Institute of Aeronautics and Astronautics, 2000.
- ⁴⁸ M. Niu. *Airframe Structural Design*. Adaso/Adastra Engineering Center, 2011.
- ⁴⁹ The International Council of Aircraft Owner and Pilot Associations (IAOPA). *IAOPA Fuel Prices*, 2017. <https://www.iaopa.eu/fuelprices>.
- ⁵⁰ Piper. *M500 by the Numbers*, (accessed: Feb 20, 2018). http://www.piper.com/wp-content/uploads/2015/08/2015MeridianM500ByTheNumbers.Final_MR.pdf.
- ⁵¹ Textron Aviation Plane & Pilot. *PILOT OPERATING HANDBOOK & FLIGHT MANUAL*, (accessed: Feb 20, 2018). http://www.x-aviation.com/downloads/C400_POH.pdf.
- ⁵² McCauley Propellers. *1 Constant Speed Propeller result(s) for PIPER PA-32-301 Saratoga W/ IO-540-K1G5 (LY) Engine*, 2018. [http://mccauley.txtav.com/en/products?PropType=constant&OEM=PIPER&AircraftModel=PA32-301Saratoga&EngineType=IO540-K1G5\(LY\)](http://mccauley.txtav.com/en/products?PropType=constant&OEM=PIPER&AircraftModel=PA32-301Saratoga&EngineType=IO540-K1G5(LY)).
- ⁵³ McCauley Propellers. *1 Fixed Pitch Propeller result(s) for PIPER PA-25-260 Pawnee W/ O-540-G2A5 (LY) Engine*, 2018. [http://mccauley.txtav.com/en/products?PropType=fixed_pitch&OEM=PIPER&AircraftModel=PA-25260Pawnee&EngineType=O540-G2A5\(LY\)](http://mccauley.txtav.com/en/products?PropType=fixed_pitch&OEM=PIPER&AircraftModel=PA-25260Pawnee&EngineType=O540-G2A5(LY)).
- ⁵⁴ Brandon Ray. *In-Depth Review of the Cessna TTx T240*, 2014 (accessed April 25, 2018). <https://www.flyhpa.com/2014/10/in-depth-review-of-the-cessna-ttx-t240>.
- ⁵⁵ Daniel P. Raymer. *Aircraft Design: A Conceptual Approach*. American Institute of Aeronautics and Astronautics, 1992.
- ⁵⁶ A. Reiner. *Towards the End of Pilots*, 2017. <https://www.forbes.com/sites/oliverwyman/2017/10/25/single-pilot-commercial-flights-are-not-far-off-even-if-fully-autonomous-flight-is>.
- ⁵⁷ Kim Reynolds. *Tesla Supercharger: An In-Depth Look*, 2012. <http://www.motortrend.com/news/tesla-supercharger-an-in-depth-look/>.
- ⁵⁸ AOPA Rob Mark. *FLY-BY-WIRE: TOO MUCH RESPONSIBILITY FOR A MACHINE?*, 2013 (accessed April 20, 2018). <https://www.aopa.org/news-and-media/all-news/2013/november/pilot/fly-by-wire>.
- ⁵⁹ Jan Roskam. *Airplane Design Parts I through VII*. Darcorporation, 2003.
- ⁶⁰ M. Sadraey. *Aircraft Performance Analysis*. VDM Verlag Dr. Müller, 2011.
- ⁶¹ Mohammad H. Sadraey. *Aircraft Design A Systems Engineering Approach*. John Wiley & Sons, 2013.
- ⁶² Engineery Salary. *The Engineer's Complete Compensation Database*. <http://www.engineerssalary.com> (accessed April 9, 2018).
- ⁶³ Dieter Scholz. *Aircraft Design Chapter 9 Empennage General Design*, 2015 (accessed March 15, 2018). http://www.fzt.haw-hamburg.de/pers/Scholz/HOOU/AircraftDesign_9_EmpennageGeneralDesign.pdf.
- ⁶⁴ U.S. Consulate General Shanghai U.S. Commercial Service. *The General Aviation Industry in China 2012*, (accessed Feb 20, 2018). https://2016.export.gov/china/build/groups/public/eg_cn/documents/webcontent/eg_cn_047964.pdf.

- ⁶⁵ US General Conglomerate Shanghai. *The General Aviation Industry in China — 2012*, 2012 (accessed April 20, 2018). https://2016.export.gov/china/build/groups/public/@eg_cn/documents/webcontent/eg_cn_047964.pdf.
- ⁶⁶ SkyBrary. *Flight Controls*, 2017 (accessed April 23, 2018). <https://cirrusaircraft.com/innovation/esp-by-garmin/>.
- ⁶⁷ Aircraft Spruce and Specialty Co. *PRINCETON CAPACITANCE FUEL PROBES*, 2018 (accessed April 24, 2018). <http://www.aircraftspruce.com/catalog/inpages/princefuelprobes.php>.
- ⁶⁸ What to Fly.com. *Beech Baron 58*, (accessed: Feb 20, 2018). http://www.what2fly.com/manufacturer/operating_cost/BEECH/58+BARON+58/69.
- ⁶⁹ What to Fly.com. *Mooney Acclaim*, (accessed: Feb 20, 2018). http://www.what2fly.com/manufacturer/operating_cost/MOONEY/ACCLAIM/2153.
- ⁷⁰ Wiki Wings. *Fuel, Cost of Ownership of Cirrus SR22*, (accessed: Feb 20, 2018). <https://wikiwings.com/2015/08/07/fuel-cost-of-ownership-cirrus-sr22/>.
- ⁷¹ Ni Huajin Zhang Ming Yin Yin, Nie Hong. *Reliability Analysis of Landing Gear Retraction System Influenced by Multifactors*, 2016 (accessed April 30, 2018). https://www.researchgate.net/publication/299498831_Reliability_Analysis_of_Landing_Gear_Retraction_System_Influenced_by_Multi
- ⁷² J. Zimmerman. *Continental Motors - Betting Big on Diesel*, 2013. <https://airfactsjournal.com/2013/10/continental-motors-betting-big-on-diesel>.